NASA CONTRACTOR REPORT 158927

NASA-CR-158927
19840024297

DEVELOPMENT OF TWO UNDERSEAT ENERGY ABSORBERS FOR APPLICATION TO CRASHWORTHY PASSENGER SEATS FOR GENERAL AVIATION AIRCRAFT

JAMES C. WARRICK AND S. P. DESJARDINS

SIMULA INC.
2223 S. 48TH ST.
TEMPE, ARIZONA 85282

CONTRACT NAS1-14583
SEPTEMBER 18, 1979

NATIONAL AERONAUTICS AND
SPACE ADMINISTRATION

LANGLEY RESEARCH CENTER
HAMPTON, VIRGINIA 23665

All Blank Pages

Intentionally Left Blank

To Keep Document Continuity

ABSTRACT

This report presents the methodology and results of a program conducted to develop two underseat energy absorber (E/A) concepts for application to nonadjustable crashworthy passenger seats for general aviation aircraft. One concept utilizes an inflated air bag, and the other, a convoluted sheet metal bellows. Prototypes of both were designed, built, and tested. Both concepts demonstrated the necessary features of an energy absorber (load-limiter); however, the air bag concept is particularly encouraging because of its light weight. Several seat frame concepts also were investigated as a means of resisting longitudinal and lateral loads and of guiding the primary vertical stroke of the underseat energy absorber. Further development of a seat system design using the underseat energy absorbers is recommended because they provide greatly enhanced crash survivability as compared with existing general aviation aircraft seats.

TABLE OF CONTENTS

TABLE OF CONTENTS (CONTD)

TABLE OF CONTENTS (CONTD)

LIST OF ILLUSTRATIONS

LIST OF ILLUSTRATIONS (CONTD)

LIST OF TABLES

DEVELOPMENT OF TWO UNDERSEAT ENERGY ABSORBERS FOR APPLICATION TO CRASHWORTHY PASSENGER SEATS FOR GENERAL AVIATION AIRCRAFT

James C. Warrick and S. P. Desjardins
Simula Inc.

SUMMARY

Two energy-absorbing, crashworthy seating system designs were developed for general aviation aircraft. Each design utilizes an underseat energy absorber (E/A) to attenuate vertical crash deceleration magnitudes to within the range of human tolerance. The E/A of one seat system is an inflated air bag, and of the other, a convoluted sheet metal bellows. The seat bucket and occupant are allowed to stroke vertically, crushing the E/A against the floor. A seat frame was deemed necessary in order to prevent the seat system from overturning during horizontal loading. Several seat frame systems were evaluated, but hardware was not built. Project emphasis was on development of the underseat E/As.

Analytical models for both the bellows and air bag type E/As were developed. Subscale preliminary models of the bellows were built and tested; then, full-scale models of each type of E/A were designed, built, and tested statically and dynamically. Dynamic testing was performed in a drop tower facility with the E/As mounted in a fixture that simulated the motion and moving mass of an actual seat.

The air bag is intended to remain inflated under the seat at all times, thus avoiding the complexity of crash sensors and pressurization systems. An orifice uncovered at the beginning of the stroke allows expulsion of the gas within the air bag. The orifice size and air bag shape were optimized by use of a computer program in order to most uniformly and completely decelerate the occupant.

The testing proved the acceptability of the air bag for its intended use. Tests of the bellows were encouraging but somewhat inconclusive because of the loading-rate dependence of the bellows limit load.

INTRODUCTION

Purpose and Scope

The primary objective of the project documented within this report was to develop two underseat energy absorbers (E/As) for application to the passenger seats of general aviation aircraft. One E/A concept was to be a convoluted metal bellows, and the other, an inflated air bag. Analytical models of both E/As were created to predict and optimize performance. Then, subscale and full-scale E/A models were built and tested. The program emphasized the development, fabrication, and testing of practical E/A hardware for the purpose of attenuating vertical crash deceleration magnitudes to within the limits of human tolerance. A secondary purpose of the program was to investigate methods of resisting forward and lateral decelerations. For this purpose, frame concepts were designed and stress-analyzed, but fabrication and testing of these frames were not within the scope of the program.

Background

Historically, seats for general aviation aircraft have been designed for four major characteristics. These include appearance and customer acceptance, low cost, low weight, and reasonable comfort. Strength requirements for the seats, as specified in NAS809, the National Aircraft Standards Committee Specification for Aircraft Seats and Berths, are so low that they provide totally unacceptable protection to their occupants in a crash. These strengths for Type II Seats, which are for normal and utility aircraft, are:

forward 9.0 G

sideward 3.0 G

upward 3.0 G

downward 7.0 G

(G is defined as the acceleration of gravity = 9.807 m/sec^2 = 32.17 ft/sec^2)

Requirements for military aircraft far exceed the requirements for general aviation. With no energy absorption, the same comparative requirements for the Army's rotary- and light fixed-wing aircraft are:

forward 35.0 G

sideward 20.0 G

upward 8.0 G

downward 48.0 G (this is the peak input deceleration that must be attenuated to a value not exceeding 23.0 G to provide occupant safety)

The requirements for military aircraft were developed from extensive studies of crashes and the statistical distribution of crash environment severities encompassed within potentially survivable limits. Of course it is useless to provide seat strengths far exceeding the capability of the aircraft to provide a protective environment for a well-restrained occupant. However, past tests have shown that the survivability of existing aircraft exceeds that of the seats and restraint systems with which they are equipped. It is desirable, therefore, that the strengths and energy-absorbing characteristics of the seating systems for general aviation aircraft should be improved to provide the maximum protection possible consistent with the overall crashworthiness of the aircraft frame.

Methodology

In the first phase of the project, a systems analysis was performed to identify the constraints upon the seat system. These constraints included the range of occupant weights, crash impulse requirements, and load limiting required to provide safety for the occupant, restraint method for the occupant, and other general requirements of the seat system and its interface with the cabin of a typical light aircraft. Then, several preliminary seat concepts employing underseat E/As were analyzed in terms of their ability to provide the necessary vertical stroke while at the same time resisting overturning moment due to longitudinal and lateral forces. Two frame concepts, which were capable of resisting the applied loads, were selected, and a stress analysis was performed on each of them to verify their structural integrity and to predict deflections.

Then, attention was directed towards the actual detail design of the underseat E/As. An analytical model of the bellows was developed in order to predict the crushing load. A number of different variations of convolution shapes were tested and the data were used to check the accuracy of the analytical model. No preliminary models of the air bag were built or tested because the analytical

model developed to predict the air bag's behavior had a high confidence level. The air bag analytical model consisted of a computer program accounting for the transient dynamic response by stepwise integration of all of the parameters affecting the escape of air from the air bag orifice.

Full-scale test samples of both the bellows and the air bag were fabricated, and a test fixture that simulated the stroking of an actual seat was constructed. The air bags were dynamically tested using a drop tower facility, and the bellows were statically tested using a standard combination tensile-and-compression test machine. Also, one sample of the bellows was dynamically tested in the drop tower to determine the dependence of the limit load upon loading rate.

Information gained during the tests was used to refine the preliminary seat system design to produce a final design that is recommended for further study as a practical crashworthy general aviation aircraft seat.

Units of Measurement

Measurements of most quantities were made in U.S. Customary Units, which were then converted to SI Units for presentation in this report. For convenience, the U.S. Customary Unit equivalent is included in parentheses following the SI quantity.

SEAT SYSTEM DESIGN CRITERIA

In this section, the functions of the seat, constraints upon its design, its interface with the aircraft, the crash impulse it is to withstand, and the range of occupant sizes it is to accommodate and protect are described and defined. The environment in which the seat is to operate defines seat characteristics which in turn define the characteristics required of the underseat E/As.

Seat System Required Characteristics

The general requirements of a seat system are that it be:

- Crashworthy
- Lightweight
- Compact
- Low Cost
- Comfortable
- Pleasing in appearance
- Acceptable to the end user.

Design crashworthiness is treated in detail in later sections of this report. The other characteristics are elaborated upon in the following paragraphs:

The seat must be light in weight to gain acceptance by aircraft manufacturers. An upper limit of 6.8 to 9.1 kg (15 to 20 lb) was chosen; a greater weight than this would probably be unacceptable to aircraft manufacturers, and a lesser weight than this would not allow the frame to be strong enough to carry its required loads.

Another consideration was that the seat should be compact in size to fit into the cramped quarters of light aircraft. The total width of the seat was limited to 45.7 cm (18 in.). Height and length were minimized consistent with stroke requirements and frame strength requirements. A simple design using no elaborate materials or fabrication techniques was sought to minimize cost.

Of course, the seat must be comfortable and have a pleasing appearance to be acceptable to the end user.

Another consideration was the method by which the occupant would be restrained to the seat. A lap belt together with a single diagonal shoulder strap, the minimum acceptable system, appeared to be most practical. A full shoulder harness, of course, would be more crashworthy, but it is doubtful that a great percentage of passengers would wear it. A single diagonal shoulder strap is considered to be the best compromise between crashworthiness and what the public will accept. The importance of wearing the installed restraint system, however, must be stressed, as failure to do so renders much of the crashworthiness of the seat ineffective.

Candidate seat systems were evaluated on the basis of the above-mentioned characteristics, as well as upon their crashworthiness. The intention was to create a practical, crashworthy seat design that could gain acceptance in future light aircraft. Suitability of the designs for retrofit was not considered.

Most of the emphasis in the remaining portion of this report is devoted to the crashworthiness aspect of the seat system design and, specifically, in later sections, to the detailed development of the underseat E/As.

Crash Impulse Requirements

The crash impulse requirements used in this project are shown in Table 1. They are design conditions representative of the 95th-percentile survivable crash and are criteria established for passenger seats of light fixed-wing aircraft contained in the Crash Survival Design Guide, USAAMRDL TR 71-22 (Reference 1). Minimum strengths of 8 G and 12 G, respectively, are required in the upward and backward directions. The downward vertical deceleration of the seat must be attenuated to not more than 23 G for durations longer than approximately 5.5 ms in order to prevent spinal damage. Also, per recommendations of Reference 1, the vertical energy-absorber limit load was set at 14.5 G so that deceleration peaks caused by dynamic overshoot would not exceed 23 G. (Dynamic overshoot is a term referring to transient acceleration peaks of masses in a system --i.e., seat pan, cushion, buttocks, chest-- which are coupled to each other elastically. It is defined in Reference 1 as "the amplification of decelerative force on cargo or personnel beyond that of the floor input decelerative force.") The load in the lateral direction was suggested by NASA/Langley Research Center and was based upon preliminary information from crash tests being conducted there. In the forward direction, it is not necessary to attenuate the acceleration to prevent occupant injury; however, some energy absorption was necessary in order to reduce the frame strength requirements and, thus, reduce the seat weight to an acceptable level.

TABLE 1. CRASH IMPULSE DESIGN REQUIREMENTS

Impulse Direction	Velocity Change m/sec (ft/sec)	Peak Acceleration	Pulse* Duration (sec)	Reference
Forward	15.24 (50)	24 G dynamic attenuated to 15	0.130	p. 42 & 138, Ref. 1
Side	-	10 G static	-	Input from NASA/Langley Research Center
Down	12.80 (42)	48 G attenuated to 14.5 G at occupant	0.054	p. 42, Ref. 1
Upward	-	8 G static	-	p. 152, Ref. 1
Rearward	-	12 G static	-	p. 152, Ref. 1

*Pulse shape is isosceles triangle.

Occupant Weights

The inertial load, which is applied to the seat frame in a given loading direction, is equal to the acceleration load factor for that direction (from Table 1) multiplied by the sum of the occupant weight plus the seat bucket weight (e.g., 14.5 G x 62.1 kg = 14.5 x 9.808 x 62.1 = 8831 Newtons). For all loading directions except downward-vertical, the entire body weight, including clothes, of the 95th-percentile occupant is included in the calculation. In the downward-vertical direction, the weight of the 50th-percentile occupant is used, and only 80 percent of the body weight is included because the lower legs of the occupant are supported by the floor. The effective weight in the downward-vertical direction then is equal to 80 percent of the occupant weight plus the seat bucket weight. Occupant weights and effective weights are shown in Table 2 for the 5th-, 50th-, and 95th-percentile weight adults.

Load Limiting

The limit load of the underseat E/A was sized to provide 14.5 G deceleration of the effective weight of the 50th-percentile occupant. The weight of the 50th-percentile occupant was chosen because this provides the best protection to that large percentage

TABLE 2. ADULT OCCUPANT WEIGHTS

Percentile Occupant	Occupant Weight, W_o kg (lb)*	Seat Bucket Weight, W_b kg (lb)	Effective Weight, W_e kg (lb)**
5th (Female)	43.09 (95)	3.63 (8)	38.10 (84)
50th (Male)	73.26 (161.5)		62.14 (137)
95th (Male)	97.52 (215)		81.65 (180)

*From Reference 2.
**Applicable only to downward-vertical loading direction. Effective weight = $0.8 \times W_o + W_b$

of passengers whose weights are close to the 50th-percentile, as can be seen on a typical bell-shaped distribution. A minimum of 30.5 cm (12 in.) of vertical stroke is recommended (for adjustable crewseats) by Reference 1 as being necessary to decelerate the 50th-percentile occupant in the 95th-percentile survivable crash.

The 95th-percentile occupant would be expected to bottom out against the floor in the 95th-percentile vertical crash, because his greater weight is decelerated at a lesser rate by the fixed limit load of the underseat E/A. The 5th-percentile (female) occupant, on the other hand, may be subjected to deceleration peaks greater than 23 G because of her lesser weight in relation to the fixed limit load. She would not utilize a very great portion of the available stroke. These off-design conditions are unavoidable but represent the rare extremes of crash severity combinations.

A forward stroke of 15.2 cm (6 in.) is recommended by Reference 1 as the requirement to safely attenuate the 24 G peak longitudinal crash pulse to 15 G.

The forward stroke is measured at the center of gravity (c.g.). Since the final seat design does not merely translate forward but, rather, pitches forward about a pivot point at floor level, the head can be expected to move forward a distance at least twice as great as the center of gravity.

The limit load in the forward direction is sized for the 95th-percentile occupant, and the stroke requirement calculated above is for the 95th-percentile survivable crash. In this extreme combination, representing only a small fraction of survivable crashes, the occupant would stand a chance of head impact against some portion of the cabin interior but would at least remain restrained in his seat. In the majority of crashes where occupant weights are near the 50th percentile, or 73 kg (161 lb), little, if any, seat stroking would take place in the forward direction.

Seat Attachment Points

The final criteria required that the shoulder strap inertia reel be mounted to the seat back rather than to the cabin sidewall. Such a freestanding, floor-mounted seat requires more frame strength in order to resist overturning moment in forward loading directions than would a seat in which the inertia reel is attached to the cabin sidewall. However, attaching the reel to the seat makes the seat immune to loads resulting from large cabin sidewall buckling deflections that occur in crashes. If it were possible to mount the shoulder straps to hard points on the airframe that would not deform greatly relative to the floor mounting of the seat, it would be possible to reduce the frame weight. The great forward overturning moment on the seat could be carried by the shoulder strap to the airframe.

A preliminary design concept was developed utilizing a cabin sidewall attachment of the shoulder strap, and a method was found to prevent this arrangement from interfering with the vertical stroke of the seat. The concept is illustrated in Appendix A. This method of shoulder strap attachment would be valuable for seats located in front of bulkheads.

SEAT SYSTEM DESIGN

Much effort was expended in developing practical seat system designs that resisted the severe longitudinal and lateral overturning loads while at the same time maintaining the seat weight at an acceptably low level. Of particular importance is the requirement that the seat perform its vertical stroke in the presence of any combination of longitudinal and lateral loads as well as the vertical load. The combined loading case in which the maximum longitudinal and lateral loads are applied to the seat simultaneously is the most severe loading condition, not only because it tends to overturn the seat to the front and the side, but also because the bucket is cantilevered somewhat forward from the frame causing the frame to yaw.

The bellows underseat E/A is inherently rigid in torsion and is capable of reacting this yaw moment that occurs during combined loading. The air bag, however, is not rigid in torsion; therefore, the seat frame design of the air bag underseat E/A must incorporate its own means of resisting the yaw moment. Because of the structural bonus from the bellows underseat E/A, a frame design was first developed for it. Then, a slightly more sophisticated frame was developed for the air bag underseat E/A.

The structural members of both seats were rough sized by hand calculation to carry the occupant inertial loads to the floor. A stress and deflection analysis was performed on both seat frame concepts using the finite element program, STARDYNE, which is available from Control Data Corporation. The results of this study indicated that the seat designed for the air bag E/A was more efficient from a strength-to-weight standpoint; therefore, it is the one recommended for use with either underseat E/A.

Kinematics and Load Path Analysis

Early in the seat system conceptual design phase, it was learned from the kinematics and load path analysis that the underseat E/As by themselves would not be capable of resisting the longitudinal and lateral overturning moments while at the same time performing their necessary vertical load-limiting stroke. A free-standing seat with no support other than that provided by the underseat bellows and occupied by a 215-lb passenger was calculated to overturn at a horizontal acceleration of 1.6 G. The analysis behind this conclusion can be found in Appendix B. Under the same conditions, the air bag E/A would allow the seat to overturn at an even lower horizontal deceleration due to the force from the pressure in the air bag being spread uniformly over the area of the air bag rather than being concentrated at the perimeter as it is with the bellows.

Several simple concepts were evaluated as means of resisting the longitudinal and lateral loads, one of them being to provide a frame to support the front of the seat. A hinge would attach the frame to the front of the seat. This concept would have required the seat to pitch backwards during the vertical stroke. For the seat to rotate in this manner requires a torque applied by the inertial load, but the torque is dependent upon the direction as well as the magnitude of the inertial load vector. During combined longitudinal and vertical loading, the resultant vector could pass directly through the hinge, and stroking would be impossible regardless of the magnitude of the inertial load vector. This concept and any others requiring the vertical stroke to occur in a largely rotational manner were determined to be unacceptable for the reason just stated.

For the vertical stroke to be independent of the other influences, it was concluded that a semirigid frame, separate from the stroking portion of the seat, would be necessary. The frame had to resist the longitudinal and lateral loading and be provided with linear bearings to guide the vertical stroke of the seat bucket. Therefore, for loading directions other than downward-vertical, the kinematics and load path analysis concentrated on load paths through the frame.

The underseat E/A does not necessarily have to resist longitudinal and lateral loading; however, the location of the E/A under the seat does provide some resistance to forward overturning moment, and in the case of the bellows, also provides resistance to seat deflection in other directions as well (yaw). The underseat E/A in such a system can be designed to perform its primary function as a vertical load limiter without compromising its characteristics in order to resist loading in other directions.

For loading directions other than downward-vertical, the inertial load is based upon the sum of the 95th-percentile occupant weight, 97.5 kg (215 lb), plus the weight of the moving portion of the seat, 3.6 kg (8 lb), multiplied by the acceleration load factor shown in Table 1. Several seat system frame designs were developed and analyzed on the basis of carrying these inertial loads safely to the anchor points on the aircraft floor.

The location of the underseat E/A below the center of gravity of the occupant made it unnecessary to analyze the load paths through the frame in the downward-vertical loading case; in this case, the load is carried by the E/A directly to the floor, bypassing the seat frame.

Preliminary Seat System Design, Bellows Equipped

Description. - Figure 1 shows the preliminary bellows-equipped seat design. The seat consists of three major parts: the fixed

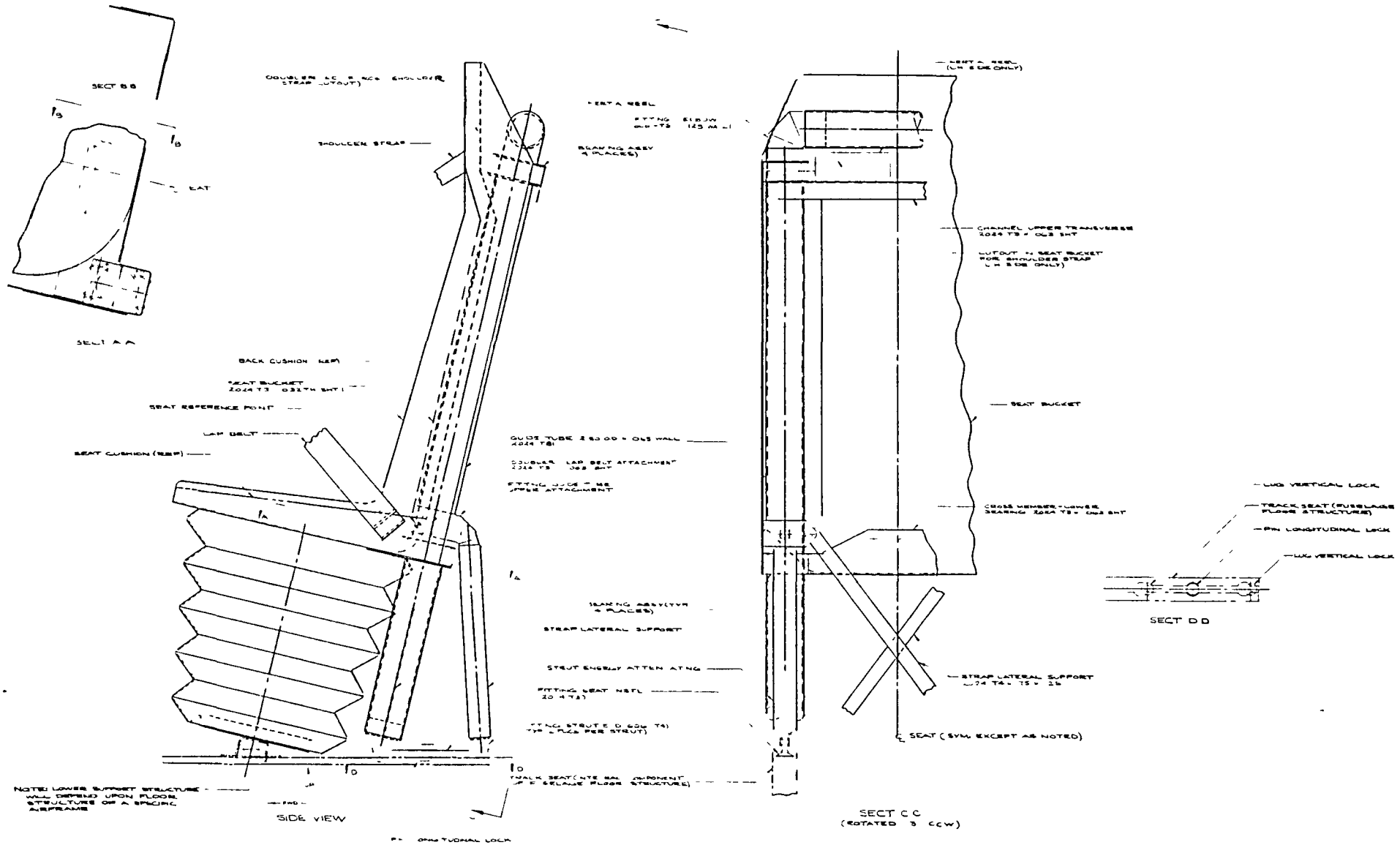

Figure 1. Preliminary bellows-equipped seat, Drawing No. SK10077.

seat frame consisting of upright guide tubes held erect by rear tubular energy-absorbing struts, the moving seat bucket formed of aluminum sheet metal, and the underseat bellows E/A. Its calculated weight is approximately 10 kg (22 lb).

The seat bucket is guided in its vertical stroke by its attachment to the tubular upright guide tubes by use of spool-shaped rollers. The rollers wrap around the guide tube to transmit lateral as well as longitudinal loads from the seat bucket to the guide tubes. Low friction for lateral as well as longitudinal loading conditions is ensured by the use of needle thrust bearings as well as needle radial bearings at the roller support areas.

In the important forward loading case, the greatest loads are applied at concentrated points by the lap and shoulder belts. The bearings have been positioned so that the concentrated belt loads are transmitted directly to them with a minimum amount of intervention by the relatively fragile seat bucket.

It is necessary for the bellows to be attached to both the seat bucket and the floor in order to resist the yaw moment that occurs during combined longitudinal and lateral loading. Otherwise, one of the energy-absorbing rear struts would be loaded much higher than the other and would stroke, allowing the seat to twist excessively.

Stress Analysis. - The stress analysis of this design indicated that the guide tubes were overstressed in the region where they connect with the energy-absorbing struts, while, at the same time, they are underutilized at their upper extremities. This problem could be remedied by starting with a heavier walled guide tube, then thinning the wall where the tube is less highly stressed, or by starting with a guide tube with a thickness sized for the least highly stressed region, then adding sleeves or bushings to the inside of the guide tube to strengthen the more highly stressed regions.

Discussion. - Rear struts, as opposed to front struts, are recommended to hold the seat erect. Rear struts were chosen for two reasons: first, the rear struts are in tension during forward loading when they are required to stroke. This avoids buckling problems associated with slender, compressive-type E/As. Second, the front struts have to be far enough apart to permit the moving portion of the seat to stroke down between them. Their thick sections, necessary to prevent buckling, plus clearances between them and the seat bucket make the frontal profile of a seat with front struts wider than can be accommodated by most light aircraft. The rear struts do not greatly reduce leg room for the passenger located behind the seat in question since the passenger's feet can rest between the struts. Also, an optional sheet metal panel, which would prevent a passenger's feet from being in a position to

be crushed by the stroking seat in front of him, could be placed between the guide tubes.

In order to provide the required minimum 30.5 cm (12 in.) vertical stroke, allowance must be made for the crushed height of the bellows. Because the crushing load of the bellows starts to rise beyond tolerable levels after the bellows has been stroked approximately 80 percent of its original height, this would require that the seat pan be located approximately 38 cm (15 in.) above the cabin floor.

Preliminary Seat System Design, Air Bag Equipped

Description. - Figure 2 shows the layout of the seat system designed for the air bag. Its weight is approximately 7.2 kg (16 lb), about 2.7 kg (6 lb) lighter than the bellows-equipped design discussed previously. Only 1.1 kg (2.4 lb) of this weight reduction is due to the difference in weight between the air bag plus its accessories and the bellows plus its accessories. The remaining weight reduction of 1.6 kg (3.6 lb) is due to more efficient use of material in the frame, specifically: the utilization of truss construction in the moving seat back, the elimination of redundant fixed-frame structure above waist level, and the substitution of sleeve bearings for the lower bearings.

Another important feature of this design is its ability to resist the twisting (yaw) effect of lateral forces while at the same time stroking forward to attenuate the longitudinal deceleration. This feature, one of the primary design objectives, is made possible by the energy-absorbing crossmember shown in Figure 3. A consideration of the geometry reveals that both left and right guide tubes must stroke forward equally (within the elastic limits) in spite of one being more heavily loaded during the combined forward and lateral load case.

The emphasis in this design was to position the upper bearings at a location level with the center of gravity of the 95th-percentile occupant, and to make the moving part of the seat an independent structure, strong enough to transmit all lateral and longitudinal occupant inertial loads to the upper bearings. Only a small portion of the longitudinal or lateral inertial load should find its way to the lower bearings, permitting Teflon-lined sleeve bearings to be used there in place of the heavier, bulkier, and more expensive roller bearing assemblies. Each lower bearing does carry a forward load of about 4450 N (1000 lb) when no occupant inertial load is applied as it acts in combination with the upper bearings to counteract the rearward overturning torque applied to the moving portion of the seat by the upward force of the air bag. However, when the downward inertial load of the occupant matches the upward force of the air bag and stroking is ready to commence, that torque becomes insignificant and the lower bearing loads approach zero.

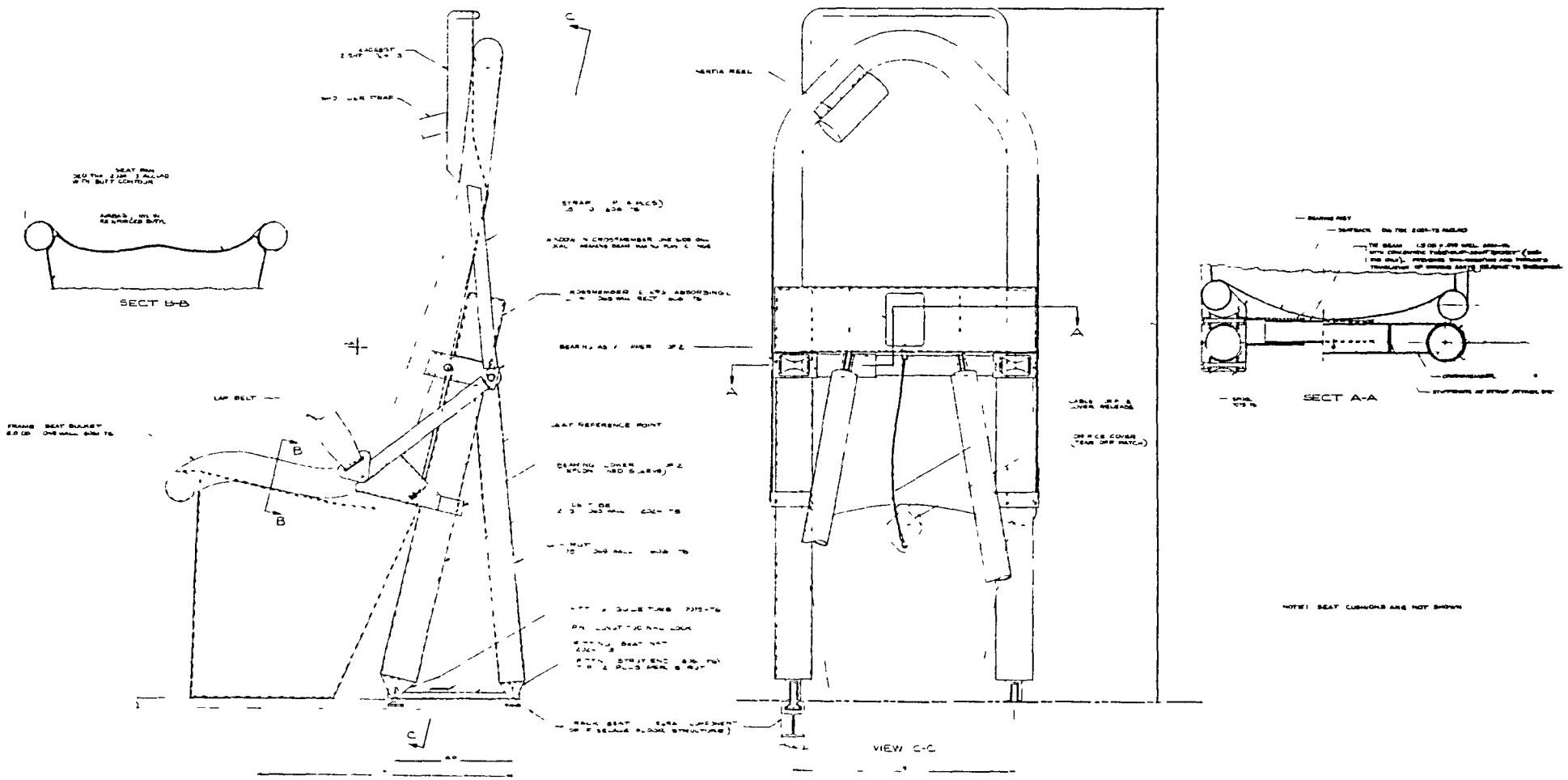

Figure 2. Preliminary air bag-equipped seat, Drawing No. SK10078.

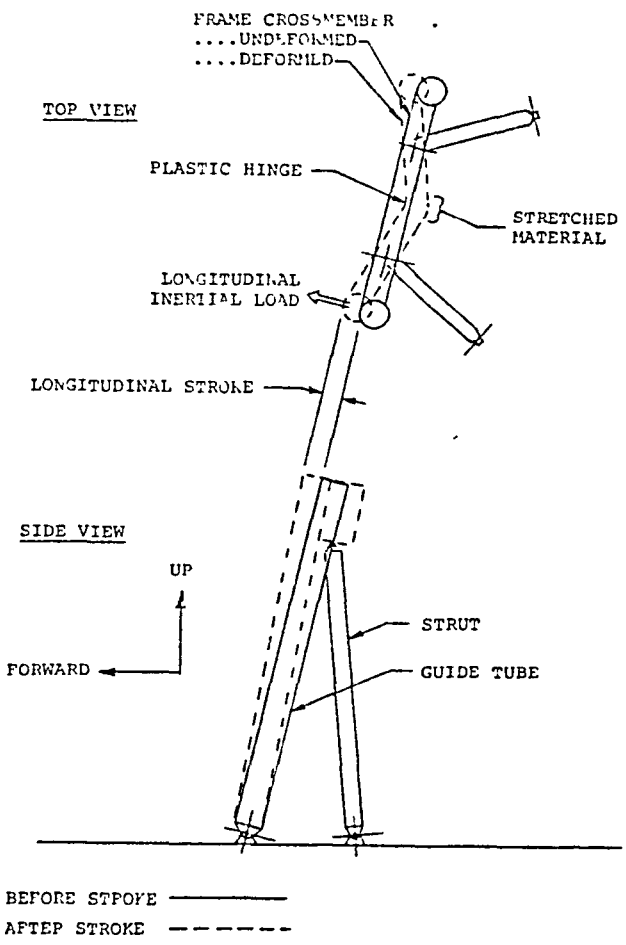

Figure 3. Operation of energy-absorbing crossmember for preliminary air bag-equipped seat.

Thus, the sliding friction of the sleeve bearings does not contribute significantly to the vertical limit load.

The tubing construction around the periphery of the moving portion of the seat shown in Figure 2 provides a more reliable means than that shown in Figure 1 for carrying all of the possible load combinations that could be subjected upon it by the occupant inertial load in the different loading configurations.

Stress Analysis. - As with the bellows-equipped design, the frame for the air bag-equipped design was originally sized on the basis of hand calculation of the loads and stresses and then verified and refined by use of the finite element STARDYNE program available from Control Data Corporation. Stresses in the structural members of this design can be found in Table 3 with the members identified in Figure 4.

Discussion. - This seat design demonstrates an inherently more efficient structure and is recommended for use with either the bellows or the air bag type of underseat energy absorber. The frame design for the final seat system design, found in a later section of this report, is the same as for the preliminary air bag-equipped seat with the exception of the longitudinal energy-absorbing crossmember mechanism.

TABLE 3. FRAME STRESSES OF AIR BAG-EQUIPPED SEAT, CALCULATED BY FINITE ELEMENT COMPUTER ANALYSIS

Member Number	Minimum Margin of Safety	Critical Loading	Critical Stress
1	+.64	Combined	Bending
2	+.17	Combined	Bending
3	+.05	Combined	Bending
4	+.12	Combined	Bending
5	+1.12	15 G Forward	Bending
6	-.06	Combined	Bending
7	-.20	Combined	Bending
8	+.32	15 G Forward	Tension
9	-.01	Combined	Tension
10	+4.01	Combined	Bending
11	+3.96	10 G Lateral	Bending
12	+.96	10 G Lateral	Bending
13	+.09	Combined	Bending
14	+.08	Combined	Bending
15	+.40	Combined	Bending
16	+3.83	15 G Forward	Bending
17	+.43	15 G Forward	Bending
18	+.47	Combined	Tension
19	+.00	Combined	Bending
20	1.64	10 G Lateral	Bending
21	+.05	15 G Forward	Bending
22	-.05	Combined	Bending
23	+.12	Combined	Bending
24	+1.99	10 G Lateral	Bending
25	+.01	Combined	Bending
26	+1.69	10 G Lateral	Bending
29	+.06	Combined	Bending
30	+.53	Combined	Bending
31	-.09	Combined	Bending
32	+.89	10 G Lateral	Bending
33	3.33	Combined	Bending
34	1.42	Combined	Tension
35	5.26	10 G Lateral	Tension
36	.33	Combined	Bending

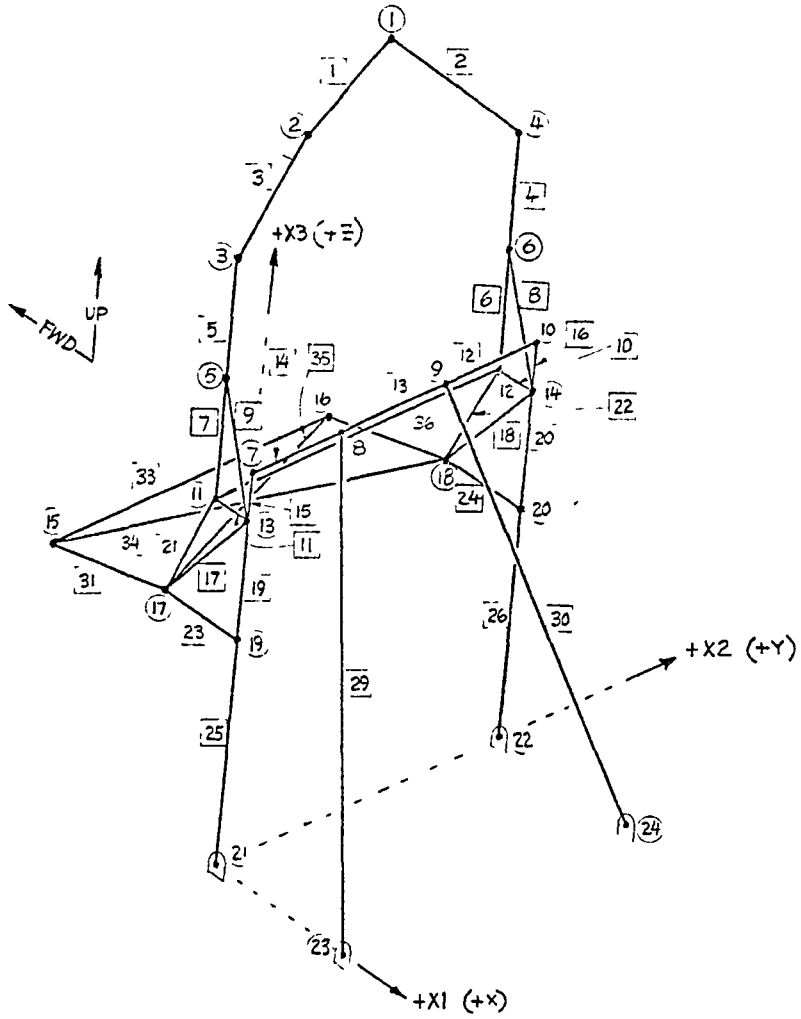

Figure 4. Structural model of preliminary air bag-equipped seat, showing member numbers referenced in Table 3.

ENERGY ABSORBER DEVELOPMENT

Required Characteristics

Briefly, the required characteristics of underseat E/As include the following:

- Near-constant limit load during plastic deflection
- High spring rate during initial elastic deflection
- Short crushed height
- Light weight
- Tolerant to end misalignment
- Tolerant to abuse (dents, punctures)
- Reliable, with low maintenance
- Manufacturable and reproducible
- Low cost.

Detailed Bellows Development

Preliminary Model Design. - An analytical model that considered the edge bending and the hoop stressing of a circular convoluted bellows as the bellows deforms was developed. The hoop stress results from the outer diameter enlarging and the inner diameter contracting as the bellows is compressed. To take advantage of the hoop stress, the convolutions were made relatively large in comparison with the diameter of the bellows. In the samples fabricated for preliminary testing, variations in convolution size, wall thickness, and overall bellows diameter were provided in order to check the analytical model and to provide a range of samples from which the correct design for the final models could be interpolated.

The material chosen for the preliminary bellows models was 6061 aluminum. This material was chosen because of its availability, formability, and weldability. Also, it can be heat treated to relatively high strength/weight ratios. Some models were heat treated to the -T4 temper, some to the -T6 temper, and one was left in the original annealed condition.

Most of the preliminary models were subscale, approximately half size, and two were full-scale. All were comparatively short in relation to their diameter; they represented short segments taken from the middle of the longer bellows. Two and one-half complete convolutions were included in the length of each model.

Preliminary Model Tests. - Results of the preliminary model tests provided useful but somewhat inconclusive information on the parameters that affect the bellows limit load. The bellows had been fabricated from convolution segments in the shape of short truncated cones that were welded to each other at their edges. During the bellows tests, many of the welds, especially on the subscale and thinner-walled models, broke. This relieved much of the stiffness that otherwise would have been gained by bending at the convolute edges. It was discovered later, during the final model test cycle, that these preliminary models were not satisfactorily representative of the final design for another reason: the close proximity of the end constraints to the midsection of the preliminary models prevented a peculiar type of wave-shape buckling that occurred in the final full-length models. Nevertheless, the preliminary models showed that the design at least was within reason. One model in particular, fabricated from 1.3 mm (0.050 in.)-thick 6061-T4 with a 30.5 cm (12 in.) outside diameter, a 90 degree included convolution angle, and 2.54 cm (1.0 in.) convolution segment length, produced a limit load of 13344 N (3000 lb) and maintained that limit load almost constant while being crushed to 25 percent of its original height.

The included angle between adjacent bellows segments was a parameter that was not varied in the tests. The 90-degree included angle used was judged to be an acceptable compromise between lesser angles, which might have caused unpredictable local buckling of the straight convolution segments, and greater angles, which might have increased weight and/or reduced strength. Uniform, predictable folding of the segments is required to ensure that the bellows can stroke to its fullest possible extent and thus reach a short crushed height. Convolutions of triangular rather than sinusoidal shape were chosen because it was believed that this would minimize the elastic deflection portion of the load deflection curve.

Design of Full-Scale Bellows Models. - Two full-scale model cycles were conducted: the planned one in May 1977, and a subsequent, unscheduled test cycle in August to improve upon the generally poor performances of the previous models.

The design of the full-scale models for the May test was based upon a theoretical model, which had been developed for the preliminary models, with corrections applied to compensate for the percentage by which the actual loads were observed to exceed the calculated loads; that was approximately 50 percent.

Bellows of 6061 aluminum, heat-treated to both the -T4 and -T6 temper had been built in the preliminary model cycle. The -T4 temper models had exhibited more uniform, flat load plateaus. There was a good deal of uncertainty about the performance of the -T6 temper preliminary models because of the greater amount of weld

breakage that occurred with them than with the -T4 temper models. However, heat-treated to the stronger -T6 temper, the bellows could be made from a 30 percent thinner material for an attractive weight savings. Therefore, bellows of both -T4 and -T6 tempers were provided in the final model phase according to Part Numbers SK10082-1 through -5 shown in Figure 5.

The final bellows models were of one-piece construction without the troublesome welds that broke during the first model phase. The final models were fabricated by spinning truncated sheet metal conical blanks over a wooden collapsible form. Several different wall thicknesses of bellows were tried in the final model cycle in order to bracket the desired limit load. This was necessary because of the uncertainty that remained about how well the analytical model would predict the behavior of the final bellows models and also because of the incremental sizes that were available in the sheet stock from which the bellows truncated cone starter blanks were made.

The tests in May showed that the bellows were unsatisfactory because their static loads were less than half of what was desired. Therefore, an unscheduled model build-and-test cycle was conducted in August to try again to demonstrate the feasibility of the bellows as an underseat E/A. The reasons for the poor performance of the models tested in May and the rationale behind the modified designs built and tested in August are covered in the Discussion section of this report.

Detailed Air Bag Development

Design Analysis. - Several different air bag shapes were investigated by means of a computer model, printout examples of which can be found in Appendix C. The computer program simulates the crash performance of the air bag by incrementing the time variable in .001 sec intervals, and, at each increment, by calculating and integrating all dynamic processes. Some interesting discoveries were made by the use of this program. For instance, an air bag of simple cylindrical shape (with a fixed orifice size) allows the pressure to decay so rapidly, as the seat velocity slows during the end of the stroke, that the seat cannot be decelerated fully and bottoms out with considerable residual velocity.

A bell-shaped air bag was discovered to be inherently better than a cylindrical air bag for maintaining the decelerative force level as the seat slows to a halt. The increasing area of the bell-shaped air bag near the end of the stroke acts to compensate for the diminishing pressure, the product of the two being force. At the beginning of the stroke of the bell-shaped air bag, the small end of the air bag has a relatively small area that requires a relatively high charging pressure in order to provide the force level needed for the desired limit load. Then, as the air bag begins to

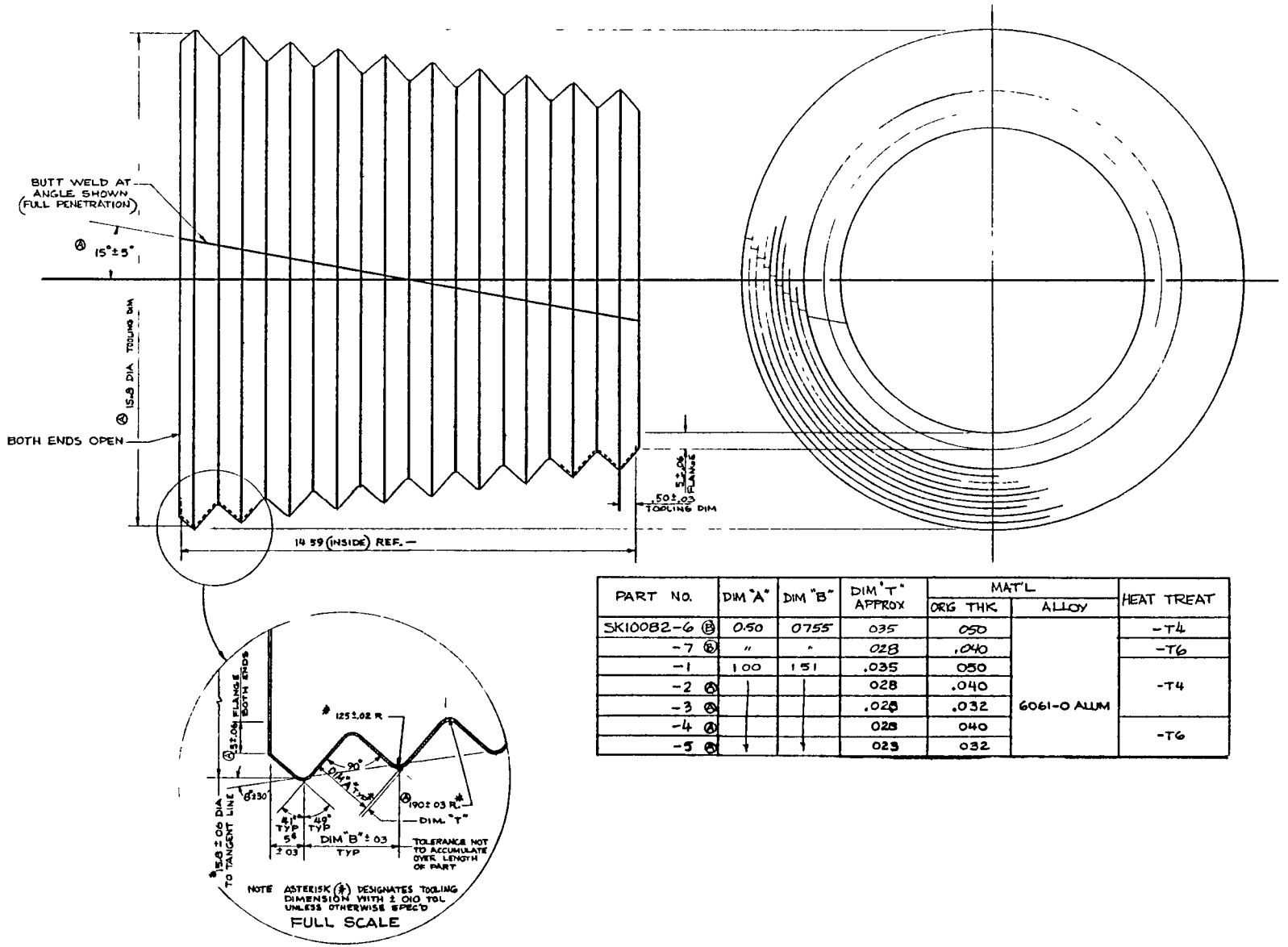

PART NO.	DIM "A"	DIM "B"	DIM "T" APPROX	MAT'L ORG THK	MAT'L ALLOY	HEAT TREAT
SK10082-6 Ⓑ	0.50	0755	035	050	6061-0 ALUM	-T4
-7 Ⓑ	"	"	028	.040		-T6
-1	1.00	1.51	.035	050		-T4
-2 Ⓐ	↓	↓	028	.040		
-3 Ⓐ			.028	.032		
-4 Ⓐ			028	040		-T6
-5 Ⓐ			028	032		

Figure 5. Convoluted bellows energy absorber.

stroke, the orifice opens up and allows the air to begin escaping. However, the large volume still remaining in the bag relative to the escape rate maintains the pressure in the bag during this part of the stroke. The relative velocity between the ends of the air bag very quickly reaches a peak near 20 ft/sec, which is the velocity for which the orifice is sized to maintain constant pressure within the air bag. During the last 5 in. of stroke, as the relative velocity between the ends of the air bag slows down, the pressure begins to decay because the diminished rate of contraction of the volume does not keep pace with the flow out of the orifice. It is over this portion of the stroke that it is desirable to rather abruptly increase the air bag diameter in order to compensate for the decaying pressure. The shape of this section of the air bag was adjusted with the computer model by trial and error in order to maintain a constant force level over the greatest stroke.

Another air bag shape, a truncated cone the same shape as the final bellows models, also was investigated. This shape held particular interest because of the possibility of designing a hybrid system consisting of a very thin-walled, pressurized bellows that could combine the advantages of both the bellows and the air bag. Its conical shape would serve to maintain the limit load during pressure decay somewhat like the bell-shaped air bag although not optimized to the same degree. A lower charging pressure would be permitted in the conical air bag because the area of its small end is larger than the area of the bell-shaped air bag. The conical shape can be manufactured more readily because of its simplicity. The conical and bell-shaped air bag designs are shown in Figures 6 and 7.

Samples of both the bell-shaped and conical air bag were built for testing in the final test phase. The material from which they were constructed was 0.25 mm (.010 in.)-thick Kevlar impregnated and sealed with polyurethane elastomer to a total thickness of approximately 0.51 mm (.020 in.). The Kevlar fabric properties are as follows: weight = 0.17 kg/m^2 (5.0 oz/yd^2); linear tensile strength = 1140 N/cm (650 lb/in.); tensile modulus = 4.5 x 10^{10} Pa (6.5 x 10^6 psi). The bell-shaped air bag weighs 0.425 kg (15 oz) and the conical weighs 0.397 kg (14 oz). The high strength and low elongation properties of the Kevlar fabric made this low weight possible; however, the relatively great rigidity of the air bag membrane walls led to a problem described in the Discussion Section of this report.

Orifice Design. - The purpose of the orifice is to allow expulsion of the gas within the air bag as the internal volume contracts during the energy-absorbing stroke. It must be sized

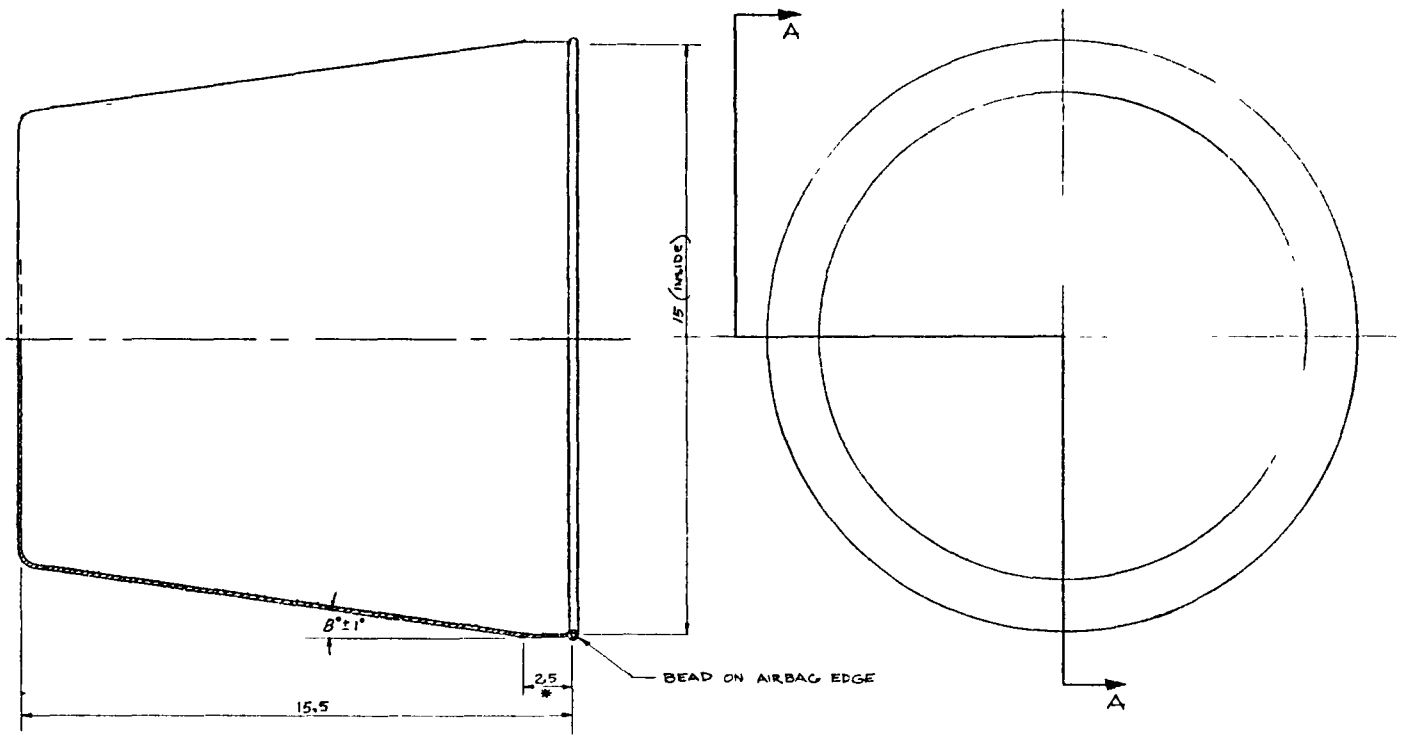

Figure 6. Conical air bag.

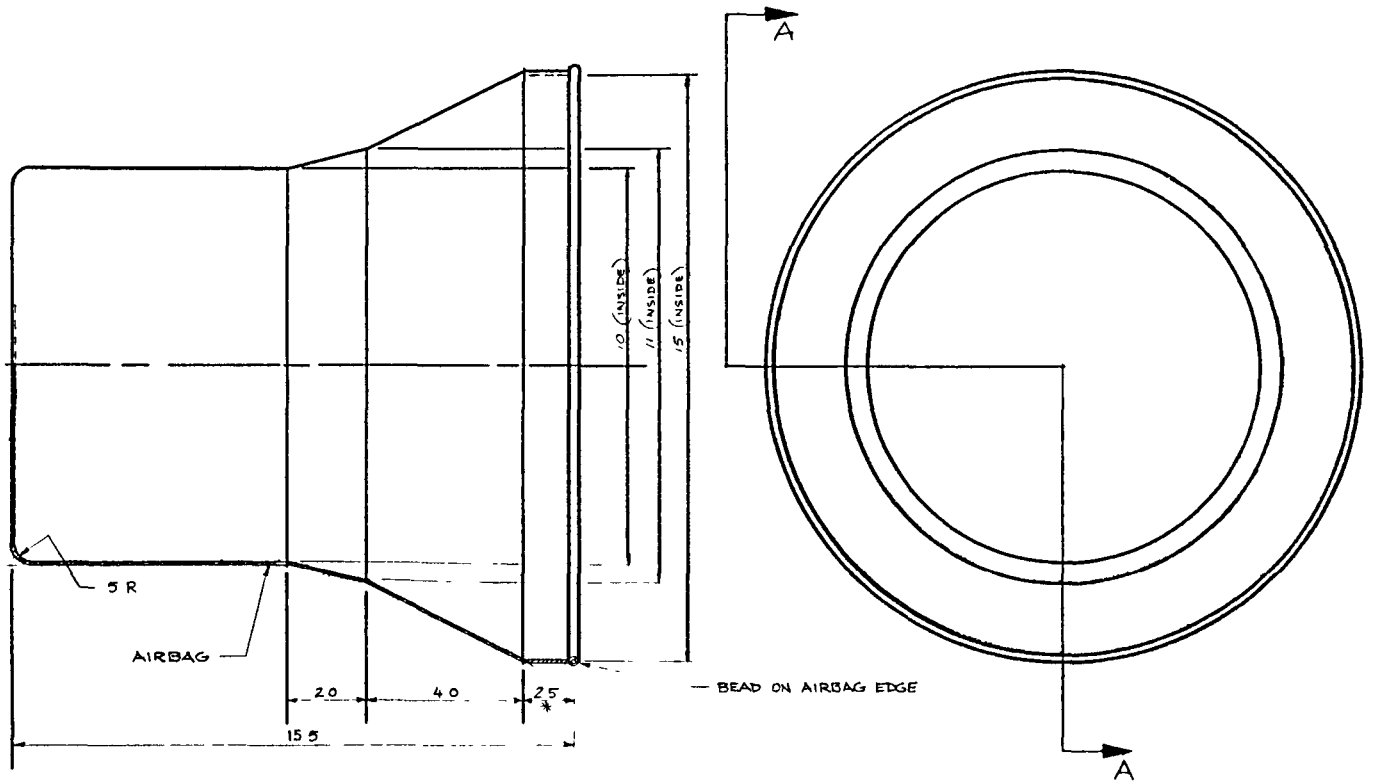

Figure 7. Bell-shaped air bag.

properly to maintain the correct internal pressure. Two basic types of orifice mechanisms are possible:

- A fixed orifice, sealed by a cover that is released at the start of the stroke.
- A variable orifice, whose degree of opening is controlled by some parameter such as time, deceleration, velocity, or stroke.

A deceleration-controlled variable orifice was considered and would be ideal because the escaping air would be automatically throttled by the orifice mechanism to maintain the required deceleration for any occupant weight. However, such a device would require a very large orifice size, very light weight, and very high frequency response -- all in a compact package. To develop such a device would require a development effort outside the scope of this project.

Another obvious type of variable orifice would be one that is pressure controlled, operating like a pressure relief valve. It would be nearly as complex and cumbersome as the deceleration-controlled orifice and would have an additional disadvantage: it would allow some pressure to escape at high altitude, leaving insufficient pressure for crashes at low altitude.

A velocity-controlled variable orifice offers no advantage and would be no less complex or cumbersome than the types previously discussed.

A stroke-controlled variable orifice may be practical. An orifice located on the moving portion of the seat could be obstructed by a baffle facing it on the fixed seat frame. The baffle could be contoured to obstruct the orifice opening more over the last portion of the stroke, thus compensating for the tendency for the pressure to decay during that time.

All variable orifices, with the possible exception of the stroke-controlled type, suffer from the same problem: complexity. Careful attention to frequency response and critical damping would be necessary in the design of such a device in order for the device to be useful during its transient operating span of only 100 ms.

The orifice configuration chosen for this project was the simple fixed orifice, which is sealed by an orifice cover until the stroke begins. The same parameters discussed above could have been used as methods to release the orifice cover. The method chosen was that the orifice cover be released after the seat stroked a specific distance. This was accomplished simply by locating the orifice at the top of the air bag on the stroking portion of the

seat and connecting the orifice cover trip mechanism to the fixed frame. Relative motion between the moving portion of the seat and the fixed frame at the commencement of stroking provides positive release of the orifice cover after a predictable and repeatable stroke. Figure 2 shows an orifice configuration that could be used on a production seat. The orifice cover is a "patch" on the air bag which is torn off by a cable connecting it to the fixed portion of the seat frame.

For test purposes in this development project, a reusable orifice cover mechanism was required. A means of substituting different sized orifices during a series of tests to determine the optimum orifice size also was needed. To meet these requirements, the orifice mechanism shown in Figure 8 was used. The orifice cover in this design is an 11.4 cm (4.5 in.)-diameter disk sealed by an O-ring into a counterbore in the upper air bag mounting plate. The cover is hinged on one side and held down on the other by a toggle clamp. As the upper air bag mounting plate begins to stroke, the handle of the toggle clamp is lifted by a cable attaching it to the nonmoving portion of the test fixture. This releases the orifice cover, which is then blown open by pressure within the bag, exposing the orifice beneath the orifice cover. The orifice is located in a 1.6 mm (.063 in.)-thick plate fastened by four screws to the bottom of the counterbore beneath the orifice cover. Nine orifice plates with orifice diameters ranging from 4.2 to 8.5 cm (1.64 to 3.34 in.) were prepared prior to the air bag tests for substitution in case the predicted orifice size was not correct.

The adjustment of the orifice cover release cable caused the orifice cover to be released after approximately 3.2 cm (1.25 in.) of stroke. The pressure rise during this portion of the stroke is practically insignificant because of the small percentage change in volume. By waiting until the stroke is underway before releasing the orifice cover, the relative velocity between opposite ends of the air bag, and thus the rate of contraction of the volume, is allowed to reach a level that can sustain the pressure near the desired value during discharge from the orifice. If the orifice cover were released at the very onset of the stroke, the pressure would decrease significantly before the relative velocity could build up sufficiently to sustain the pressure.

The orifice-release mechanism just described provided the flexibility required for the repeated testing that was performed. The hardware, of course, is much too heavy to be recommended for an actual production seat, but the same dependable principle of operation can be found in the lightweight orifice-release mechanism of Figure 2.

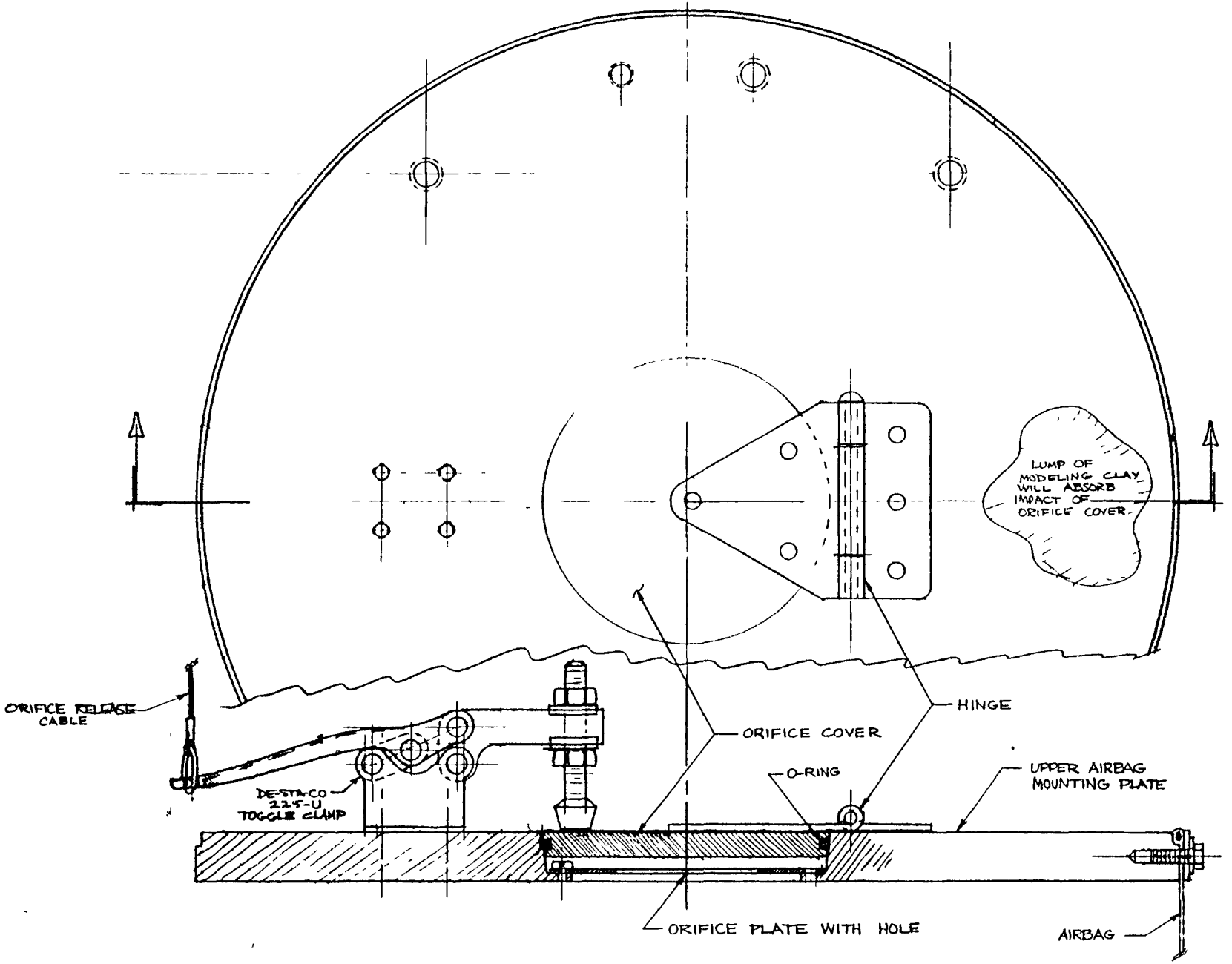

Figure 8. Orifice mechanism used for dynamic air bag tests.

TEST PROGRAM DESCRIPTION

Introduction

The underseat E/As were dynamically tested in a drop tower using a fixture that simulated the vertical stroke of an actual seat. All the air bag tests were dynamic with the exception of one static test performed to evaluate the buckling strength of the air bag membrane itself. The bellows were statically tested using a standard combination tensile-and-compression test machine at a rate of 8.5×10^{-4} m/sec (2 in./min). One bellows was dynamically tested in the same manner as the air bags in order to determined the rate-dependence of the bellows limit load. Another bellows was shear tested to determine its contribution to the longitudinal strength of the seat.

The objectives of the test program are summarized as follows:

- To record and evaluate the load/stroke histories of each of the E/As for applicability to attenuation of the 95th-percentile, survivable, vertical crash pulse.
- To determine what contribution the bellows-type E/A makes to the longitudinal stiffness of the seat system.
- To determine what effect the shear displacement of the bellows ends has upon the bellows' ability to perform its primary vertical stroke.
- To determine the optimum orifice sizes required by the air bag to decelerate the 50th-percentile weight occupant.
- To determine the accuracy of the air bag computer simulation and the bellows theoretical model as design tools for future refinement of the E/As.

Test Equipment and Procedure

Dynamic Tests. - The drop cage shown in Figure 9 with the test fixture bolted securely to it was dropped from a height of 5.33 m (17.5 ft) onto a pyramidal target of paper honeycomb. The shape of the honeycomb stack shown in Figure 10 was determined during preliminary calibration drops in order to satisfy the following desired conditions as set forth in Reference 1:

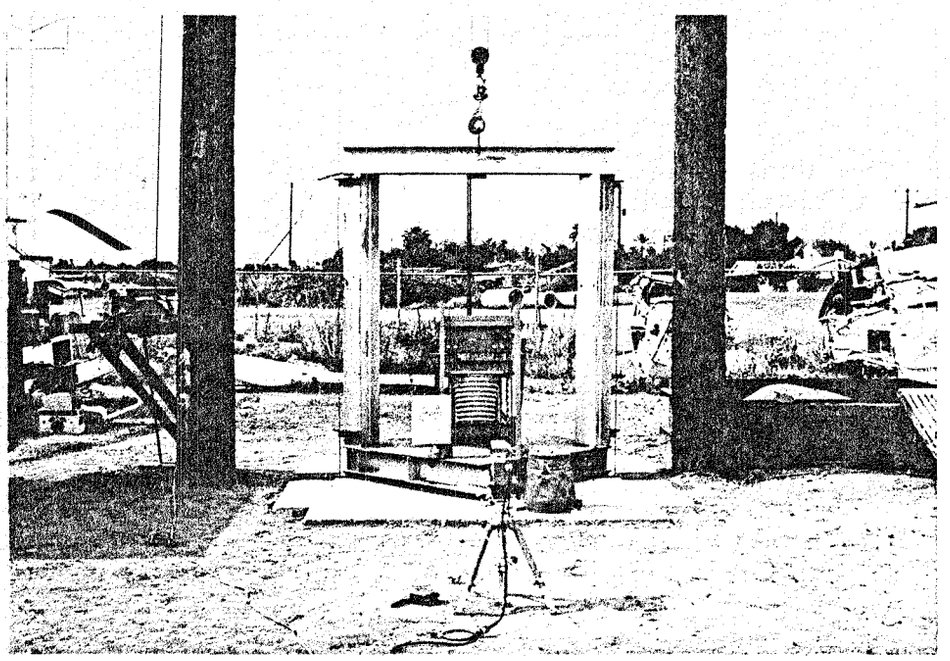

Figure 9. Drop cage at base of tower.

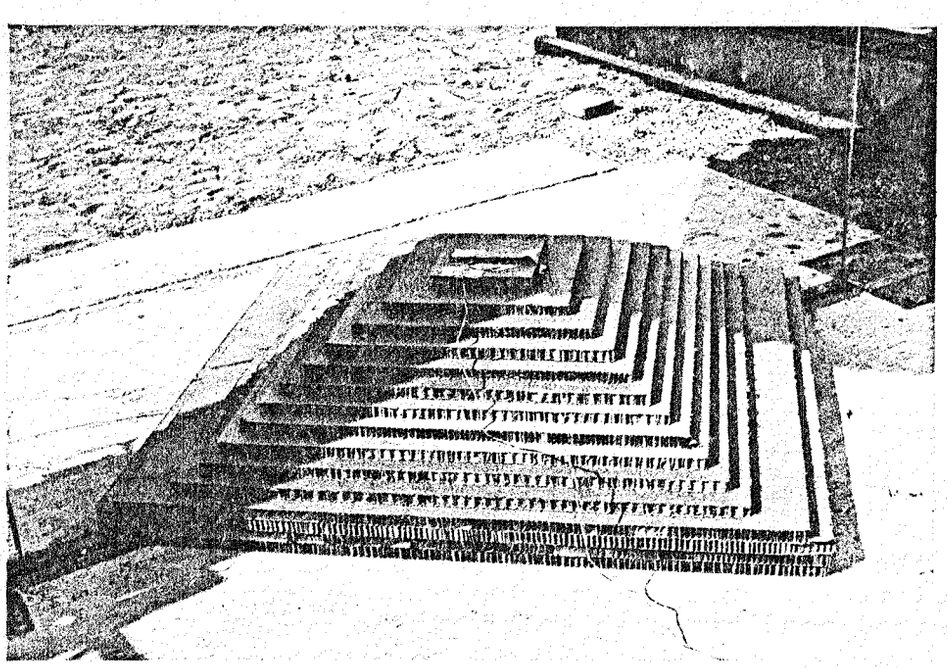

Figure 10. Paper honeycomb impact target.

- Vertical velocity change of 12.8 m/sec (42 ft/sec), including rebound.
- Pulse duration of 0.054 sec.
- Triangular pulse shape with peak occurring between .022 sec and 0.043 sec.

The paper honeycomb used was type KP1/2-80(0) EDF purchased from Hexcel Corporation in California.

The dynamic test fixture is shown in Figure 11. The fixture was made of steel channel in order to be durable enough to withstand repeated drop tests; it was not intended to represent an actual seat construction. The moving portion of the test fixture was constructed of 1.3 cm (0.5 in.)-thick steel plate to add the weight necessary to simulate the weight of the 50th-percentile occupant. The primary purpose of this fixture was to guide the E/A test specimen during the dynamic test along the same path as would an actual seat. The secondary purpose of the fixture was to provide a method of imposing shear deformation on the bellows to simulate a longitudinal stroke of the seat.

In the dynamic test, the longitudinal stroking capability of the fixture was locked out by bolting the upper side rails to the front uprights. In this configuration, the guide tubes of the fixture were maintained at an angle of 13 degrees from the vertical. The moving portion of the fixture traveled along these guide tubes on rollers. It weighed 62.6 kg (138 lb), very nearly the 50th-percentile total effective weight of 62.1 kg (137 lb). Either a bellows or an air bag E/A could be mounted using the proper interface adapter plate between the moving portion of the fixture and the fixture's lower E/A mounting plate.

Most of the weight of the moving portion of the fixture was concentrated in the weight plates near the outboard edge of the fixture. With this design feature, if the available stroke was exceeded for some reason, the weight plates would impact heavy gussets on the fixed portion of the fixture without damaging the test fixture or the air bag sample.

An accelerometer on the upper adapter plate and another on the lower E/A mounting plate sensed the attenuated acceleration and the input acceleration along the stroking direction of the E/A. Another accelerometer mounted on the fixed portion of the test fixture measured acceleration in the vertical direction to monitor the input crash pulse. A pressure transducer monitored pressure within the air bag. Signals from the pressure transducer and the accelerometers were amplified and recorded on an oscillograph. The time base reference was provided internally by the oscillograph, and calibration test signals of known amplitude were recorded prior

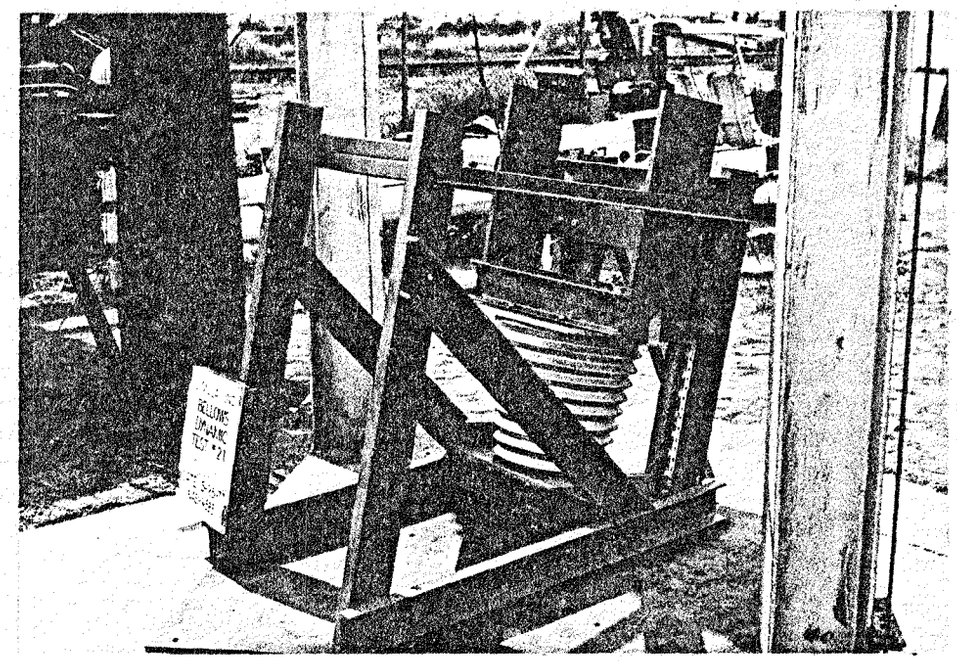

(a) Side view

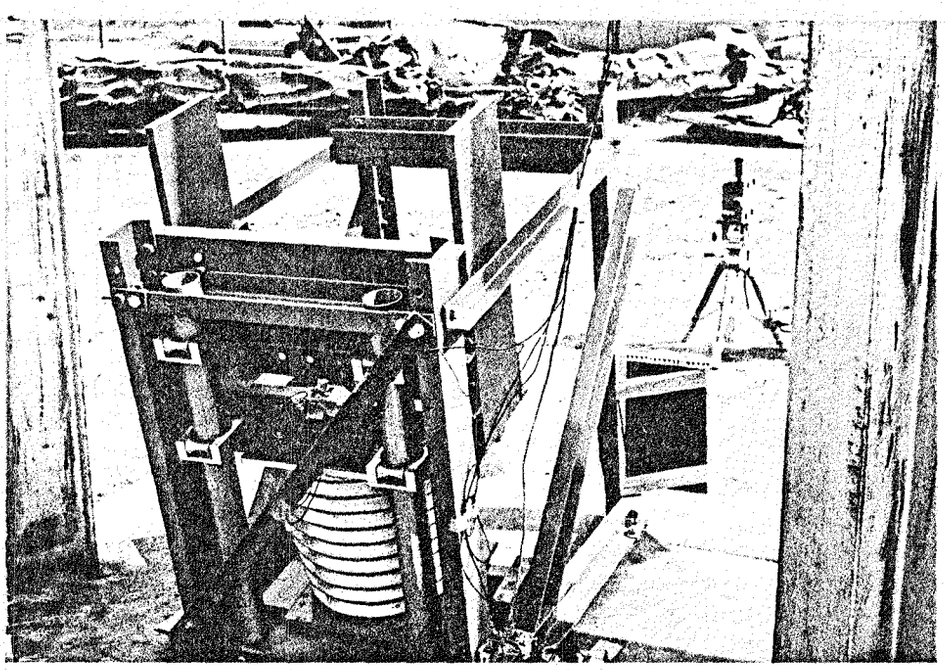

(b) Rear view

Figure 11. Dynamic test fixture.

to each drop test to provide the reference to which the data could be scaled. A high-speed (500 frames per second) motion picture camera recorded the progressive folding of the air bags and bellows during their strokes. Still photographs were taken before and after each drop test. A complete list of instrumentation can be found in Table 4.

TABLE 4. DYNAMIC TEST INSTRUMENTATION

Instrument	Quantity	Range or Limit	Use
Oscillograph, CEC Model 5-124 with Galvanometers, CEC Model 7-316	1 4	64 in./sec 1000 Hz	Record three accelerometer channels plus one pressure transducer channel.
Accelerometers, Endevco Model 2235C	1	0-100 G	Measure input deceleration vertically.
	1	0-100 G	Measure input deceleration along 13° stroking angle of the seat.
	1	0-100 G	Measure attenuated deceleration of moving portion of fixture along stroking direction.
Charge Amplifier, Endevco Model 2713A	3	-	Amplify accelerometer signals.
Pressure Transducer, Taber Model 227	1	0-50 psi	Measure internal pressure in air bag.
Signal Conditioner, Alinco Model SAM-1	1		Amplify pressure transducer output.
Load Cell, BLH Model U-1	1	0-2000 lb	Measure overturning load during static shear test. Alinco Model SAM-1 used as signal conditioner.
High-Speed Camera, LOCAM with 24 mm lens. Film, 16 mm Kodak Ektachrome 7241 EF	1	500 frames per second	Record visual events of stroke.

Static Tests. - The static tests were performed in May on an Instron tensile and compressive test machine shown in Figure 12. The rate of loading was 8.5×10^{-4} m/sec (2.0 in./min), and the load was continuously monitored and recorded on a strip chart recorder, which is a part of the test machine. After a stroke of 5.1 cm (2.0 in.), and again at 30.5 cm (12.0 in.), the loading direction was temporarily reversed to obtain a plot of the unloading spring rate of the bellows. The static tests performed in August were done on a Baldwin tensile and compressive test machine shown in Figure 13. Continuous strip chart recording was not available; therefore, load readings were taken at .32 cm (0.125 in.) increments during the initial 2.5 cm (1.0 in.) of stroke and at 1.3 cm (0.5 in.) increments thereafter.

In the static shear test, the dynamic test fixture provided the means for simulating the effect upon an underseat E/A of the seat stroking longitudinally, or pitching forward. This was accomplished by unbolting the upper side rails from the upper uprights, loosening the bolts securing the frame that supports the guide tubes, and installing a jack and a load cell between the upper front and upper rear of the fixture. Operation of the jack caused the guide tube support frame to pitch forward, misaligning the bellows ends. The force required to impose this motion was monitored by means of the load cell and translated into terms of torque by multiplying the load by the moment arm. This torque represents the contribution that the bellows makes to prevent the seat from pitching forward during longitudinal loading.

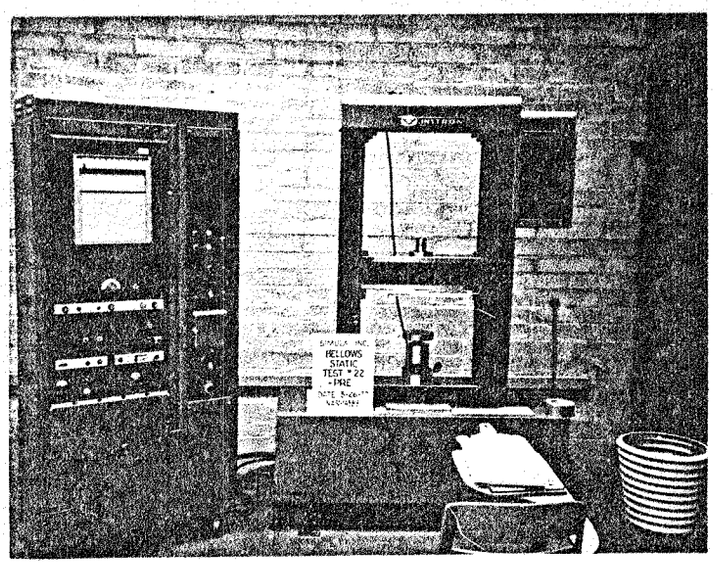

Figure 12. Static test facility, Instron.

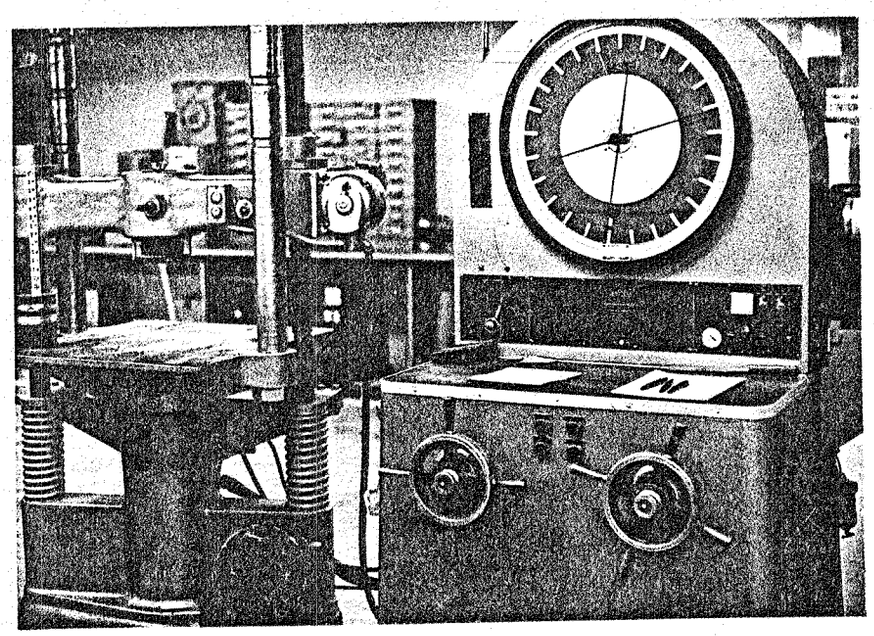

Figure 13. Static test facility, Baldwin.

TEST RESULTS

During the regularly scheduled test series in May 1977, the air bags performed well, but the bellows did not reach the limit loads expected. Additional bellows models were built to try to increase the limit load. The additional models were tested in August and demonstrated more favorable strength/weight ratios.

The air bags were dynamically tested in a drop tower. The bellows were statically tested, with the exception of one sample that was dynamically tested to determine loading rate sensitivity. The results of all tests are summarized in the following tables and graphs. Additional comments on the results can be found in the Discussion section.

Dynamic Test Results

A careful analysis of the oscillograph data plus correlation with observations of the high-speed films yielded the information documented in this section of the report.

The air bags, which performed in the dynamic tests almost as predicted by the analytic model, demonstrated their potential usefulness as underseat E/As. A summary of each dynamic test condition can be found in Table 5. The measured accelerations for each test are plotted in Figure 14. Pretest and posttest photos of the air bags are shown in Figure 15.

Test Numbers 1 and 10, in particular, limited the deceleration of the moving mass to 19 G and 21.9 G, respectively, which is close to the desired level of 14.5 G. Decelerations in all the air bag tests were somewhat higher than expected due to the buckling strength of the rather rigid air bag membrane and/or other resistances to motion, such as rolling resistance of the fixture. Test Number 3 with an orifice diameter of 4.8 cm (1.89 in.) maintained the pressure at the proper level during the majority of the stroke.

The acceptability of the bellows as an underseat E/A could not be determined from the dynamic test performed on it. It reached its design load with a little help from its loading-rate dependence. However, the test mass bottomed out with considerable residual velocity at the end of the 31.8 cm (12.5 in.) available stroke due to the slow buildup of load in the bellows E/A during the initial low-velocity portion of the stroke.

Static Test Results

During the regularly scheduled test program in May 1977, the bellows that were tested did not perform as expected. In the static tests, they provided less than half the desired limit load.

TABLE 5. SUMMARY OF DYNAMIC TEST CONDITIONS AND RESULTS

Test No.	Device Tested	Orifice Diameter cm (in.)	Charging Pressure kPa (psig)	Input Acceleration/Time History @ 13° Angle: Peak Acceleration (G)	Input Acceleration/Time History @ 13° Angle: Peak Time (sec)	Input Acceleration/Time History @ 13° Angle: Duration (sec)	Input Acceleration/Time History @ 13° Angle: Velocity Change m/sec (ft/sec)	Attenuated Acceleration/Time History: Peak Acceleration (G)	Attenuated Acceleration/Time History: Peak Time (sec)	Attenuated Acceleration/Time History: Max. Stroke cm (in.)	Attenuated Acceleration/Time History: Max. Stroke Time (sec)
1	Bell-Shaped Air Bag SK10083-1	5.54 (2.18)	168.9 (24.5)	46.0	.039	.067	13.72 (45.0)	19.0	.040	30.48 (12.0)	.100
2	Bell-Shaped Air Bag SK10083-1	4.17 (1.64)	172.4 (25.0)	46.0	.038	.065	12.65 (41.5)	22.0	.066	24.13 (9.5)	.091
3	Bell-Shaped Air Bag SK10083-1	4.80 (1.89)	172.4 (25.0)	49.2	.038	.066	14.23 (46.7)	23.4	.051	23.50 (9.25)	.084
10	Conical Air Bag SK10084-1	6.38 (2.51)	129.3 (18.75)	44.8	.037	.066	12.98 (42.6)	21.8	.054	25.40 (10.0)	.102
11	Conical Air Bag SK10084-1	5.54 (2.18)	172.4 (25.0)	45.4	.038	.066	13.56 (44.5)	24.7	.044	15.24 (6.0)	.076
12	Conical Air Bag SK10084-1	4.80 (1.89)	128.9 (18.7)	46.0	.037	.066	12.83 (42.1)	25.8	.060	16.51 (6.5)	.075
21	Bellows SK10082-1	-	-	44.2	.038	.063	12.56 (41.2)	40.7	.081	31.75 (12.5)*	.081

*Bottomed out.

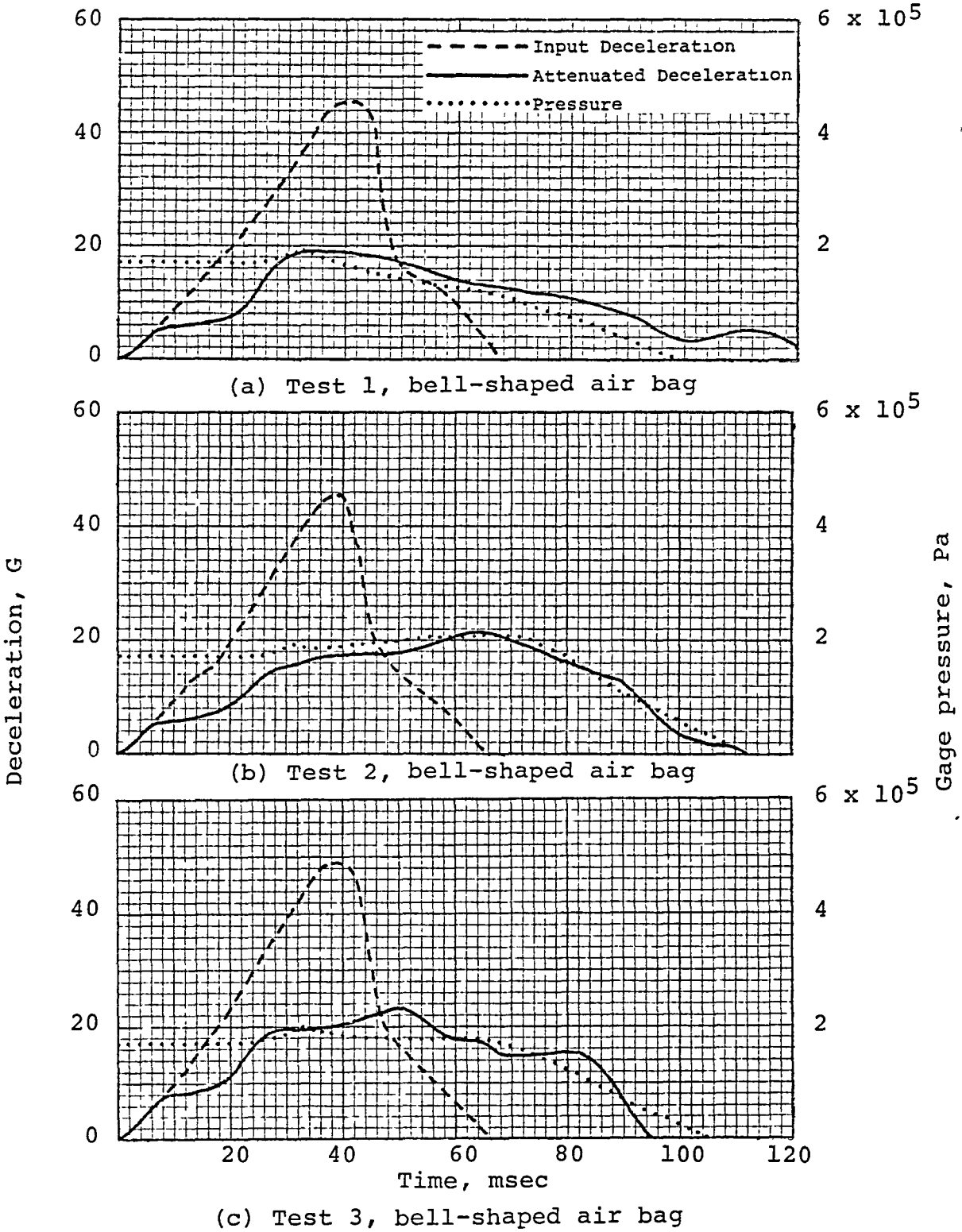

Figure 14. Dynamic test deceleration/time histories.

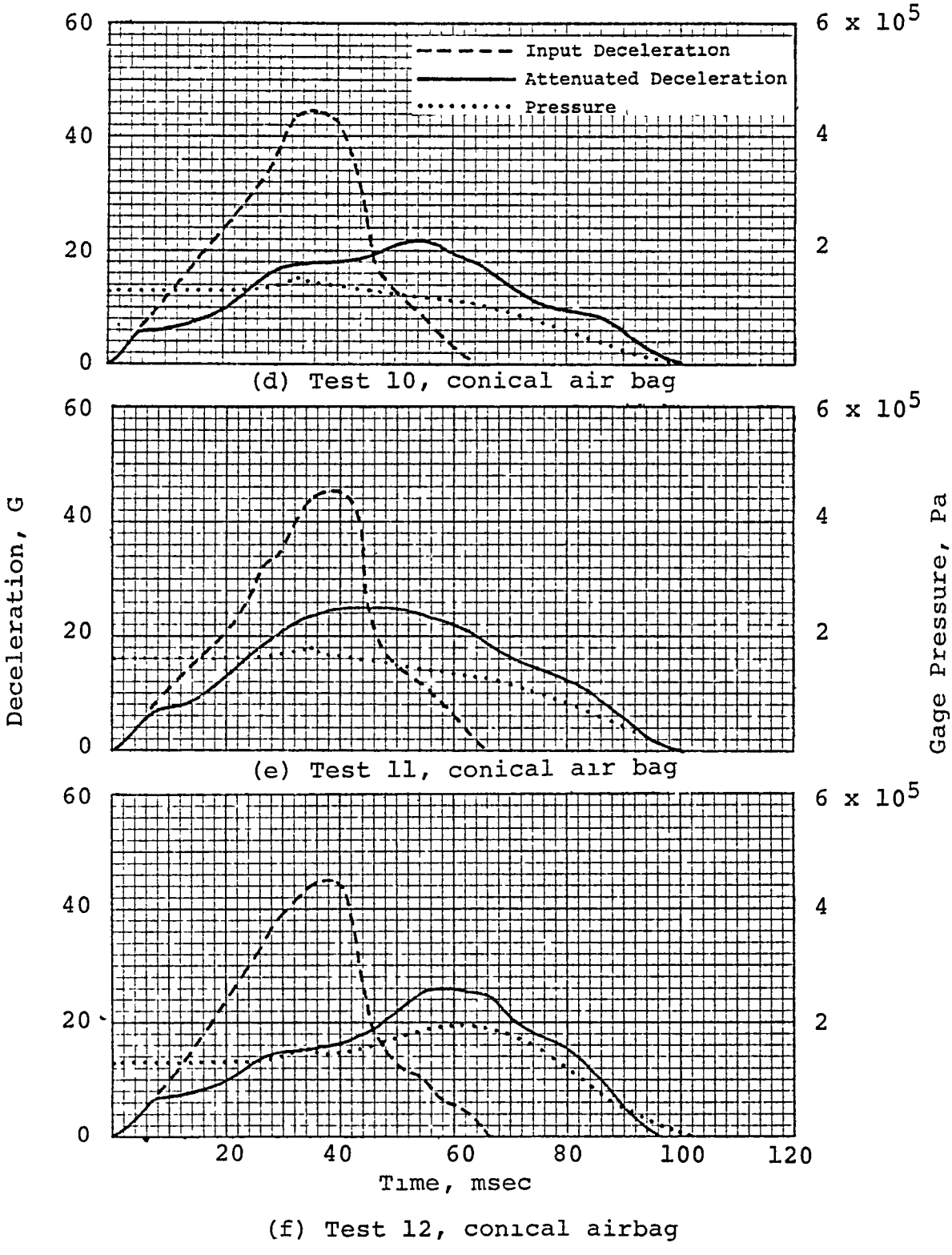

Figure 14. Dynamic test deceleration/time histories (contd).

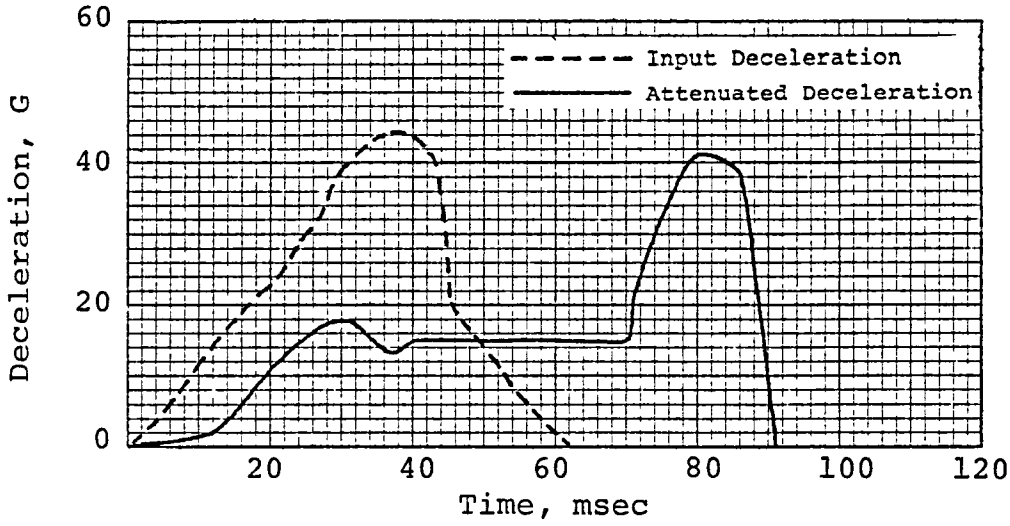

(g) Test 21, bellows

Figure 14. Dynamic test deceleration/time histories (contd).

Their strength/weight ratio was unfavorably low, and their low initial spring rate and high loading-rate dependence made inefficient use of the available stroke.

To correct these problems, an additional bellows fabrication-and-test cycle was performed in August 1977. The results of the August tests were much more encouraging and demonstrate that a favorable strength/weight ratio and stroke can be achieved by a bellows E/A.

Table 6 provides a list of tests performed, a description of the samples tested, and a brief summary of results. Load/deflection curves for the static-tested samples can be found in Figure 16. The performance of the shear-tested bellows can be found in Table 7.

In the static tests, it was hoped the bellows would stroke at a constant load of 8800 N (1987 lb). Tests 23, 24, 26, and 27, performed in May 1977, fell far short of this as can be seen on Figure 15. Only Tests 23 and 24 are plotted; Tests 26 and 27 have been omitted for clarity. Test 26 had almost the same load/ deflection curves as Test 23, and Test 27 had almost the same curve as Test 24.

In the static tests performed in August, two samples (Tests 32 and 33) stroked at near the desired load, and two others (Tests 30 and 31) stroked at a load nearly twice what was desired. The bellows of Tests 32 and 33 were of the same design tested in May but with stiffeners added to control the wave-shaped buckling that

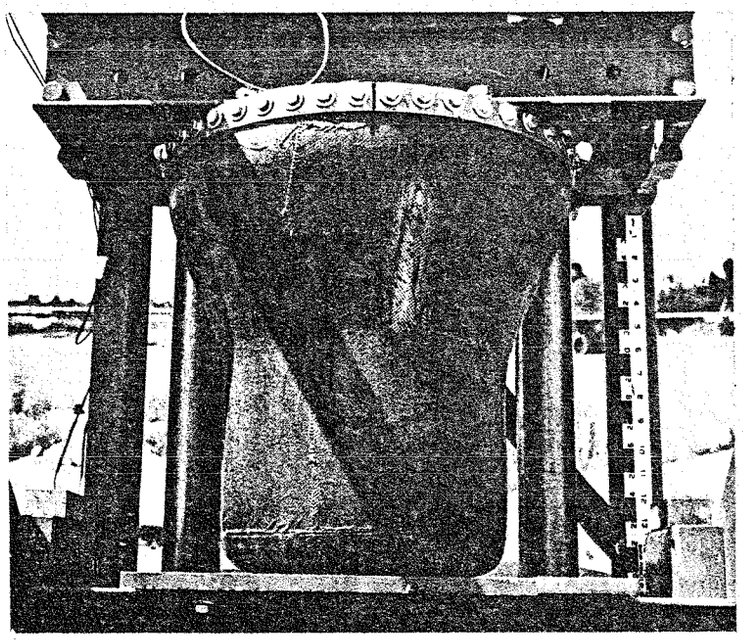

(a) Inflated bell-shaped air bag

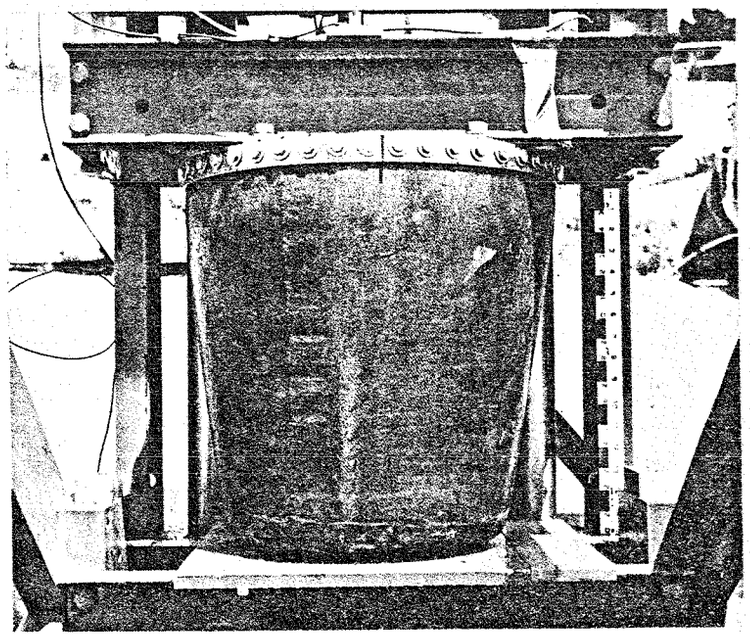

(b) Inflated conical air bag

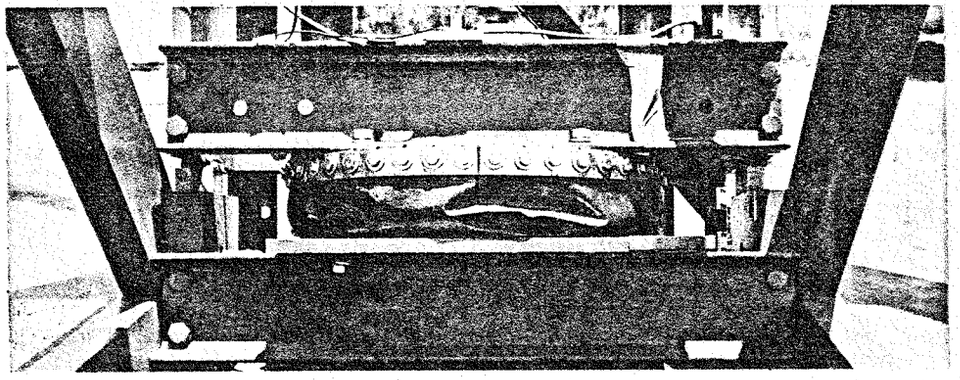

(c) Typical crushed condition

Figure 15. Air bag underseat energy absorbers.

TABLE 6. SUMMARY OF BELLOWS TEST CONDITIONS AND RESULTS

Test			Bellows Description			Results		
Number	Description	Month of Test	Part No.	Average Wall Thickness mm (in.)	Heat-Treat Aluminum Alloy 6061-	Weight kg (lb)	Average Load N (lbf)	Usable Stroke cm (in.)
21	Dynamic	May	SK10082-1	0.89 (0.035)	-T4	1.54 (3.4)	8900 (2000)	28 (11)
22	Shear		SK10082-1	0.89 (0.035)	-T4	1.54 (3.4)	See Table 7	
23	Static		SK10082-1	0.89 (0.035	-T4	1.54 (3.4)	3500 (790)	26 (10.2)
24	Static		SK10082-2	0.71 (0.028)	-T4	1.22 (2.7)	2500 (560)	26 (10.2)
26	Static		SK10082-4	0.71 (0.028)	-T6	1.22 (2.7)	3500 (790)	26 (10.2)
27	Static		SK10082-5	0.58 (0.023)	-T6	1.00 (2.2)	2500 (560)	26 (10.2)
30	Static	August	SK10082-7	0.71 (0.028)	-T6	1.13 (2.5)	16000 (3600)	30 (11.8)
31	Static		SK10082-6	0.89 (0.035)	-T4	1.41 (3.1)	19000 (4300)	17 (6.7)
32	Static		SK10082-3*	0.89 (0.035)	-T4	1.63 (3.6)	9500 (2100)	28 (11.0)
33	Static		SK10082-1**	0.58 (0.23)	-T4	1.59 (3.5)	8000 (1800)	26 (10.2)

*Stiffened by 1.6 mm (.063 in.)-diameter annealed aluminum wires, 15 on outside, 15 on inside. See Figure 20.
**Stiffened by 0.64 mm (0.026 in.)-thick 6061-0 aluminum sheets, 10 pieces on outside only. See Figure 21.

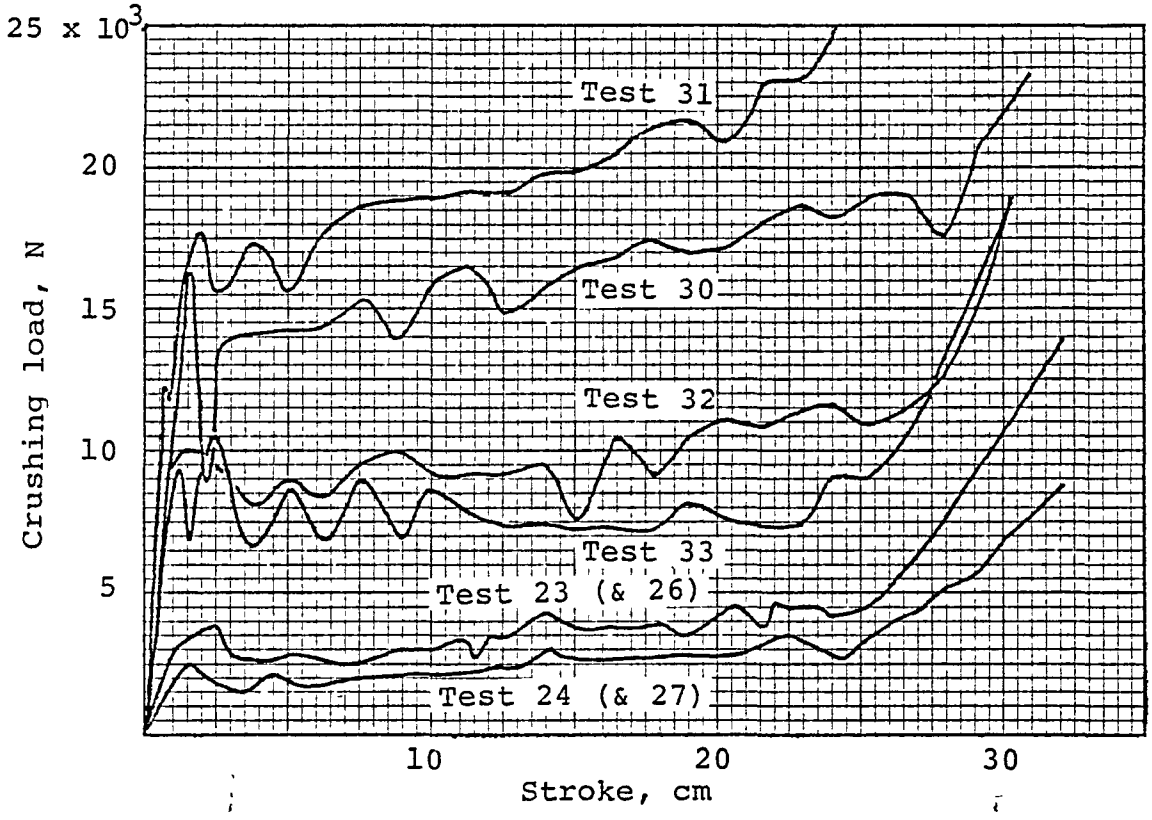

Figure 16. Bellows static load/deflection.

TABLE 7. SHEAR TEST

Angular Displacement (deg)	Overturning Torque N-m (ft-lb)
0	0 (0)
1	247 (182)
1.5	493 (364)
2	1015 (749)
4	1540 (1136)
6	1350 (997)
8	1525 (1125)

had previously relieved the hoop stresses. The bellows of Tests 30 and 31 had convolution sizes one-half the size of the previous models.

In the bellows shear test, the fixture frame was pitched forward by a mechanical jack with the force measured by a load cell. Then, the overturning torque was calculated from the force and is tabulated in Table 7.

When the overturning torque was removed, the fixture returned to an angular displacement of 6.5 degrees. Localized crushing at the small end of the bellows was the only damage sustained.

The final portion of the shear test, the axial compression test, was not conducted because the minor local damage would not have caused the performance in the static axial compression test to be any different than that of the other bellows. It was thought that more useful information could be obtained if the bellows could be reworked to increase its static limit load. Therefore, it was set aside for this purpose.

DISCUSSION

This section of the report describes the methods by which the data were analyzed, discusses results, and explains the significance of the results.

Analysis of Air Bag Test Data

The analysis was to proceed in two stages: first, the oscillograph acceleration traces were to be analyzed during the test and corrections were to be made to the orifice size in order to approach a 14.5 G acceleration level for the moving portion of the fixture. Second, a comparison of the actual air bag test results with the predictions of the analytic computer model was desired as a means of refining the computer model in order to create a tool for optimizing the future performance of air bags.

Desired results of the first part of the analysis were not wholly realized because of data interpretation problems and because it was not recognized that a portion of the load was being carried by the air bag membrane itself. However, Test Numbers 1 and 10 held the peak deceleration of the moving portion of the fixture to 19 G and 21.9 G, respectively, somewhat higher than the 14.5 G desired but close enough to demonstrate feasibility. All tests provided important data for the second part of the analysis.

In the second part of the analysis, the acceleration/time history of the moving portion of the fixture together with initial pressure, air bag diameter data, orifice size, temperature, and weight of the moving portion of the fixture were used as inputs to the analytic computer model. The coefficients in the analytic model were then refined to obtain agreement with the measured acceleration/time history of the moving portion of the fixture. As a further check on the accuracy of the accelerometer data and of the analytic model, the stroke integrated by the computer model was compared with measured stroke data obtained from the high-speed movies. The close agreement between the computed and actual strokes lends strong support to the accuracy of both the measured accelerations and the computer model.

The following refinements to the analytic model were required to obtain agreement with the measured accelerations and thus to provide a useful tool for optimizing future air bag performance: the flow coefficient, C, was increased from .6 to .75 for the conical air bag and from .6 to .85 for the bell-shaped air bag; a 5 G correction factor, K, was added to account for load that was apparently being carried by the air bag membrane itself and/or the resistance to motion of the moving part of the test fixture.

The probable cause for the difference between the two flow coefficients was that the bell-shaped air bag contained, upstream

from the orifice, a volume-filling spacer that the conical air bag did not have. The spacer was a disk of 36.8 cm (14.5 in.) diameter, 3.8 cm (1.5 in.) thickness, and with a 10.2 cm (4.0 in.) diameter hole in its center. Its purpose was to reduce the volume of the air bag, but it also had the undesirable side effect of guiding air more gradually (lower velocity gradient) toward the orifice, thus increasing the flow coefficient. The purpose of the volume-filling spacer was to shorten the effective length of the bell-shaped air bag to 33 cm (13 in.), which was the length and volume for which the shape of the bag had been designed.

To account for the dynamic crushing strength of the air bag, the correction factor, K, was assumed to be linearly dependent upon internal pressure and stroking velocity. The correction factor is of the form

$$K = \frac{P}{P_{max}} \frac{V}{V_{max}} K_1 \qquad (1)$$

where P is pressure, V is velocity, and K_1 is a constant. The equation can be found in the computer program of Appendix C in the statement following the comment card "calculate seat acceleration, GC." Correction factor K is called FC in the program.

The correction factor had to be pressure dependent because increased pressure stiffened the sides of the bag (the unpressurized bag was relatively easy to crush). Also, the correction factor had to be velocity dependent to account for the peak in the acceleration data that occurred during maximum relative velocity. The velocity-dependence was also indicated to a certain extent by the static test of the air bag, although the speed during the static test of 8.47×10^{-3} m/sec (20 in./min) was many orders of magnitude less than the 6.1 m/sec (20 ft/sec) reached during the dynamic test.

Some relationship other than linear is likely to be more exact than the linear relationship assumed for the correction factor. However, considering the experimental error, the relationship chosen appears adequate. In fact, its use produced very close agreement between predicted and experimental acceleration levels for Test Number 1 (see Appendix C). The accuracy of the analytic model was further substantiated by close agreement with the pressure transducer data and also with the stroke data obtained from the high-speed films. Actual measured stroke and pressure data together with acceleration data has been entered in pencil on the computer output of Appendix C.

The value for the term K_1 in equation (1), which gave the best agreement with results from Test Number 1, was 5.0. This same factor was applied to all the other dynamic air bag tests in order to provide a common base for test comparisons.

In order to obtain more information on the buckling strength of the pressurized air bag membrane, a static test of a bell-shaped air bag pressurized to 172 kPa (25 psig) was performed to detect any difference between the actual crushing load and the product of pressure times area. An Instron tensile test machine was used for this purpose at its maximum obtainable crosshead speed of 8.47 x 10^{-3} m/sec (20 in./min). The measured load was not conclusively higher than the product of pressure times area; however, each time the stroke was halted at one-inch intervals, an abrupt 3 percent drop in the load was noted. The following additional observations were made: 1) the buckling of the air bag appeared to progress much further ahead of the base platform in the static test, than in the high-speed movies, 2) groaning and squeaking sounds were present as the air bag folds rubbed against each other.

Analysis of Bellows Test Data

Several variations of bellows wall thickness and heat-treat strength were provided for the May 1977 static test. It was believed that one or more of these models would have a limit load close enough to the design point to demonstrate the effectiveness of the bellows as an underseat E/A. Even if the sample closest to the design point had a limit load, for example, 30 percent from the design point, it would have been possible to interpolate or extrapolate the correct bellows configuration from the data points provided by the range of samples. The correct bellows configuration could have been selected on the basis of the empirical test data alone, or on the basis of the analytical model with an empirical correction.

Unfortunately, the bellows configurations tested in May had static limit loads less than half of those needed. This was due to an elastic instability that allowed wave-shaped buckling, or twisting, of the convolutions, as shown in Figure 17. This buckling apparently relieved hoop stresses at the roots and crests of the convolutions, which had been counted on to supply up to half of the crushing load of the bellows. The primary material stresses that remained to support the load were probably the bending stresses at the roots and crests of the convolutions. Some additional strain energy to support the bellows probably came from the twisting of the convolutions, but the convolution cross-section is not rigid to torsion, therefore this contribution was probably small.

The bellows convolution shape did not make the best use of material. The degrees of freedom existing for the convolutions

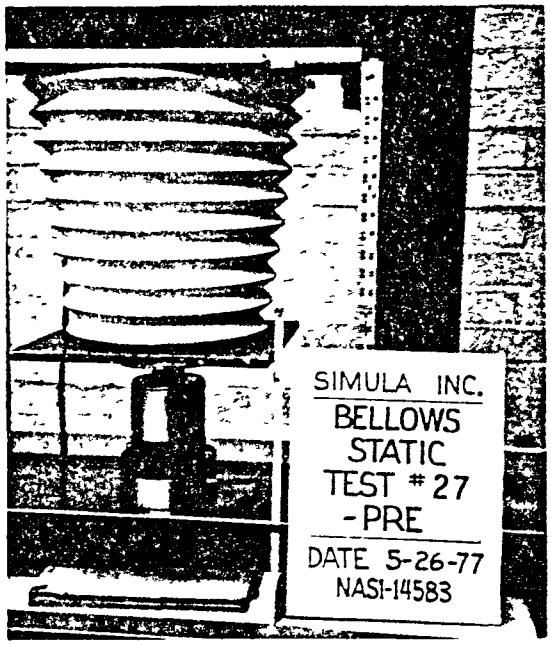

(a) Pretest

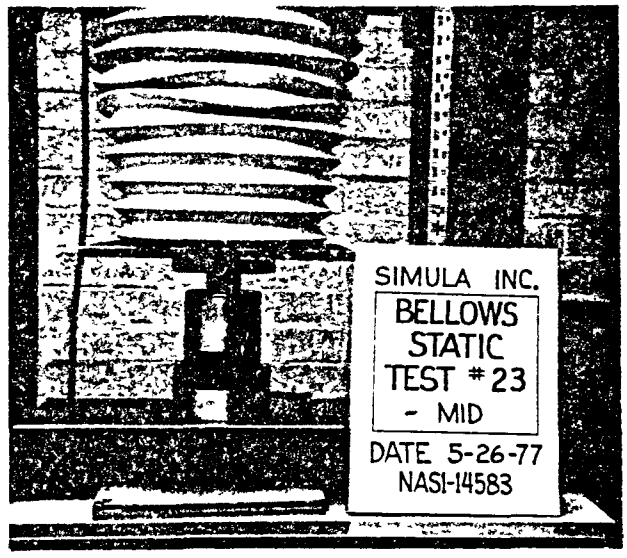

(b) Wave-shaped buckling begins

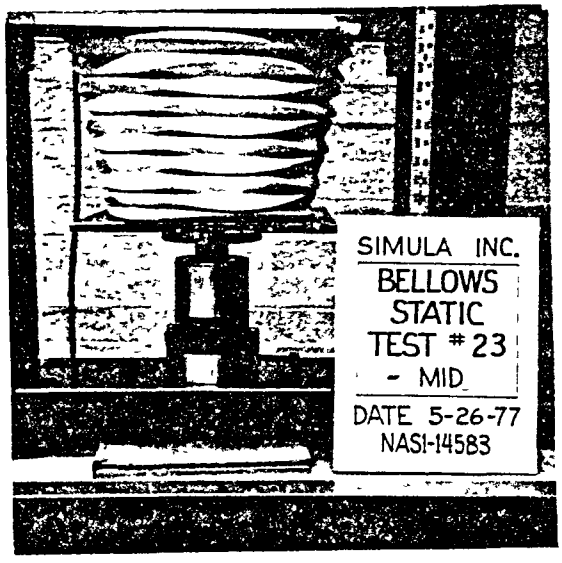

(c) Fully developed wave-shaped buckling

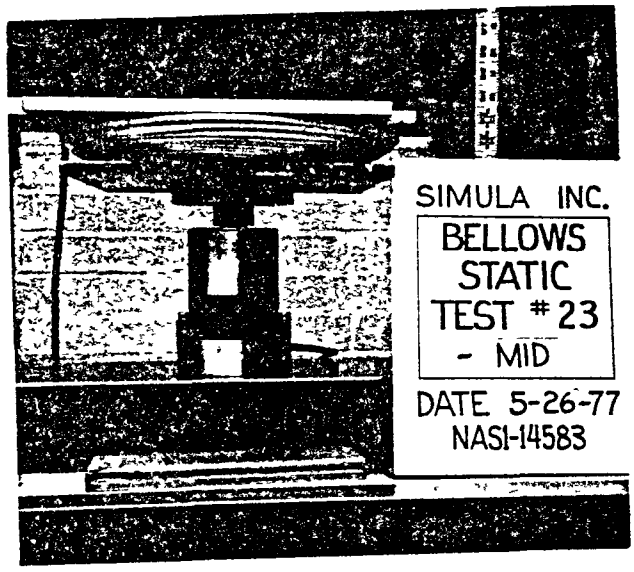

(d) Posttest, stroke = 33 cm

Figure 17. Test 23, bellows P/N SK10082-1.

allows strain to occur in a manner that did not provide stresses high enough to develop the required crushing load. Therefore, the design was inefficient from a strength/weight standpoint.

The convolution shape had been selected to take advantage of the hoop stresses, but these stresses did not materialize in the full-scale models because the material chose to "duck out" into a lower strain energy mode, namely, twisting of the convolution. Some wave-shaped buckling or twisting of the convolutions had been observed in the short preliminary models but apparently had not progressed to a serious degree because of the close proximity of the end constraints. The limit load of the preliminary models had in fact been greater than required.

In the dynamic bellows test, the moving portion of the fixture bottomed out because the limit load of the bellows built up slowly over the first 2.5 cm (1.0 in.) of stroke. The slow buildup of load, due to the low initial spring rate of the bellows and to the loading-rate dependence of the limit load, is detrimental in that, early in the stroke, it allows the buildup of a large relative velocity that then, prematurely, consumes the remaining available stroke. The load reached and maintained a level near the design goal and would have been sufficient to decelerate the mass within the available 31.8 cm (12.5 in.) stroke had it not built up so slowly at the start of the stroke.

The dynamic stroking load of the bellows was more than twice the static load of its twin static tested at 8.47×10^{-4} m/sec (2.0 in./min), indicating a large loading-rate dependence. Loading-rate sensitivity is not in itself undesirable as it can be used to optimize the protection provided over a range of crash severities. However, the large magnitude seen here should be reduced to allow the load to reach the desired plateau sooner without the extent of velocity buildup that occurred in Dynamic Test Number 21.

Additional Bellows Models

Rather than let the matter rest with the above explanation, it was decided to perform another bellows test cycle with modified designs to evaluate modifications that might cause the bellows to perform as desired. Two different approaches were taken to increase the limit load: first, a different convolution shape was chosen to maximize bending stresses and decrease dependency upon hoop stresses. Second, stiffeners were welded onto bellows of the old convolution shape in order to remove the degrees of freedom that had allowed relief of the hoop stresses.

The first approach resulted in the design of Part Numbers SK10082-6 and -7 shown in Figure 6. These bellows had convolution depths only half as deep as those tested in May. A given bending moment at the root of one of their convolutions produces twice the

resistance to crushing, because the moment arm connecting that root to the adjacent crests is half as long as on the earlier models.

In the second approach, two types of reinforcements were tried on two different bellows. First, on one bellows, wires connecting adjacent roots to each other and adjacent crests to each other were used to prevent the connected portions of the convolutions from spreading further apart from each other (this was observed to occur in the May tests even while the overall length of the bellows was decreasing). Second, on another bellows, sheet metal panels were welded across the crests to make the convolutions into box beams that were inherently rigid in torsion and capable of resisting the convolution twisting characteristic of the wave-shaped buckling.

The additional bellows models were tested in August and demonstrated much greater limit loads, as described in the following paragraphs.

Bellows With Smaller Convolutions. - Part Numbers SK10082-6 and -7 crushed at loads of 19 000 N (4300 lb) and 16 000 N (3600 lb), respectively, which is about twice the desired 8 840 N (1987 lb). The fact that their loads were much greater than needed is not discouraging as it indicates that an acceptable limit load can be achieved with a favorable strength/weight ratio. This is achieved by a compromise in convolution shape and wall thickness as described in the previous section.

As can be seen in Figures 18 and 19, the bellows with the smaller convolution size buckled somewhat unpredictably. Also, it should be noted that the wave-shaped buckling was still present. Part Number SK10082-6 was limited to only about 23 cm of usable stroke, because the nonuniformly crumpled convolutions failed to nest properly. The convolutions of SK10082-7 also crumpled unpredictably, but ultimately nested well and provided the longest usable stroke of any bellows tested. The ratio of convolution depth to diameter in these bellows is assumed to be slightly less then the minimum at which predictable folding can be depended upon. End misalignment during longitudinal stroking would be expected to further lessen the probability of the convolutions nesting well, thus preventing the full vertical E/A stroke.

A compromise between the convolution sizes of the bellows tested in May and August would probably yield a bellows with acceptable tolerance to end misalignment, tolerance to unpredictable buckling, and with the correct limit load. It is recommended that the configuration be as shown on Figure 5 but with: a convolution pitch of 2.8 cm (1.1 in.) (dimension B on Figure 5); material of 1.0 mm (0.04 in.)-thick 6061-T6 aluminum.

Reinforced Bellows with Large Convolutions. - The reinforced bellows models with the large convolution size stroked at nearly

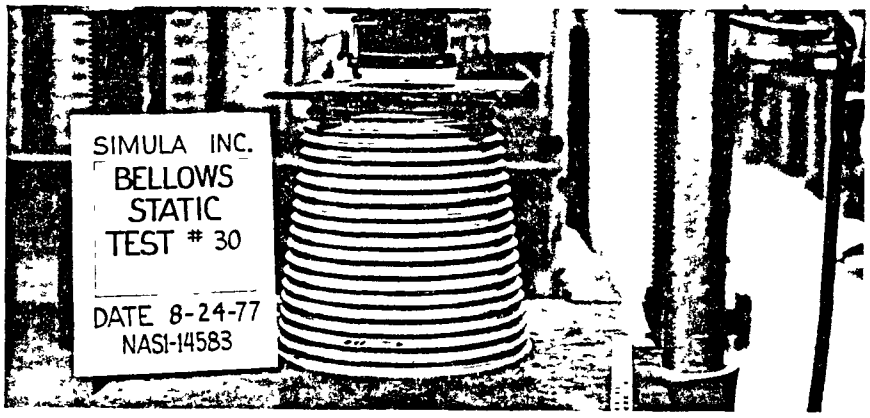

(a) Pretest

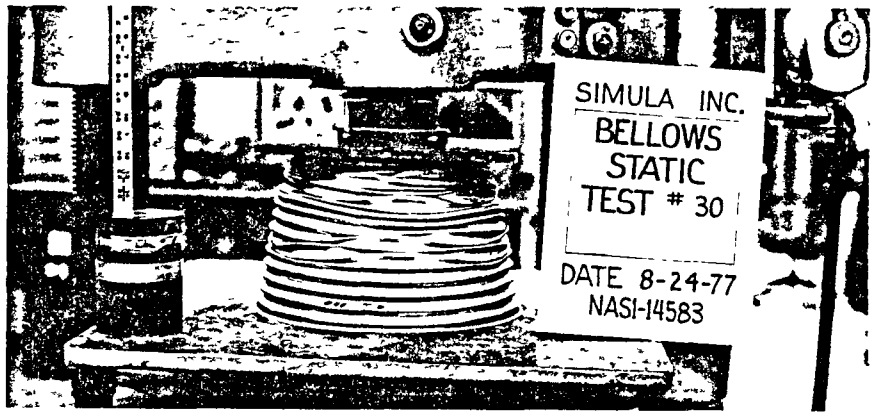

(b) Midtest, stroke = 15.2 cm

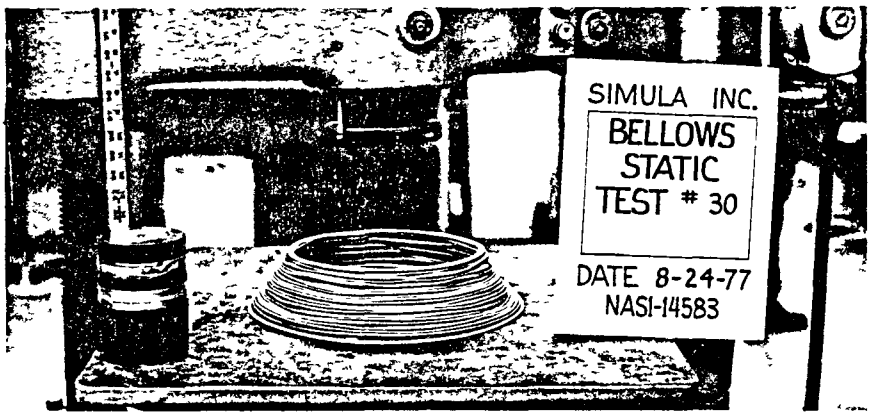

(c) Posttest, stroke = 30.5 cm

Figure 18. Test 30, bellows P/N SK10082-7.

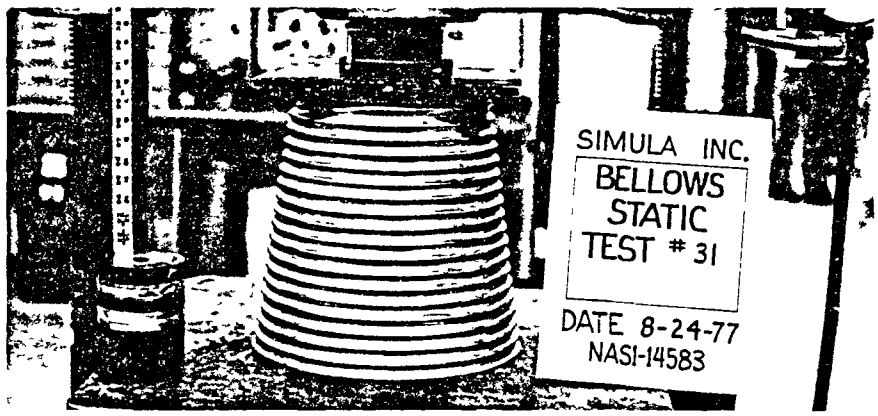

(a) Pretest

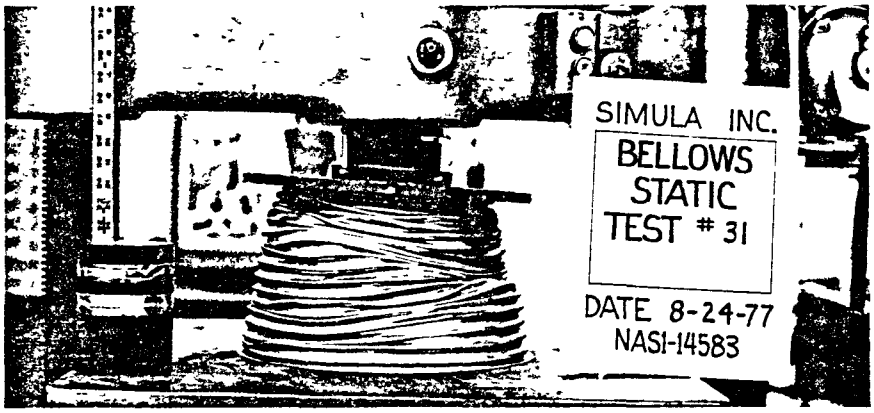

(b) Midtest, stroke = 16.5 cm

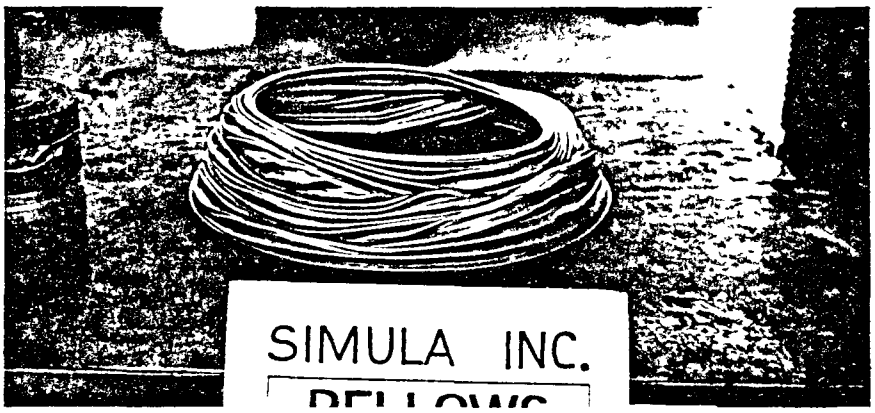

(c) Posttest, stroke = 30.5 cm

Figure 19. Test 31, bellows P/N SK10082-6.

the required load. As expected, wave-shaped buckling was still present in the wire-reinforced model but was prevented from reaching its fullest extent. The wires tying the adjacent convolution crests together prevented them from spreading apart, except where the wires broke in tension.

No wave-shaped buckling was observed in the model reinforced by sheet metal panels because of the torsional rigidity of the closed convolutions.

The wires and panels undoubtedly added some stiffness of their own to the bellows. The final strength of the reinforced bellows is a combination of the strength of the bellows itself, whose degrees of freedom have been limited by the reinforcements, plus the buckling strength of the reinforcements. Photographs of these bellows can be seen in Figures 20 and 21.

Bellows Static Shear Test

This test was to measure the contribution of the bellows to the strength of the seat in the forward loading condition.

The overturning torque from a 95th-percentile occupant subjected to a 15 G forward deceleration is approximately 9450 N-m (6970 ft-lb). The bellows underseat E/A that was tested supplied an average torque of 1300 N-m (960 ft-lb), 14 percent of the reaction torque necessary to prevent the seat from overturning. This bellows was identical to one in the static axial load test that supplied a load of 3600 N (809 lb), less than half of that desired. If the strength of the bellows had been closer to that desired, its contribution to the seat strength in the longitudinal direction would be expected to be greater than 14 percent.

The fixture was designed to simulate the motion of a seat frame pitching forward about a pivot point at the floor attachment of the guide tubes. The action of the seat upon the bellows causes two displacements: axial crushing; and misalignment of the bellows ends. The axial crushing contributes a torque equal to the crushing load of the bellows, 3600 N (809 lb), multiplied by the distance between the bellows axis and the seat pitch axis, 22 cm (8.5 in.), or 777 N-m (573 ft-lb). The difference between the total overturning torque 1300 N-m (860 ft-lb) and 777 N-m (570 ft-lb) is the contribution from the misalignment, or shear, of the bellows ends and is approximately 500 N-m (370 ft-lb).

Initial E/A Elastic Spring Rate

Neither type of E/A, bellows or air bag, reached its design limit load immediately at the start of the stroke. This is undesirable for efficient use of the stroke available, but it is not an inherent problem with the E/As and can be remedied.

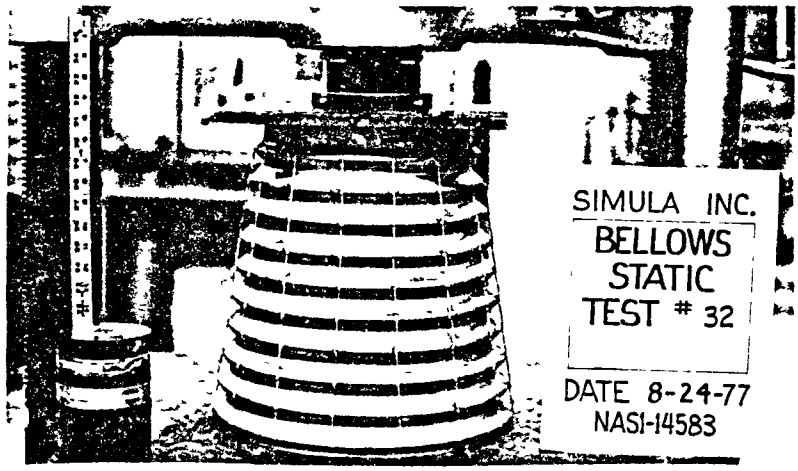

(a) Pretest

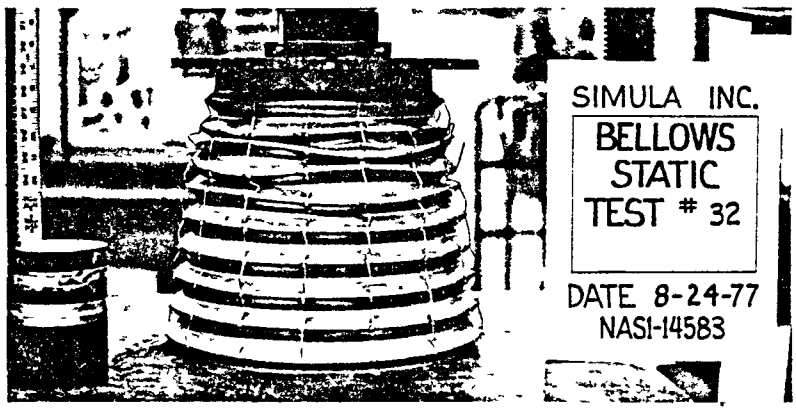

(b) Midtest, stroke = 5.8 cm

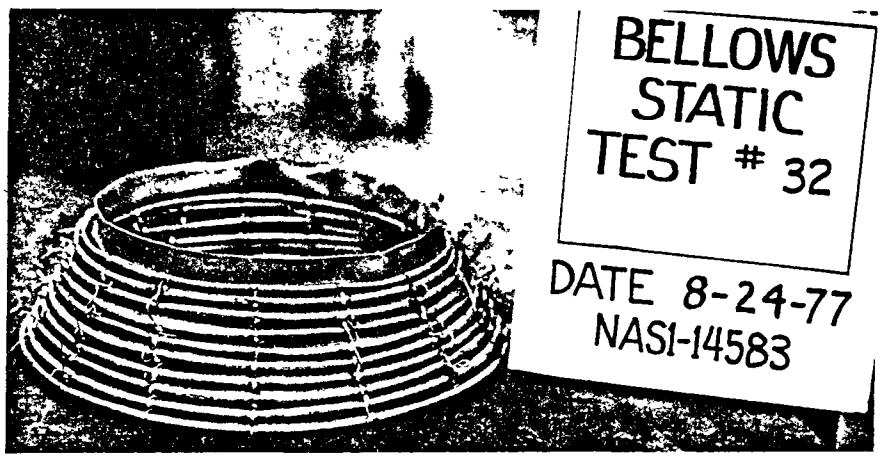

(c) Posttest, stroke = 30.5 cm

Figure 20. Test 32, wire-reinforced bellows.

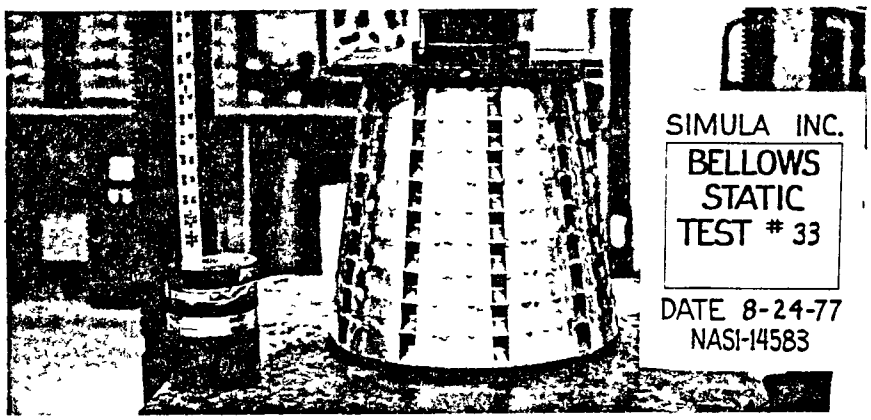

(a) Pretest

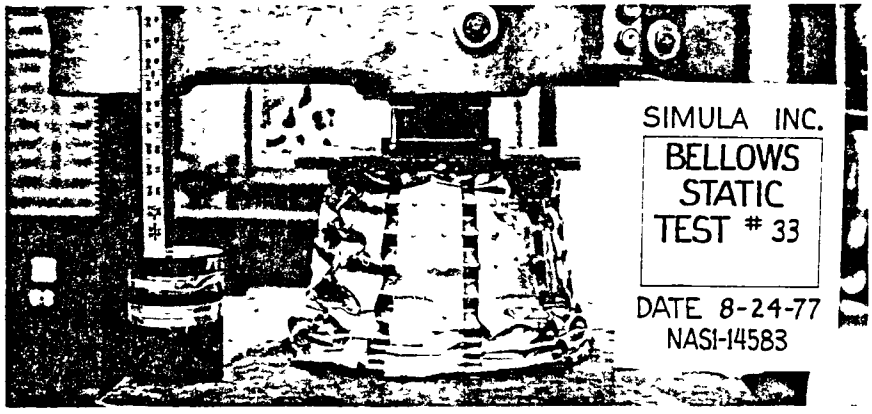

(b) Midtest, stroke = 12.7 cm

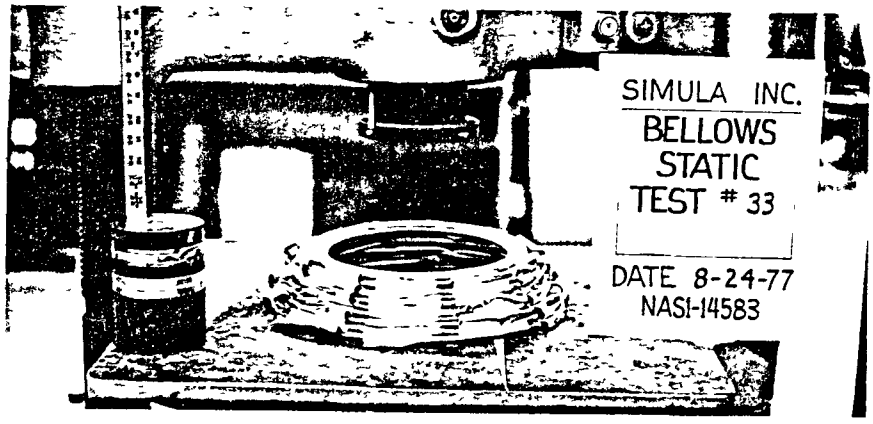

(c) Posttest, stroke = 30.5 cm

Figure 21. Test 33, sheet metal-reinforced bellows.

The bellows did not reach its static limit load until after 1.0 to 1.5 cm (.39 to .59 in.) of stroke. Some of the deflection of the bellows during initial load application was due to flaring of the relatively unsupported end convolution segments. In the dynamic test, the bellows required a stroke of over 2.5 cm (1.0 in.) before the load began to be increased by the loading rate dependence. The air bag did not reach its design limit load until after approximately 0.7 cm (.28 in.) of stroke because of a dome-shaped bulge on the small (bottom) end of the bag caused by stretching of the air bag fabric. This resulted in a smaller than planned contact area being available for the internal pressure to act upon. Even though the bulge was completely flattened out after approximately .6 cm (.25 in.) of stroke, it caused a reduction in the desired deceleration over an extended time period as can be seen at the beginning of the acceleration/time histories of Figure 14.

In a flexible, lightweight production seat, the air bag could cause another problem; one that did not occur with the dynamic test fixture because of the fixture's rigidity. That is, the upward force from the air bag could be expected to displace the seat pan upward by deflecting the seat bucket and frame. This would prevent the full design limit load from being applied to the occupant until the seat pan had been deflected back down to the position it had occupied before the air bag was pressurized. The amount of displacement would be significant because of the flexibility of the necessarily lightweight seat system. Thus, even though the air bag load would be maximum from the start (assuming no bottom end bulge), the spring rate of the predeflected seat would prevent that load from immediately being applied to the occupant.

A possible solution would be to preload the air bag E/A by means of a tensioning cable or cables inside the bag that connected between the seat pan and the floor. In addition, the airbag should be made approximately 1.3 cm (0.5 in) longer than the space it is to occupy to prevent the formation of the bulge on the bottom of the bag. The bellows, too, could be preloaded by cables. Also, it is important for the bellows loading rate dependence to be reduced. The flanges at both ends of the bellows must be attached to the seat pan and to the floor in such a way that the last convolution is not permitted to flare or buckle at a load less than the better-supported convolutions in the middle of the bellows.

It is very important for the E/A's design limit load to be reached quickly in order to take advantage of the energy absorption of the airframe. As an illustration of this, using rigid body analogy, an occupant stroke of only about 28 cm (11.0 in.) relative to the floor is required to fully decelerate the occupant from 12.8 m/sec (42 ft/sec) at 14.5 G if the occupant deceleration rises simultaneously with the airframe deceleration. Compare this with the 33 cm (13 in.) of stroke required if the E/A load builds up to its limit load linearly over the first 0.6 cm

(0.25 in.) of stroke. In the extreme case, if the 14.5 G deceleration is not applied to the occupant until after the airframe deceleration is complete, 91 cm (36 in.) of stroke is required between the seat and the aircraft floor. Appendix D shows the computer program used to double integrate the relative acceleration between the seat and the airframe. Also shown are the output plots of the first two acceleration cases described above.

In reality, the occupant does not behave like a rigid mass as assumed in the above illustration. Flexibilities between the seat bucket and hips, and hips and thorax, the thorax and head, etc., make it impossible to begin the deceleration of all parts of the occupant at once. However, the illustration proves a useful point concerning energy management during the stroke.

Reference 3 indicates the seat pan can be subjected to an initial deceleration in excess of 23 G without causing spinal damage, provided that the duration is less than 0.0055 sec. When the full limit load of the E/A is initially applied to the seat/occupant, it does not act to decelerate all of the mass at once. The mass that the force first acts upon, the seat bucket, is only a fraction of the total moving mass and, therefore, initially, is decelerated at greater than 23 G. Then, once the springs between the seat pan, hips, thorax, and head have been compressed, and the E/A load begins to act upon all of the mass, the deceleration of the composite mass returns to a level near 14.5 G.

Air Bag Construction

A bell-shaped air bag was leak tested at 152 kPa (22 psig) for six weeks. After that period, the pressure had dropped by 10.3 kPa (1.5 psi). No leaks could be detected by immersing the air bag in water, but some minute leaks may have existed nonetheless. The polyurethane elastomer with which the air bag fabric was sealed does not have good impermeability and is not recommended by plastic design references for sealing applications.

A butyl rubber membrane of the same thickness would be expected to allow much less leakage because of its superior gas impermeability. The pressure-sealing membrane could be made separate from the fabric reinforcement to make the air bag more flexible and to facilitate replacement or repair should a leak develop.

Pressurized Bellows

Based on the tests, a pressurized metal bellows combines the best features of both the air bag and bellows. The advantages of this combination are:

- The bellows contributes more strength to the seat frame during longitudinal and lateral loadings.

- Because part of the limit load is supplied by the internal pressure, the bellows walls can be made thinner to reduce weight.

- The thinner bellows walls can be crushed to a shorter compressed height.

- As the bellows convolutions close upon each other near the end of the stroke, the crushing load rises. This could be used to compensate for the decaying internal pressure.

- The seat bucket would be held by the bellows at whatever position to which it strokes, preventing rebound.

- The metal bellows will protect the inner pressure membrane, if used, from puncture.

FINAL SEAT SYSTEM DESIGN

The final seat system design for both the bellows and air bag E/As incorporate most of the structural features of the preliminary air bag-equipped seat frame discussed earlier in the report. Therefore, the stress analysis performed on the preliminary seat was sufficient for the final design.

Bellows-Equipped Seat, Final Design

A layout of the final bellows-equipped seat can be found in Figure 22. This design uses the same frame structure as the preliminary air bag-equipped seat with the exception that the E/A crossmember is replaced by a simple rigid crossmember. Longitudinal energy absorption is provided by the rear struts which elongate. If one strut has reached its limit load and the other one has not, the seat is prevented from yawing by the torsional rigidity of the bellows.

Air Bag-Equipped Seat, Final Design

A layout of the final air bag-equipped seat is shown in Figure 23. This seat differs from the preliminary air bag-equipped seat in two places: (1) it has a different longitudinal E/A mechanism; and (2) it has an aluminum honeycomb seat pan.

The longitudinal E/A mechanism operates as shown in Figure 24. It permits the seat to stroke forward without yawing. The top of each strut is attached to a short lever arm on a rigid torque tube. The ends of the torque tube are connected by torque-limiting axles to fittings at the top of each guide tube. When the struts become loaded to react the forward overturning moment of the seat, they exert a torque upon the torque tube. When the torque exceeds the limit that can be carried by the load-limiting axles, the torque tube rotates and allows the seat to stroke forward. Both levers rotate the same amount because they are connected by the rigid torque tube, thus constraining the seat to stroke forward without yawing to the side.

This mechanism provides at least 15.2 cm (6.0 in.) of forward stroke; whereas, the preliminary design allowed only approximately 5 cm (2.0 in.). (Reference 1 recommends 6.0 in. of longitudinal stroke to attenuate the longitudinal crash impulses to 15 G.) This assumes that the shoulder and lap belts are snug and have little elastic stretch. If they are loose or have considerable elastic stretch, more than 15.2 cm (6.0 in.) of forward stroke may be required.

The primary purpose of the honeycomb seat pan is to provide the rigidity needed to maintain the buttocks contour in the presence of the upward load applied by air bag internal pressure. The

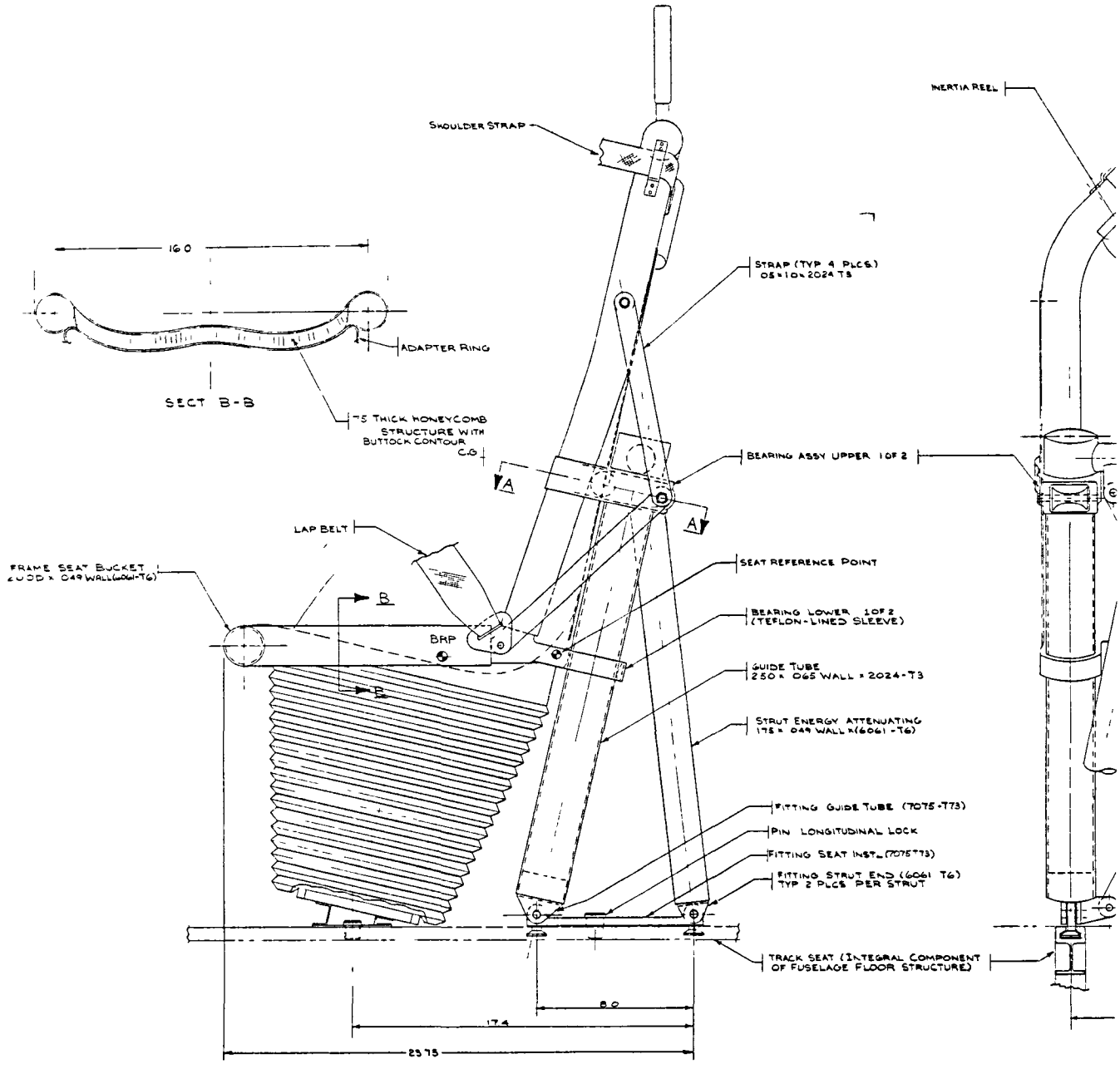

Figure 22. Layout of bellows-equipped seat.

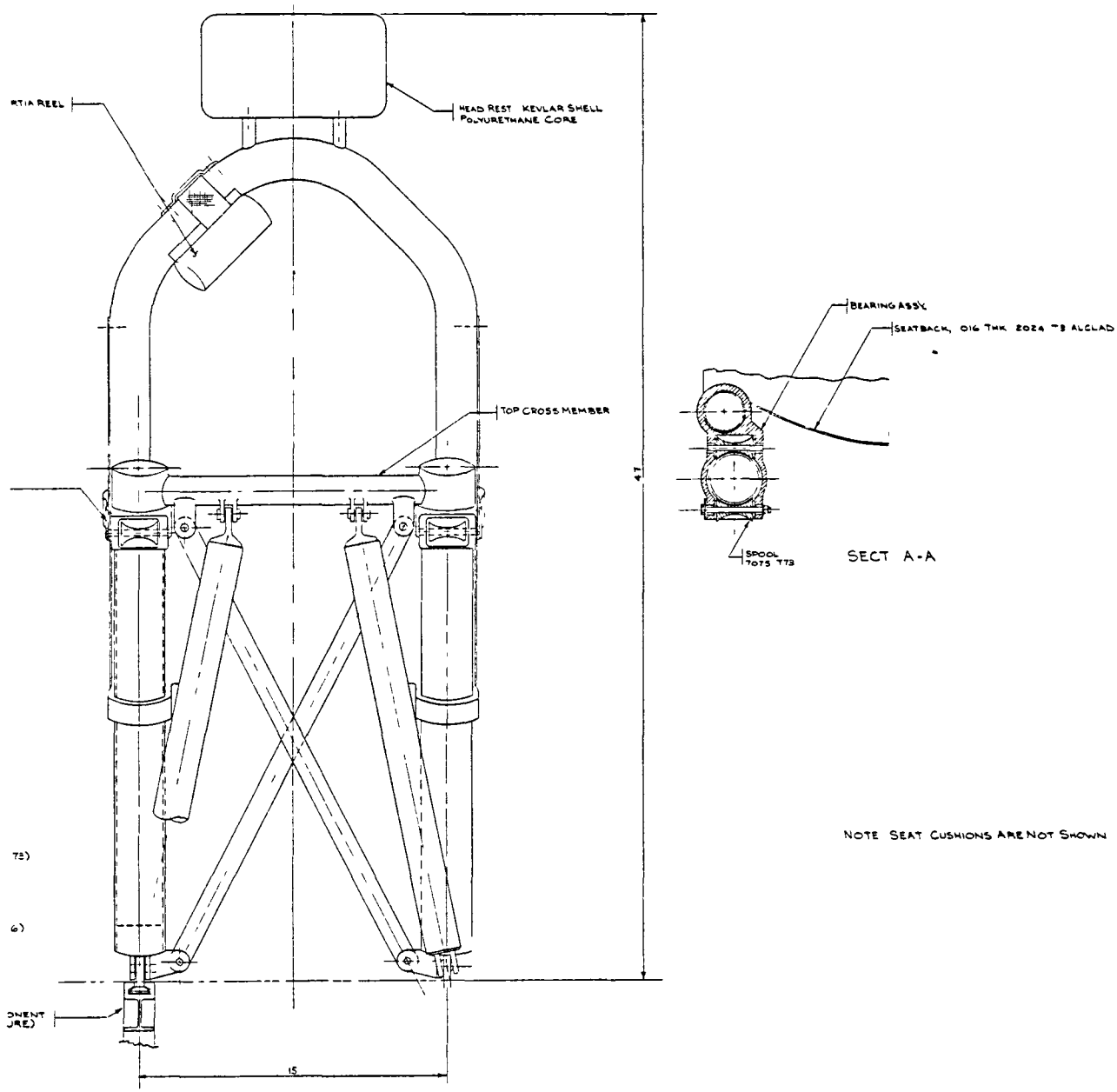

Figure 22. Layout of bellows-equipped seat (contd).

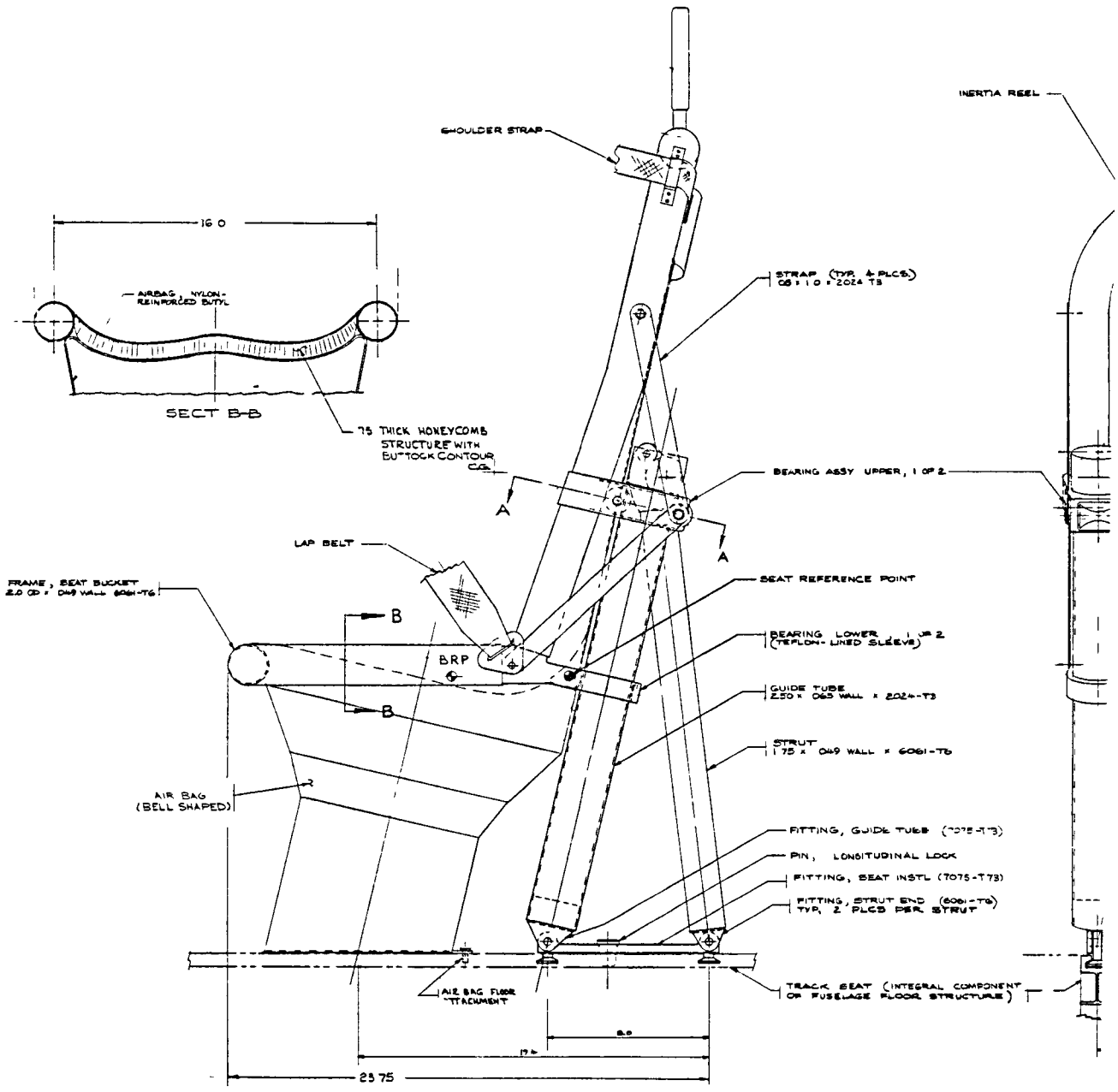

Figure 23. Layout of air bag-equipped seat.

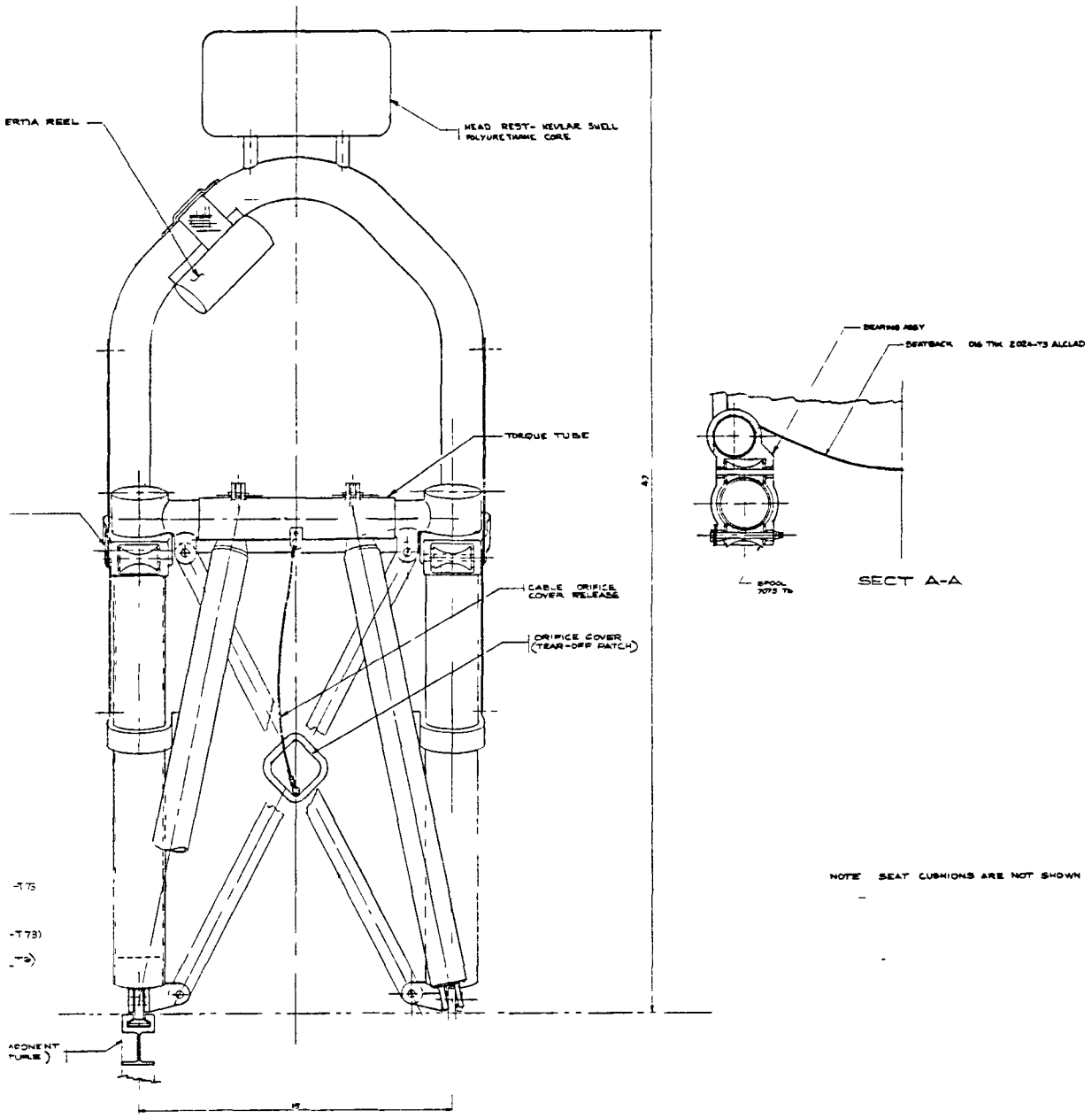

Figure 23. Layout of air bag-equipped seat (contd).

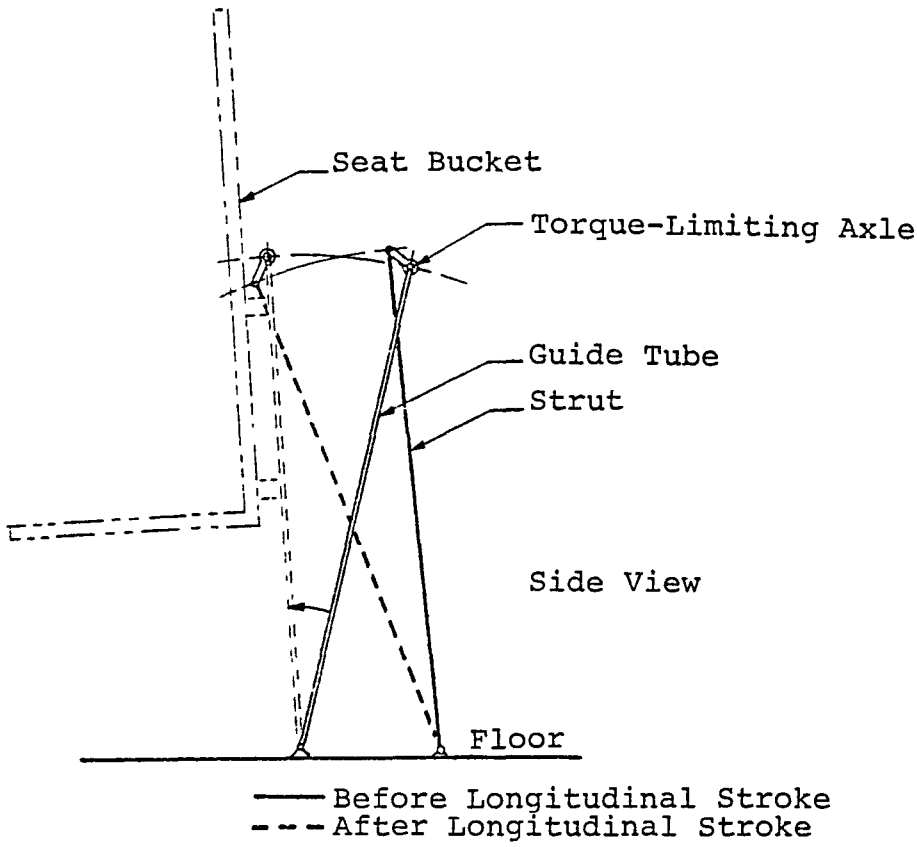

Figure 24. Geometry change of frame equipped with torque-limiting crossmember during forward E/A stroke.

honeycomb seat pan also can provide additional energy absorption. If the crushing strength of the 1.9 cm (0.75 in.)-thick seat pan were adjusted to provide 14.5 G deceleration to the 50th-percentile occupant, it could decelerate the occupant by 2.32 m/sec (7.6 ft/sec). This would provide additional end-of-stroke protection in case the air bag failed to decelerate the occupant fully.

CONCLUDING REMARKS

The object of this program was to develop seat concepts and underseat energy absorbers (E/As) for crashworthy, general aviation aircraft seats. Two types of E/As were investigated: an inflated air bag and a convoluted metal bellows. Both types of E/As were designed, built, and tested to evaluate their potential for attenuating the residual vertical crash energy of a 95th-percentile survivable crash to a level within the range of human tolerance. Seat frame concepts were evaluated for their ability to permit the vertical E/A stroke while concurrently resisting crash impulses in the longitudinal and lateral directions. A practical frame design, which is recommended for further study, was developed, but no frame hardware was built in this program. In the following paragraphs, specific conclusions concerning the suitability of the underseat E/As and seat frame concepts for providing a practical crashworthy seat for use in general aviation aircraft are presented.

Underseat Energy Absorbers

General. - Underseat E/As have some inherent advantages over E/As mounted elsewhere on the seat frame:

- The underseat E/A provides a direct load path to the cabin floor for the downward occupant inertial loads. This makes it possible for the decelerative force to be applied to the occupant at the beginning of the crash pulse without being delayed by flexibilities in the necessarily lightweight seat bucket and frame. Therefore, best use of the available stroke can be provided.

- The position of the underseat E/A enhances reliability by providing a load path, which bypasses the frame, directly to the floor. This placement eliminates the imposition of large moments on the frame structure such as occurs in seats supported by E/As located in back of the bucket.

- The underseat E/A prevents under-the-seat stowage of objects which could otherwise block the vertical seat stroke.

In order to achieve maximum benefit from the direct load path and immediately apply the decelerative load to the occupant, it is necessary for the underseat E/A to have a very high elastic spring rate; that is, its load/deflection curve must be very steep over the initial fraction of an inch of stroke. The bellows tested did not exhibit this desired characteristic, and the upward load from the air bag in precrash conditions would deflect the seat frame, thereby introducing the spring rate of the seat frame into the load path. This problem could be corrected by preloading both E/As by

a tensioning cable or cables connecting the seat pan to the floor attachment provision.

Air Bag E/A. - In the dynamic tests, the air bag proved to be well-suited for use as an underseat E/A. It fully decelerated the simulated occupant weight at a level close to that desired and within the 30.5 cm (12.0 in.) of stroke provided.

The orifice concept that was tested proved simple and effective. It consisted of an orifice hole sealed prior to impact by an orifice cover. At impact, the seat bucket begins to stroke, and the relative movement between it and the frame is utilized to release the orifice cover.

The air bag shape was found to be an important parameter that could be adjusted to compensate for pressure decay near the end of the stroke. A bell-shaped air bag proved to be more effective than cylindrical or conical shapes for fully decelerating the occupant. Near the end of the stroke as the relative velocity decreases, the internal pressure decays because of the slowing rate of volume contraction. The greater area of the bell-shaped air bag at this point in the stroke maintains the decelerative force (pressure times area) and decelerates the occupant fully.

It was discovered that the air bag membrane itself supports a significant buckling load during rapid crushing. The air bag was constructed of Kevlar fabric impregnated and sealed with polyurethane. It was stiffer than desired and should be replaced in future designs by a more flexible construction, such as Kevlar cloth with a separate inner bladder of butyl rubber.

The air bag was designed to remain pressurized at all times rather than be inflated at the time of crash impact. This avoids the cost and complexity of crash sensors and pressurization mechanisms. It does make it necessary to check the pressurization during routine maintenance. It is recommended that the air bag be fitted with a self-sealing valve similar to aircraft tire valves so that inspection and repressurization of both could be done with the same equipment at the same time.

Bellows E/A. - Several bellows with different convolution sizes, wall thicknesses, and material strengths were built and tested. Two models were built with reinforcements welded between convolution crests to control twisting of the convolutions, and these models exhibited the correct static limit load. The other simple bellows (unreinforced) exhibited static limit loads above and below the desired value, permitting the correct design parameters to be interpolated. Nearly all bellows maintained an almost constant limit load while stroking a distance equal to 70 percent of their original height. Therefore, the load/deflection characteristics make the bellows suitable as underseat E/A. However,

there are some problems and unanswered questions that will require further study before it is known whether a bellows underseat E/A can compete favorably with other types of E/A's. These problems, together with detailed conclusions, are covered in the following paragraphs.

Reinforced Bellows: Reinforcing wires and sheet metal panels were welded between convolution crests to control twisting of the convolutions. A given convolution will twist alternately one way, then the other, five to seven times around its circumference. Adjacent convolutions twist the opposite way, forming mirror images. This buckling mode relieves hoop stresses that otherwise would be generated by the expansion of the bellows OD and the contraction of the ID. The reinforcements were successful in controlling this low-energy, buckling mode and increased the limit load by a factor of 2 to 4. The strength/weight ratio, however, was no greater than that of a single unreinforced bellows having a smaller convolution depth. Although reinforcements were welded to the bellows, dip-brazing would be a less expensive attachment method.

Simple Unreinforced Bellows: The overall bellows shape was that of a truncated cone, 38 cm (15.0 in.) high, with 40 cm (16.0 in.) diameter at the top, and 30 cm (12.0 in.) diameter at the bottom. This was the most effective shape to fit under the seat pitched rearward at the prescribed 13 degree angle. The convolutions of a cone also tend to nest, allowing a shorter crushed height.

A range of convolution shapes and wall thicknesses were evaluated. Convolution depths of .95 cm (.375 in.) and 1.91 cm (.75 in.) were tried. The former did not provide the convolution with enough strength to maintain its circular shape, and unpredictable nesting resulted. The strength/weight ratio was high. The latter had much lower strength but very predictable nesting behavior. Wall thicknesses of .06, .07, and .09 cm (.023, .028, and .035 in.) were among the samples tested. Over this range of wall thicknesses, strength varied with the square of the wall thickness, and no effect upon the mode of buckling was observed.

The material chosen for the bellows was 6061 aluminum, because it could be easily welded, formed, and heat-treated. Samples of both -T4 and -T6 temper were tested, and crushing load was found to vary approximately as the square root of yield strength.

A triangular convolution with a 90 degree angle between adjacent convolution segments was used throughout the testing and appears to be nearly the optimum configuration. An angle greater than 90 degrees would increase the limit load, but would cause the root of the convolution to cripple outward during convolution twisting, thereby preventing the bellows from nesting to a short crushed height. Angles of less than 90 degrees would unnecessarily decrease the strength/weight ratio and would lower the initial elastic spring rate.

Other Bellows Features: The bellows can add significantly to the strength of the seat frame. As the seat pitches forward during longitudinal loading, the crushing and shearing action of the bellows can supply up to 30 percent of the moment required to hold the seat erect (assuming a 15 G forward load-limited seat system). During lateral loading, the bellows can resist 100 percent of the yaw moment resulting from the occupant's cantilevered position in front of the seat frame.

The bellows has a significant disadvantage in that only 80 percent of its original length is available for stroke. A bellows 43 cm (17.0 in.) long would be required to provide 30 cm (12.0 in.) of stroke necessary to safely decelerate the 50th-percentile occupant in the 95th-percentile survivable crash. Space limitations within the cabin of general aviation aircraft may require shorter bellows that cannot provide the optimum stroke.

Only one bellows was dynamically tested, and it showed an unacceptable loading rate dependence. Designed to reach the desired limit load during the high velocity portion of the stroke, the bellows would not provide sufficient load over the initial low velocity portion of the stroke, causing the occupant to bottom out at the end of the stroke. Other convolution configurations may not be so rate sensitive, and will require further dynamic testing to study their performance.

Seat Frame Concepts

There was no configuration of the underseat E/A by itself that could resist longitudinal and lateral loads while at the same time performing the essential vertical energy-absorbing stroke. Therefore, fixed frame concepts that could resist the horizontal loads and guide the seat bucket downward during its vertical stroke were used.

The shoulder strap inertia reel had to be mounted on the seat back rather than on the cabin sidewall in order to uncouple the seat from the large cabin sidewall buckling displacements that accompany light aircraft crashes. The shoulder strap, therefore, cannot help prevent the seat from overturning during forward loading, and the frame alone must hold the freestanding seat erect.

If no energy-absorbing stroke were provided in the forward direction, the seat would have to be designed to withstand a 30 G forward load factor. This would require a strong frame, very much heavier than present general aviation aircraft seats and possibly unacceptable to manufacturers of light aircraft. For this reason, it was decided to sacrifice some secondary impact safety to the occupant by designing the frame to stroke forward at a 15 G limit load, thus decreasing the frame strength requirement and weight.

The frame design finally selected has the following features:

- Three distinct parts - fixed frame, seat bucket, and underseat E/A.
- The fixed frame consists of two upright guide tubes interconnected at their tops by a crossmember and held erect by rear struts.
- The seat bucket is guided downward during the vertical stroke by rollers attaching it to guide tubes.
- The seat bucket vertical stroke is load limited by an underseat E/A.
- The seat bucket forward stroke is load limited by an E/A built into the fixed frame crossmember or the rear struts.
- There is no lateral energy absorption.

The forward load limiting is accomplished by permitting the guide tubes to pitch forward about their floor attachment points. The longitudinal energy-absorbing force, which the pitching of the guide tubes acts against, is provided by a different mechanism in the air bag-equipped seat than in the bellows-equipped seat. The longitudinal stroke can be provided in the bellows-equipped seat by allowing the rear struts to elongate at a prescribed limit load. The bellows will prevent the seat from twisting if one strut is more highly loaded. The bellows, attached to the seat bucket at its top and to the cabin floor at the bottom, is very rigid in torsion and prevents the seat from yawing during lateral load. (The yaw moment results from the seat bucket being cantilevered forward from the frame.)

Twisting (yaw) of the frame is to be minimized because it jeopardizes the structural integrity of the frame and could block the vertical stroke of the seat bucket by allowing the seat bucket to move over some obstruction, such as an adjacent seat or cabin sidewall.

The air bag cannot prevent the seat frame from twisting, therefore a different mechanism is required to provide the longitudinal energy-absorbing stroke for the air bag-equipped seat. In the final seat system design, this is accomplished by building the energy-absorbing feature into the crossmember rather than into the rear struts. A rigid torque tube parallel to the crossmember connects to both the struts by short lever arms. The torque tube is connected to the guide tube upper fittings by load-limiting axles which allow the torque tube to rotate when the moment applied by the struts exceeds the axles' limit. Because the torque tube is

rigid, both levers rotate the same amount; therefore the seat must pitch forward without yawing any more than is allowed by the elastic flexibilities of the seat.

RECOMMENDATIONS

Based on the results of this project, the following recommendations are made:

- A production prototype design of the bell-shaped air bag and of the orifice-release mechanism should be developed.

- Additional analysis of the bellows design using a finite-element computer program, such as MARC-CDC or NASTRAN, should be performed. The analytical predictions should be combined with the empirical data gathered in this program to predict the bellows parameters required to design and build two different bellows. The crushing load of one bellows would be due entirely to plastic deformation of metal. The other, with thinner walls, would produce part of its load by plastic deformation with the remainder being provided by internal air pressure.

- The two bellows concepts described above should be fabricated and tested both statically and dynamically.

- Detailed designs of seat frames for the bellows-equipped seat and for the air bag-equipped seat should be developed.

- Full-scale seat systems utilizing the air bag and the bellows should be built and tested. The testing should include:

  (1) Static testing in the longitudinal, lateral, and combined loading directions.
  (2) Dynamic testing with an anthropomorphic dummy of the seat's underseat E/A in a predominantly vertical direction.
  (3) Dynamic testing (sled test) with an anthropomorphic dummy of the seat frame in the combined longitudinal and lateral direction.

- Additional full-scale seat systems of the same or a refined design should be fabricated for flight testing and aircraft crash testing.

Simula Inc.
2223 South 48th Street
Tempe, Arizona 85282
September 18, 1979

APPENDIX A

Seat With Shoulder Strap Inertia Reel Mounted Upon Bulkhead

The shoulder strap inertia reel in the first seat configuration investigated was mounted on the cabin sidewall or bulkhead approximately 18 in. behind and several inches below the shoulder. The shoulder strap is not attached to the seat back, but rather passes through a hole in the seat back which maintains the proper strap height relative to the occupant's shoulder. As shown in Figure A1, the section of shoulder strap between the inertia reel and seat back can swing during the vertical E/A stroke to maintain occupant restraint without interfering with the vertical stroke.

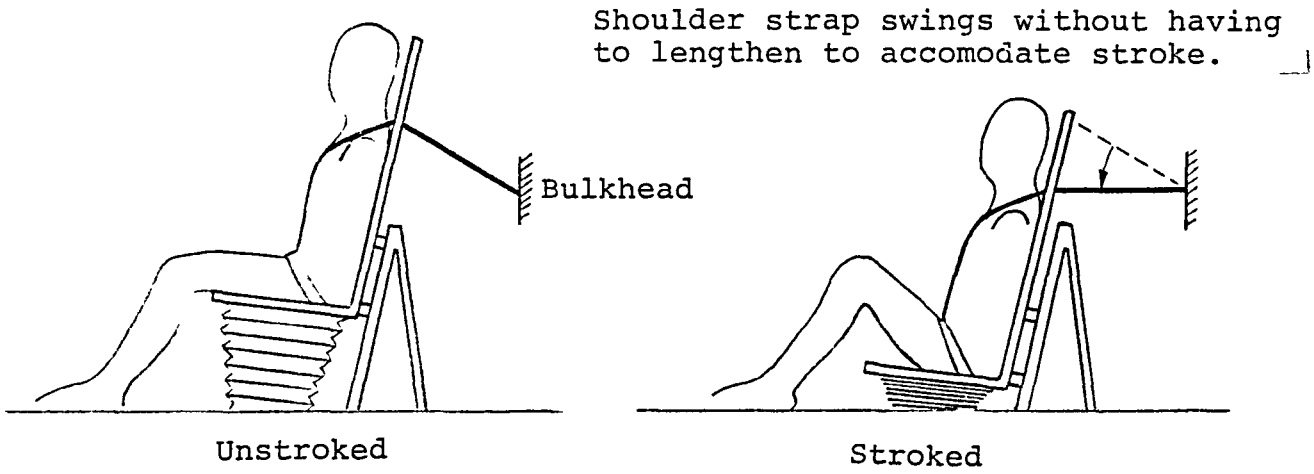

Figure A1. Stroked and unstroked configuration with shoulder strap connected to bulkhead.

When loaded in the forward direction, approximately 40 percent of the occupant's inertial load can be carried by the shoulder strap to the airframe, bypassing the seat frame. This can reduce the seat frame weight and/or increase the forward deceleration at which the occupant can be safety restrained.

However, the design has some drawbacks: the large outward buckling displacements of aircraft cabin sidewalls during a crash could pull the seat over sideways if the inertia reel were attached to the sidewall; and there is not always enough room between a seat and the bulkhead behind it for the length of shoulder strap required to prevent unhindered vertical stroke.

If the inertia reel can be mounted in the required position, and the hard point to which it is attached cannot move greatly relative to the seat floor attachments, this seat configuration should be seriously considered.

APPENDIX B

Calculation of Longitudinal or Lateral Acceleration Which Will Overturn Freestanding Seat Mounted on Bellows E/A

Assume that the seat system shown in the figure below is subjected to a forward load F applied at the c.g. of the occupant. Total occupant and seat bucket weight is 223 lb. Thickness, t, is neither the wall thickness or the convolution depth, but rather a variable representing the equivalent thickness of a dummy material whose crush strength per unit circumferential length is equivalent to that of the bellows. In other words, the physical bellows has been replaced for purposes of this calculation by a nonconvoluted, straight cylindrical tube of radius R and thickness t, whose crush strength in the axial direction is sized to provide the required vertical limit load.

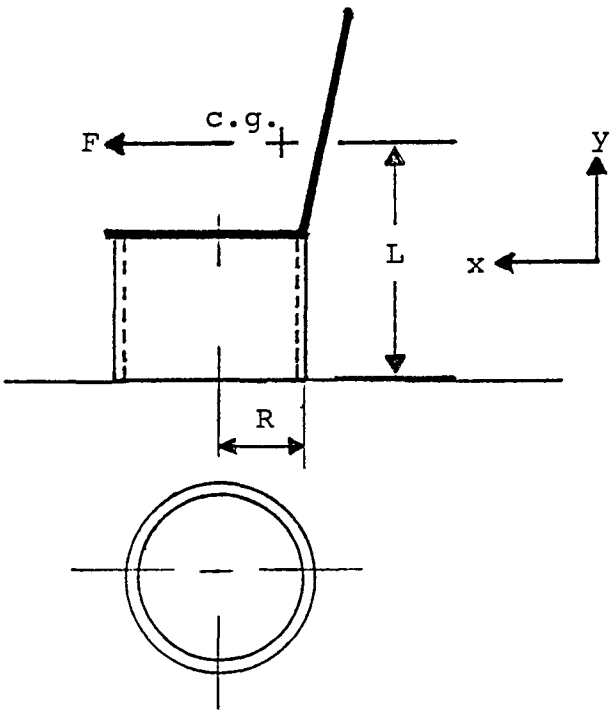

The crush strength of such a cylinder in the vertical direction is given by:

$$F = S_y A = S_y \, 2\pi Rt$$

Where F = crushing load, total, pounds

S_y = material yield strength, psi

A = area, in^2.

Solving for S_y and recalling that the desired limit load is 1987 lb:

$$S_y = \frac{1987}{2\pi RT} \qquad (1)$$

The moment of inertia, I, of a cylinder where $t \ll R$ is given by:

$$I = \pi R^3 t \qquad (2)$$

The allowable bending moment, M is:

$$M = S_y \frac{I}{R} \qquad (3)$$

Where R = radius = distance to extreme fiber from neutral axis.

Combination of equations 1, 2, and 3 yields:

$$M = \frac{1987}{2\pi Rt} \frac{R^3 t}{R} = \frac{1987\ R}{2}$$

$$M = 7948 \text{ in-lb}$$

The moment, M, is also equal to FL = WaL.

Where W = occupant weight and

a = acceleration load factor

L = distance from c.g. to floor = 25 in.

Solving for a yields:

$$a = \frac{M}{WL} = 1.42\ G$$

APPENDIX C

Air Bag Analytic Computer Program and Output From Test 1

The computer program shown in Figure C1 is designed to integrate all the dynamic processes in steps of 0.001 sec. Before integration begins, the initial conditions such as charging pressure, orifice size, moving mass, and orifice flow coefficient are set by reading data cards. The deceleration/time coordinates of the actual input crash pulse and the diameter/length coordinates of the measured air bag are also read into the model by data cards and stored in arrays.

Once the iteration is begun, input deceleration is interpolated from the deceleration/time array. The input deceleration eventually rises above the level at which it can be passed on to the test mass by the air bag force (initial pressure x initial area). Relative acceleration then begins to exist between the airframe (input) and seat (test mass). This acceleration is double integrated to obtain: first, relative velocity, then relative displacement (stroke). The new pressure due to the contracting air bag volume is calculated by adiabatic gas equations at each 0.001 sec interval and used at the following time increment to calculate the seat deceleration. After a stroke of 1.2 in., the orifice opens and air begins escaping from the air bag control volume. The mass rate of flow is calculated using a sharp-edged orifice flow equation and then integrated over each 0.001 sec time interval. The mass of air in the bag is then reduced by the amount exhausted, and the new remaining air mass is used in the gas equation to calculate the pressure for the next iteration.

The iteration proceeds in the above manner until the available stroke is used up or until the time limit is reached. At each time increment, the major variables are printed out and plotted as shown in the example of Figure C2. Figure C2 shows the theoretical performance of the air bag calculated from the initial conditions and input deceleration of Dynamic Air Bag Test Number 1. The actual measured deceleration has been penciled onto the plot in dashed lines, and measured pressures and strokes have been entered beside the theoretical tabulated values for comparison.

```
GASBAG,T40,P5.
ACCOUNT.
HEADING,51 SIMULA.
FTN,A.
LGO.
0000000000000000 00000
      PROGRAM GASBAG (INPUT, OUTPUT, TAPE1 = INPUT)
      REAL M
      DIMENSION X(1 1), TD(10), GD(10), CASE(8),SD(10), DD(10)
C  INITIALIZE CONSTANTS
      PI = 3.14159
      R=53.3
      PATM = 14.7 * 144.
      TMAX = .15
      DT = .001
C READ AND PRINT PAGE HEADING
   40 READ 50, (CASE(J), J = 1,8)
   50 FORMAT(8A10)
      IF (EOF(1)) 1000, 55
   55 PRINT 60, (CASE(J), J = 1,8)
   60 FORMAT(1H1, 8A10, /)
C READ INPUT PULSE COORDINATES, (TIME, G)
  112 READ 114,((TD(J), GD(J)), J = 1,10)
  114 FORMAT(2F10.5)
C READ AIRBAG SHAPE DESCRIPTION  (STROKE, DIA)
      READ 114, ((SD(J), DD(J)), J = 1,10)
C CALCULATE AIRBAG INITIAL VOLUME
      QINIT = 0.
      ADISK = 0.
      JS = 1
      DO 180 J = 1, 148
      S = J/10.
      IF (S .LE. SD(JS+1)) GO TO 170
      JS = JS + 1
  170 DIA = DD(JS)+(S-SD(JS))*(DD(JS+1)-DD(JS))/(SD(JS+1)-SD(JS))
      ADISK = PI*DIA**2/(4*144)
  180 QINIT = QINIT + ADISK*.1/12.
      QINIT = QINIT -(14.5**2-4.**2)*PI*1.5/4./1728.
C READ AND PRINT INDEPENDENT PARAMETERS
  140 READ 150, DR, W, P, C, FACTOR
  150 FORMAT(5F10.5)
      IF(EOF(1))1000,160
  160 PRINT 120,DR, W, C, FACTOR
  120 FORMAT(14H1ORIFICE DIA =  , F4.2, * INCH   EFFECTIVE WT, =*,
     C F4.0, * LBS,*,  *   FLOW COEF, =*, F4.2, *   FACTOR =*, F4.0/)
C SET INITIAL CONDITIONS
      Q = QINIT
      P = P * 144 + PATM
      PNEW = P
      TEMP = 570.
      M = P*Q/(R*TEMP)
      ARO = PI*DR**2/(4*144)
      JJ = 1
      JS = 1
      K = 3
      V = 0.
      S = 0.
      T = 0.
      DVA = 0.
C PRINT COLUMN HEADING
      PRINT 200
  200 FORMAT (//, ACCEL, VELOC, STROKE PRESS,  DIA,  TIME, )
      PRINT 250
  250 FORMAT(40H    G     V,FPS    S,IN    P,PSI  D,IN    SEC  /1H ,135(1H*))
C BEGIN ITERATION, CALCULATE DEPENDENT VARIABLES
      GO TO 300
  270 T = T + DT
C CALCULATE AIRFRAME ACCELERATION, GA, BY INTERPOLATION BETWEEN DATA POINTS
  300 IF (T .LE. TD(JJ+1)) GO TO 350
      JJ = JJ + 1
  350 GA = GD(JJ)+(T-TD(JJ))*(GD(JJ+1)-GD(JJ))/(TD(JJ+1)-TD(JJ))
C CALCULATE AIRBAG DIAMETER THEN AREA
      IF (S .LE. SD(JS+1)) GO TO 370
      IF(S .LT. SD(JS)) JS = JS-2
      JS = JS + 1
  370 DIA = DD(JS)+(S-SD(JS))*(DD(JS+1)-DD(JS))/(SD(JS+1)-SD(JS))
      A = PI * DIA**2 / (4*144)
C CALCULATE ORIFICE AREA, AR
      IF(S .LT. 1.2) AR = 0.
      IF(S .GE. 1.2) AR = ARO
C CALCULATE SEAT ACCELERATION, GS
      FC = (P-PATM)/144./25.*V/22.*FACTOR
      GS = (P-PATM)*(A-AR*1.29*0.6)/W + FC
      IF(S .GE. 0. .AND. GS .GT. GA) GS = GA
```

Figure C1. Air bag analytic computer program, "GASBAG".

```
C CALCULATE ACCELERATION OF SEAT RELATIVE TO AIRFRAME, GSA
      GSA = GA - GS
C INTEGRATE ACCEL TO OBTAIN VELOCITY AND DISPLACEMENT, V AND S
      V = V+GSA*DT*32.2
      S = S+V*DT*12.
      IF (S .GT. 13.) GO TO 900
C CALCULATE VOLUME CHANGE,DQ, AND INTEGRATE TO OBTAIN NEW Q
      DQ = V*A
      Q = Q - DQ*DT
      IF(Q .LT. 0.) GO TO 900
C CALCULATE MASS RATE OF EXHAUST,DMEX , AND INTEGRATE FOR NEW TOTAL MASS
      PR = P/PATM
      IF (P .LT. PATM) PR = PATM/P
      IF (P .EQ. PATM) GO TO 510
      DMEX = 2.05*C*AR*PATM*(PR**.283*(PR **.283-1.)/TEMP)**.5
  500 M = M - DMEX * DT *(P-PATM) / (ABS(P-PATM))
C SOLVE GAS EQNS FOR NEW PRESSURE AND TEMPERATURE
  510 PNEW = R * M * TEMP / C
      TEMP = TEMP*(PNEW/P)**0.283
      P = PNEW
C INTEGRATE AIRFRAME ACCEL TO OBTAIN TOTAL INPUT VELOCITY CHANGE
      DVA = DVA +GA*DT*32.2
  550 CONTINUE
C SCALE VARIABLES FOR PLOTTING
      IGA = GA*1.85 +5
      IF(IGA .GT. 95) IGA = 5
      IGS = GS*1.85 + 5
      IV = V + 5
      IF(IV .LT. 1) IV = 1
      IS = S * 2 + 5
      PP = P/144 - 14.7
      IP = PP + 5
      ID = DIA * 2 + 5
C CLEAR PLOT LINE
      DO 600 J= 1,95
      X(J) = 1H
  600 CONTINUE
C LOAD PLOT LINE WITH OUTPUT CHARACTERS
      X(ID) = 1HD
      X(IS) = 1HS
      X(IV) = 1HV
      X(IP) = 1HP
      X(IGA) = 1HC
      X(IGS) = 1HG
      X(5) = 1H*
C PLOT
      PRINT 700, GS, V, S, PP, DIA, T, (X(J), J = 1,95)
  700 FORMAT(1H , 5(F6.2,1X), F4.3, 95A1)
      IF ( T .LT. TMAX) GO TO 270
C END OF ITERATION
      GO TO 920
  900 PRINT 910
  910 FORMAT(1H , 44X, 12HBOTTOMED OUT )
  920 PRINT 930, DVA, QINIT
  930 FORMAT(/* VELOCITY CHANGE OF INPUT PULSE =*, F4.1,*FT/SEC*,
     C*,   INITIAL VOL. =*, F5.3)
      GO TO 140
 1000 STOP
      END
000000000000000000000
TEST NUMBER 1, BELL-SHAPED AIRBAG
0.        0.
0.029     32.06
0.039     46.03
0.044     43.98
0.048     17.26
0.056     13.15
0.067     0.
0.250     0.
0.250     0.
0.250     0.
0.        6.2
.15       7.1
.45       9.4
1.        10.27
7.        10.35
8.5       10.92
10.5      12.56
12.5      14.42
13.5      15.06
15.5      15.06
2.18      138.0     24.6      .85       5.
000000000000000000000
```

Figure C1. Air bag analytic computer program, "GASBAG" (contd).

Figure C2. Analytical model output using initial conditions of air bag Test No. 1.

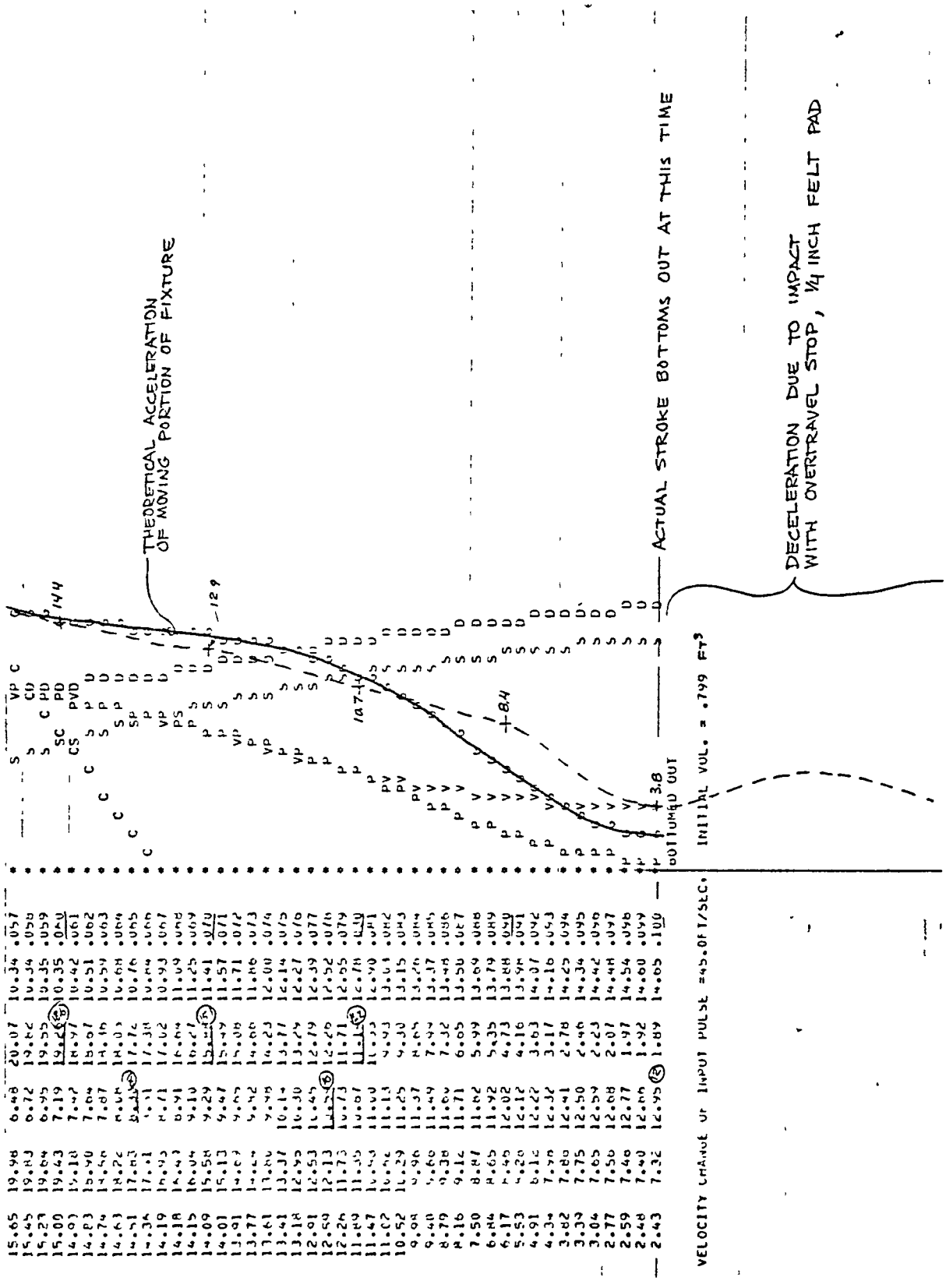

Figure C2. Analytical model output using initial conditions of air bag Test No. 1 (contd).

APPENDIX D

Double Integration of Measured Decelerations to Obtain Stroke

The integration routine shown in Figure D1 was made originally to analyze a curious set of circumstances that occurred during the bellows dynamic test. The test mass bottomed out with considerable residual velocity, even though the oscillograph record showed the deceleration to be adequate. It was thought possible that the slow rise of test mass deceleration over its first fraction of an inch of stroke could allow the buildup of a considerable relative velocity that would consume the remaining stroke prematurely. In fact, by using the integration program shown in Figure D1, this was found to be the case. The measured input deceleration and attenuated test mass deceleration were entered into the program and integrated to obtain stroke. The results showed a large residual velocity after the available stroke had been utilized.

The conclusion drawn from this, and discussed at some length in the main body of the report, is that an E/A must have a very high elastic spring rate in order to minimize the stroke requirement. Two sample printouts that illustrate this point clearly are shown in Figures D2 and D3. Figure D2 shows that a stroke of 10.9 in. is required to decelerate the test mass at 14.5 G when its deceleration rises simultaneously with the input deceleration. Figure D3 shows that a stroke of 13.9 in. is required to decelerate the test mass at 14.5 G if its initial deceleration rises linearly over the first 0.25 in. of stroke, such as would occur with an E/A having 0.25 in. of elastic deflection before reaching its limit load. On the printouts, the velocity, V, is in ft/sec, and the stroke, S, is in inches. Airframe deceleration is tabulated under the column heading "GA" and plotted with the symbol "C." Attenuated seat bucket deceleration is tabulated under the column heading "GB" and plotted with the symbol "G." This symbol "G" does not represent the acceleration of gravity as it does in the main body of the report.

```
      PROGRAM PLOT(INPUT, OUTPUT, TAPE1 = INPUT)
      DIMENSION TAD(12), GAD(12), TBD(12), GBD(12), X(105)
C READ INPUT PULSE COORDINATES
  100 READ 110,((TAD(J), GAD(J)), J = 1,12)
  110 FORMAT(2F10.5)
  120 READ 110,((TBD(J),GBD(J)), J= 1,12)
      IF(EOF(1))1000,125
  125 PRINT 130
  130 FORMAT(1H1,//*  GA    GB    V     S     T  */)
      S = 0.
      V = 0.
      T = 0.
      DT = .001
      DV = 0.
      JA = 1
      JB = 1
C COMPUTE AIRFRAME ACCELERATION
  150 IF(T .LE. TAD(JA+1)) GO TO 200
      JA = JA +1
  200 GA = GAD(JA)+(T-TAD(JA))*(GAD(JA+1)-GAD(JA))/(TAD(JA+1)-TAD(JA))
C COMPUTE SEAT BUCKET ACCELERATION
      IF(T .LE. TBD(JB+1)) GO TO 300
      JB = JB + 1
  300 GB = GBD(JB)+(T-TBD(JB))*(GBD(JB+1)-GBD(JB))/(TBD(JB+1)-TBD(JB))
C INTEGRATE
      GBA = GA - GB
      V = V + GBA*DT*32.2
      S = S + V*DT*12.
      IF(S .GT. 13.6) GO TO 900
      DV = DV + DT*GA*32.2
C SCALE VARIABLES FOR PLOTTING
      IGA = GA*2+10
      IGB = GB*2+10
      IV = V+10
      IS = S*2+10
C LOAD PLOT LINE WITH OUTPUT CHARACTERS
      DO 400  J = 1, 105
  400 X(J) = 1H
      X(IGA) = 1HC
      X(IGB) = 1HG
      X(IV) = 1HV
      X(IS) = 1HS
      X(10) = 1H*
C PLOT
      PRINT 800, GA, GB, V, S, T, (X(J), J = 1, 105)
  800 FORMAT(1H , 4(F4.1, 1X), F4.3, 105A1)
      T = T + DT
      IF(T .LE. 0.120) GO TO 150
  900 PRINT 910, DV
  910 FORMAT(/1H , *INPUT PULSE VELOCITY CHANGE = *, F5.2, * FT/SEC*)
      GO TO 120
 1000 STOP
      END
```

Figure D1. Computer program to double integrate measured decelerations to obtain stroke.

GA	GB	V	S	T
0.0	0.0	0.0	0.0	.000
1.8	1.8	0.0	0.0	.001
3.6	3.6	0.0	0.0	.002
5.3	5.3	0.0	0.0	.003
7.1	7.1	0.0	0.0	.004
8.9	8.9	0.0	0.0	.005
10.7	10.7	0.0	0.0	.006
12.4	12.4	0.0	0.0	.007
14.2	14.2	0.0	0.0	.008
16.0	14.5	.0	.0	.009
17.8	14.5	.2	.0	.010
19.6	14.5	.3	.0	.011
21.3	14.5	.5	.0	.012
23.1	14.5	.8	.0	.013
24.9	14.5	1.1	.0	.014
26.7	14.5	1.5	.1	.015
28.4	14.5	2.0	.1	.016
30.2	14.5	2.5	.1	.017
32.0	14.5	3.1	.1	.018
33.8	14.5	3.7	.2	.019
35.6	14.5	4.4	.2	.020
37.3	14.5	5.1	.3	.021
39.1	14.5	5.9	.4	.022
40.9	14.5	6.7	.5	.023
42.7	14.5	7.6	.5	.024
44.4	14.5	8.6	.6	.025
46.2	14.5	9.6	.8	.026
48.0	14.5	10.7	.9	.027
44.2	14.5	11.7	1.0	.028
44.4	14.5	12.7	1.2	.029
42.7	14.5	13.6	1.3	.03
40.9	14.5	14.4	1.5	.031
39.1	14.5	15.2	1.7	.032
37.3	14.5	16.0	1.9	.033
35.6	14.5	16.7	2.1	.034
33.8	14.5	17.3	2.3	.035
32.0	14.5	17.8	2.5	.036
30.2	14.5	18.2	2.7	.037
28.4	14.5	18.5	3.0	.038
26.7	14.5	18.8	3.2	.039
24.9	14.5	19.0	3.4	.040
23.1	14.5	19.2	3.7	.041
21.3	14.5	19.3	3.9	.042
19.6	14.5	19.4	4.1	.043
17.8	14.5	19.4	4.4	.044
16.0	14.5	19.4	4.6	.045
14.2	14.5	19.3	4.9	.046
12.4	14.5	19.3	5.1	.047
10.7	14.5	19.1	5.4	.048
8.9	14.5	18.9	5.6	.049
7.1	14.5	18.7	5.8	.050
5.3	14.5	18.4	6.1	.051
3.6	14.5	18.1	6.3	.052
1.8	14.5	17.7	6.5	.053
.0	14.5	17.2	6.7	.054
0.0	14.5	17.7	7.0	.055
0.0	14.5	17.3	7.2	.056
0.0	14.5	16.8	7.4	.057
0.0	14.5	16.3	7.6	.058
0.0	14.5	15.8	7.8	.059
0.0	14.5	15.2	7.9	.060
0.0	14.5	14.6	8.1	.061
0.0	14.5	14.0	8.3	.062
0.0	14.5	13.4	8.4	.063
0.0	14.5	12.8	8.6	.064
0.0	14.5	12.1	8.7	.065
0.0	14.5	11.4	8.8	.066
0.0	14.5	10.7	8.9	.067
0.0	14.5	10.0	9.0	.068
0.0	14.5	9.3	9.1	.069
0.0	14.5	8.6	9.2	.070
0.0	14.5	7.9	9.3	.071
0.0	14.5	7.2	9.3	.072
0.0	14.5	6.5	9.4	.073
0.0	14.5	5.8	9.4	.074
0.0	14.5	5.1	9.5	.075
0.0	14.5	4.4	9.5	.076
0.0	14.5	3.7	9.5	.077
0.0	14.5	3.0	9.5	.078
0.0	14.5	2.3	9.5	.079
0.0	14.5	1.6	9.5	.080
0.0	14.5	.9	9.5	.081
0.0	14.5	.2	9.5	.082
0.0	14.5	-.5	9.5	.083
0.0	14.5	-1.2	9.5	.084
0.0	14.5	-1.9	9.5	.085
0.0	14.5	-2.6	9.5	.086
0.0	14.5	-3.3	9.5	.087
0.0	14.5	-4.0	9.5	.088
0.0	14.5	-4.7	9.5	.089
0.0	14.5	-5.4	9.5	.090
0.0	14.5	-6.1	9.5	.091
0.0	14.5	-6.8	9.5	.092
0.0	14.5	-7.5	9.5	.093
0.0	14.5	-8.2	9.5	.094
0.0	14.5	-8.9	9.5	.095
0.0	14.5	-9.6	9.5	.096
0.0	14.5	-10.3	9.5	.097
0.0	14.5	-11.0	9.5	.098
0.0	14.5	-11.7	9.5	.099

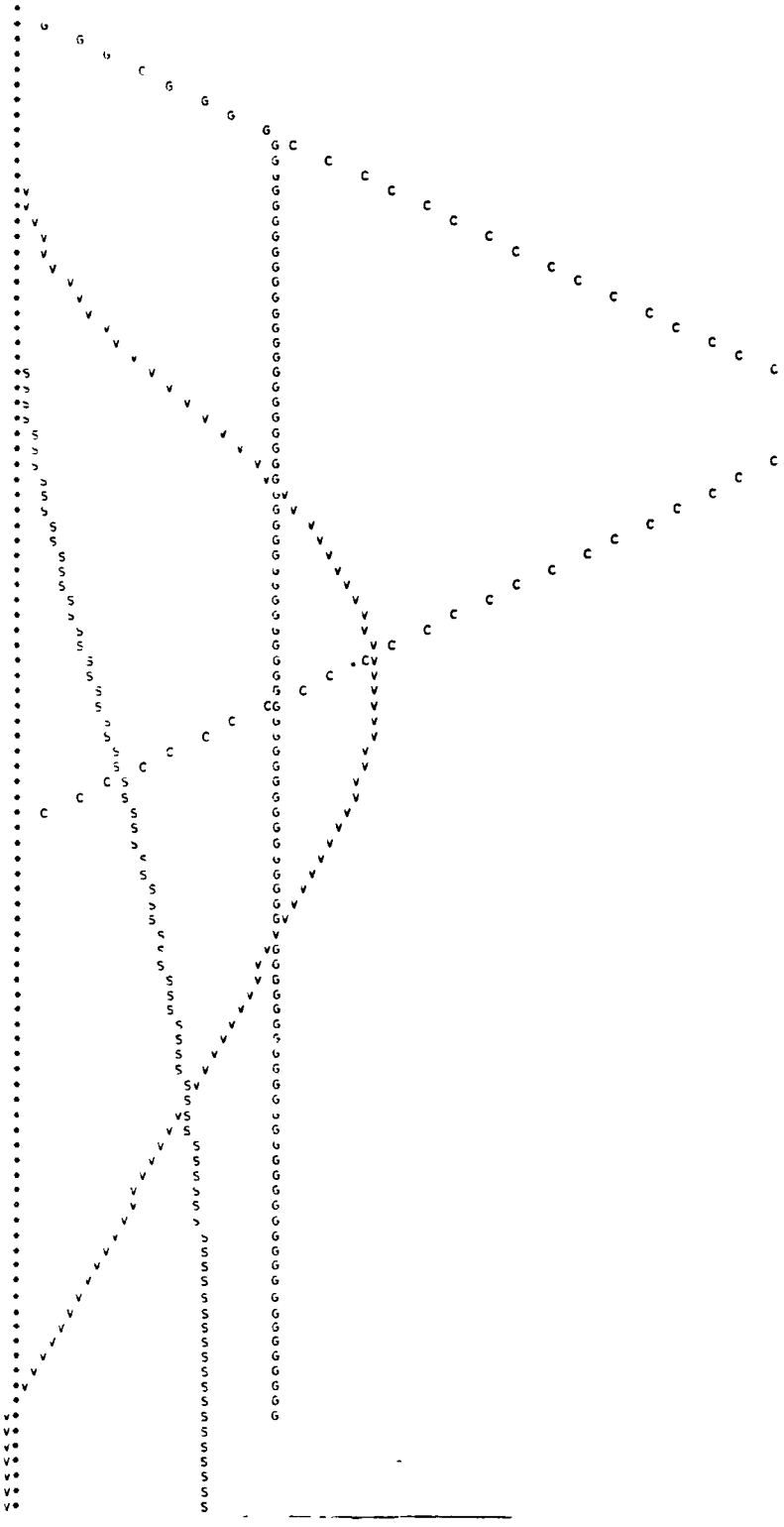

Figure D2. Integration of stroke, S, assuming that bucket deceleration, GB, rises simultaneously with airframe deceleration, GA.

GA	BB	V	S	T
0.0	0.0	0.0	0.0	.000
1.8	0.0	.1	.0	001
3.6	.0	.2	.0	.002
5.3	.2	.3	.0	.003
7.1	.4	.5	.0	.004
8.9	.6	.7	.0	.005
10.7	1.3	1.1	.0	.006
12.4	2.1	1.4	.1	.007
14.2	3.1	1.7	.1	.008
16.0	4.4	2.2	.1	.009
17.8	5.9	2.6	.1	.010
19.6	7.7	2.9	.2	.011
21.3	9.7	3.3	.2	.012
23.1	12.0	3.7	.3	.013
24.9	14.5	4.0	.3	.014
26.7	14.5	4.4	.4	.015
28.4	14.5	4.7	.4	.016
30.2	14.5	5.1	.5	.017
32.0	14.5	5.4	.5	.018
33.8	14.5	5.8	.6	.019
35.6	14.5	6.2	.7	.020
37.3	14.5	6.5	.8	.021
39.1	14.5	6.9	.9	.022
40.9	14.5	7.3	1.0	.023
42.7	14.5	10.5	1.2	.024
44.4	14.5	11.5	1.3	.025
46.2	14.5	12.5	1.4	.026
48.0	14.5	13.6	1.6	.027
46.2	14.5	14.6	1.8	.028
44.4	14.5	15.6	2.0	.029
42.7	14.5	16.5	2.2	.030
40.9	14.5	17.3	2.4	.031
39.1	14.5	18.1	2.6	.032
37.3	14.5	18.8	2.8	.033
35.6	14.5	19.5	3.0	.034
33.8	14.5	20.1	3.3	.035
32.0	14.5	20.7	3.5	.036
30.2	14.5	21.2	3.8	.037
28.4	14.5	21.7	4.1	.038
26.7	14.5	22.0	4.3	.039
24.9	14.5	22.4	4.6	.040
23.1	14.5	22.7	4.9	.041
21.3	14.5	22.9	5.1	.042
19.6	14.5	23.0	5.4	.043
17.8	14.5	23.1	5.7	.044
16.0	14.5	23.2	6.0	.045
14.2	14.5	23.2	6.2	.046
12.4	14.5	23.1	6.5	.047
10.7	14.5	23.1	6.8	.048
8.9	14.5	22.9	7.1	.049
7.1	14.5	22.6	7.3	.050
5.3	14.5	22.3	7.6	.051
3.6	14.5	21.9	7.9	.052
1.8	14.5	21.5	8.1	.053
.0	14.5	21.1	8.4	.054
0.0	14.5	20.6	8.6	.055
0.0	14.5	20.1	8.9	.056
0.0	14.5	19.7	9.1	.057
0.0	14.5	19.2	9.3	.058
0.0	14.5	18.7	9.5	.059
0.0	14.5	18.2	9.8	.060
0.0	14.5	17.6	10.0	.061
0.0	14.5	17.3	10.2	.062
0.0	14.5	16.9	10.4	.063
0.0	14.5	16.4	10.6	.064
0.0	14.5	15.9	10.8	.065
0.0	14.5	15.4	11.0	.066
0.0	14.5	15.0	11.2	.067
0.0	14.5	14.5	11.3	.068
0.0	14.5	14.0	11.5	.069
0.0	14.5	13.6	11.7	.070
0.0	14.5	13.1	11.8	.071
0.0	14.5	12.6	12.0	.072
0.0	14.5	12.2	12.1	.073
0.0	14.5	11.7	12.3	.074
0.0	14.5	11.2	12.4	.075
0.0	14.5	10.8	12.5	.076
0.0	14.5	10.3	12.6	.077
0.0	14.5	9.9	12.8	.078
0.0	14.5	9.4	12.9	.079
0.0	14.5	8.9	13.0	.080
0.0	14.5	8.4	13.1	.081
0.0	14.5	8.0	13.2	.082
0.0	14.5	7.5	13.3	.083
0.0	14.5	7.0	13.4	.084
0.0	14.5	6.6	13.4	.085
0.0	14.5	6.1	13.5	.086
0.0	14.5	5.6	13.6	.087
0.0	14.5	5.2	13.7	.088
0.0	14.5	4.7	13.7	.089
0.0	14.5	4.2	13.7	.090
0.0	14.5	3.8	13.8	.091
0.0	14.5	3.3	13.8	.092
0.0	14.5	2.9	13.9	.093
0.0	14.5	2.4	13.9	.094
0.0	14.5	1.9	13.9	.095
0.0	14.5	1.4	13.9	.096
0.0	14.5	1.0	13.9	.097
0.0	14.5	.5	13.9	.098
0.0	14.5	.0	14.0	.099
0.0	14.5	-.4	13.9	.100
0.0	0.0	-.4	13.9	.101
0.0	0.0	-.4	13.9	.102
0.0	0.0	-.4	13.9	.103
0.0	0.0	-.4	13.9	.104
0.0	0.0	-.4	13.9	.105
0.0	0.0	-.4	13.9	.106
0.0	0.0	-.4	13.9	.107
0.0	0.0	-.4	13.9	.108

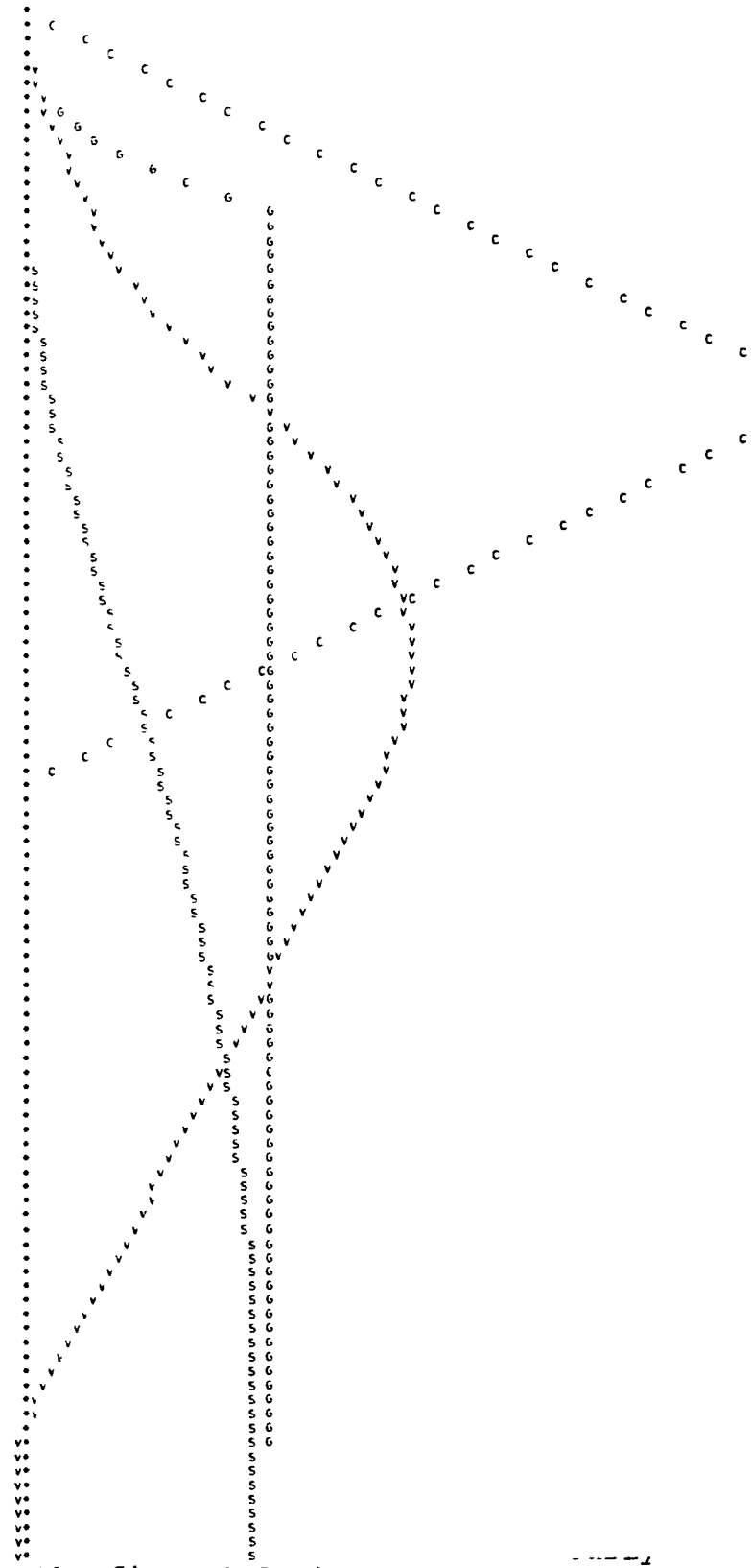

over the first 0.25 in. of stroke.

REFERENCES

1. Crash Survival Design Guide. U.S. Army Air Mobility Research and Development Laboratory Technical Report 71-22, 1971.

2. Dreyfuss, H.: The Measure of Man - Human Factors Design. Whitney Publications, Inc., 1960.

3. Desjardins, Stanley P.; and Harrison, Harold D.: The Design, Fabrication, and Testing of an Integrally Armored Crashworthy Crewseat. U.S. Army Air Mobility Research and Development Laboratory Technical Report 71-54, January 1972.

End of Document